PB82-230921

# Pilot-Scale Assessment of Conventional Particulate Control Technology for Pressurized Fluidized-Bed Combustion Emissions

Acurex Corp.
Morrisville, NC

Prepared for

Industrial Environmental Research Lab.
Research Triangle Park, NC

Apr 82

U.S. Department of Commerce
National Technical Information Service
NTIS

United States
Environmental Protection
Agency

EPA-600/7-82-028

April 1982

PB82-230921

# Research and Development

## PILOT-SCALE ASSESSMENT OF CONVENTIONAL PARTICULATE CONTROL TECHNOLOGY FOR PRESSURIZED FLUIDIZED-BED COMBUSTION EMISSIONS

## Prepared for

Office of Air Quality Planning and Standards

## Prepared by

Industrial Environmental Research
Laboratory
Research Triangle Park NC 27711

REPRODUCED BY
NATIONAL TECHNICAL
INFORMATION SERVICE
U.S. DEPARTMENT OF COMMERCE
SPRINGFIELD, VA 22161

IERL-RTP-1269

**TECHNICAL REPORT DATA**

*(Please read Instructions on the reverse before completing)*

| | | |
|---|---|---|
| 1. REPORT NO.<br>EPA-600/7-82-028 | 2. | 3. RECIPIENT'S ACCESSION NO.<br>PB82-230921 |
| 4. TITLE AND SUBTITLE Pilot-scale Assessment of Conventional Particulate Control Technology for Pressurized Fluidized-bed Combustion Emissions | | 5. REPORT DATE<br>April 1982 |
| | | 6. PERFORMING ORGANIZATION CODE |
| 7. AUTHOR(S)<br>W. O. Lipscomb III, S. R. Malani, C. L. Stanley, and S. P. Schliesser | | 8. PERFORMING ORGANIZATION REPORT NO. |
| 9. PERFORMING ORGANIZATION NAME AND ADDRESS<br>Acurex Corporation<br>Route 1, Box 423<br>Morrisville, North Carolina 27560 | | 10. PROGRAM ELEMENT NO. |
| | | 11. CONTRACT/GRANT NO.<br>68-02-2646 |
| 12. SPONSORING AGENCY NAME AND ADDRESS<br>EPA, Office of Research and Development<br>Industrial Environmental Research Laboratory<br>Research Triangle Park, NC 27711 | | 13. TYPE OF REPORT AND PERIOD COVERED<br>Final; 3/79-6/80 |
| | | 14. SPONSORING AGENCY CODE<br>EPA/600/13 |

15. SUPPLEMENTARY NOTES IERL-RTP project officer is John O. Milliken, Mail Drop 61, 919/541-7716.

16. ABSTRACT The report gives results of an evaluation of electrostatic precipitator (ESP) and fabric filter particulate control technology for the EPA/Exxon pressurized fluidized-bed combustion (PFBC) Miniplant in Linden, NJ. EPA's mobile ESP and fabric filter pilot facilities were slipstreamed downstream of the Miniplant's tertiary cyclone to simulate the flue gas stream exiting a PFBC combined-cycle gas turbine. Results presented include control-device operating characteristics and performance based on mass and fractional collection efficiencies. ESP mass collection efficiency varied from 80 to 90%. The mobile baghouse efficiency was 99.3%. EPA's mathematical performance models for the ESP, fabric filter, and venturi scrubber were exercised to generate a basis for an economic analysis of conventional particulate control alternatives. Control costs for a 350-MW PFBC ranged from 0.33 to 0.51 mills/kWh for fabric filters and from 0.30 to 0.57 mills/kWh for ESPs. Venturi scrubbing costs were considerably higher (0.66 mills/kWh).

17. KEY WORDS AND DOCUMENT ANALYSIS

| a. DESCRIPTORS | | b. IDENTIFIERS/OPEN ENDED TERMS | c. COSATI Field/Group | |
|---|---|---|---|---|
| Pollution | Fabrics | Pollution Control | 13B | 11E |
| Dust | Scrubbers | Stationary Sources | 11G | 07A |
| Aerosols | Flue Gases | Particulate | 07D | 21B |
| Electrostatic Precipitators | Fluidized Bed Processing | Fabric Filters | 13I | 13H |
| Filtration | Combustion | | | |

| | | |
|---|---|---|
| 18. DISTRIBUTION STATEMENT<br>Release to Public | 19. SECURITY CLASS *(This Report)*<br>Unclassified | 21. NO. OF PAGES<br>132 |
| | 20. SECURITY CLASS *(This page)*<br>Unclassified | 22. PRICE |

EPA Form 2220-1 (9-73)

# RESEARCH REPORTING SERIES

Research reports of the Office of Research and Development, U.S. Environmental Protection Agency, have been grouped into nine series. These nine broad categories were established to facilitate further development and application of environmental technology. Elimination of traditional grouping was consciously planned to foster technology transfer and a maximum interface in related fields. The nine series are:

1. Environmental Health Effects Research
2. Environmental Protection Technology
3. Ecological Research
4. Environmental Monitoring
5. Socioeconomic Environmental Studies
6. Scientific and Technical Assessment Reports (STAR)
7. Interagency Energy-Environment Research and Development
8. "Special" Reports
9. Miscellaneous Reports

This report has been assigned to the INTERAGENCY ENERGY-ENVIRONMENT RESEARCH AND DEVELOPMENT series. Reports in this series result from the effort funded under the 17-agency Federal Energy/Environment Research and Development Program. These studies relate to EPA's mission to protect the public health and welfare from adverse effects of pollutants associated with energy systems. The goal of the Program is to assure the rapid development of domestic energy supplies in an environmentally-compatible manner by providing the necessary environmental data and control technology. Investigations include analyses of the transport of energy-related pollutants and their health and ecological effects; assessments of, and development of, control technologies for energy systems; and integrated assessments of a wide range of energy-related environmental issues.

## EPA REVIEW NOTICE

[illegible]

This document is available to the public through the National Technical Information Service, Springfield, Virginia 22161.

EPA-600/7-82-028
April 1982

# PILOT-SCALE ASSESSMENT OF CONVENTIONAL PARTICULATE CONTROL TECHNOLOGY FOR PRESSURIZED FLUIDIZED-BED COMBUSTION EMISSIONS

by

W.O. Lipscomb III, S.R. Malani, C.L. Stanley, and S.P. Schliesser

Acurex Corporation
Route 1, Box 423
Morrisville, North Carolina 27560

Contract No. 68-02-2646

EPA Project Officer: **John O. Milliken**

Industrial Environmental Research Laboratory
**Office of Environmental Engineering and Technology**
Research Triangle Park, North Carolina 27711

Prepared for

U.S. ENVIRONMENTAL PROTECTION AGENCY
Office of Research and Development
Washington, DC 20460

# DISCLAIMER

This report has been reviewed by the Industrial Environmental Research Laboratory, U.S. Environmental Protection Agency, and approved for publication. Approval does not signify that the contents necessarily reflect the views and policies of the U.S. Environmental Protection Agency, nor does mention of trade names or commercial products constitute endorsement or recommendation for use.

# ABSTRACT

This report presents the results of a performance evaluation of conventional particulate control technology applied to the EPA/Exxon pressurized fluidized-bed combustion (PFBC) miniplant in Linden, New Jersey. The EPA mobile electrostatic precipitator (ESP) and fabric filter pilot facilities were slipstreamed downstream of the miniplant's tertiary cyclone to simulate the flue gas stream exiting a PFBC combined-cycle gas turbine. Results presented include control-device operating characteristics and performance based on mass and fractional efficiencies. ESP mass efficiency varied from 80 to 90 percent and appeared to be sensitive to miniplant operating conditions. The mobile baghouse efficiency was 99.3 percent. The EPA mathematical performance models for the ESP, fabric filter, and venturi scrubber were exercised to generate a basis for an economic analysis of conventional particulate control alternatives. Costs of control for a 350 MW PFBC ranged from 0.33 to 0.51 mils/kWh for fabric filters and from 0.30 to 0.57 mils/kWh for ESPs. Venturi scrubbing costs were considerably higher (0.66 mils/kWh).

# CONTENTS

Page

Abstract.................................................... iii

List of Figures.............................................. v

List of Tables............................................... vii

Conversion Factors for British and SI Units..................... ix

Acknowledgments............................................... x

Section 1. Introduction and Objectives........................... 1

Section 2. Conclusions........................................... 3

Section 3. Recommendations....................................... 4

Section 4. Description of Facilities............................. 5

Section 5. Program Methodology................................... 13

Section 6. Results and Discussion................................ 26

References.................................................... 88

Appendices

A. Exxon miniplant run summaries.............................. A-1

B. Mobile baghouse operational problems....................... B-1

C. ESP inlet and outlet differential size distribution curves................................................. C-1

## FIGURES

Number Page

1 Exxon pressurized fluidized-bed combustion miniplant schematic.......................................... 6

2 Plan view of mobile ESP facility.......................... 7

3 Removable high voltage field.............................. 10

4 Mobile baghouse schematic................................. 12

5 Schematic of the mobile baghouse installation at the Exxon miniplant................................................ 15

6 Representative ESP V-I curve for miniplant run 103........ 34

7 Representative ESP V-I curve for miniplant run 104........ 35

8 Representative ESP V-I curve for miniplant run 105........ 36

9 Laboratory resistivity for ash samples from pilot ESP..... 37

10 ESP average inlet cumulative size distribution for runs 103, 104, 105............................................ 46

11 ESP average inlet differential size distribution for run 103.................................................. 47

12 ESP average inlet differential size distribution for run 104.................................................. 48

13 ESP average inlet differential size distribution for run 105.................................................. 49

14 ESP average inlet differential size distribution for runs 103, 104, and 105, with 50 percent confidence intervals.. 51

15 ESP average outlet differential size distribution for runs 103, 104, and 105 with 50 percent confidence intervals... 52

16 ESP average penetration characteristics for runs 103, 104, and 105................................................ 53

FIGURES (continued)

Number Page

17 Baghouse inlet and outlet cumulative size distributions, including probe wash........................................ 60

18 Baghouse inlet and outlet cumulative size distributions, excluding probe wash........................................ 61

19 Baghouse average inlet differential size distribution for runs 106, 107, and 108, with 50 percent confidence intervals..................................................... 63

20 Baghouse outlet differential size distributions for run 107.......................................................... 64

21 Baghouse outlet differential size distributions for run 108.......................................................... 65

22 Baghouse average penetration characteristics for run 107... 66

23 Baghouse average penetration characteristics for run 108... 67

24 Laboratory resistivity for ash samples from the pilot baghouse ...................................................... 69

25 Tertiary cyclone outlet particle size distributions from Coulter Counter and cascade impactors.................... 72

26 Comparison of ESP empirical and predicted fractional penetrations............................................... 75

27 Typical drag versus loading curves......................... 76

28 Estimation of $K_2$ and $S_E$ values............................ 77

29 ESP costs versus SCA and emission level.................... 85

30 Baghouse costs versus air/cloth ratio and emission level... 86

Appendices

ESP inlet and outlet differential size distribution curves................................................C-1

# TABLES

Number Page

1 PFBC Coal and Sorbent Specifications.......................... 8

2 Full-Scale and Pilot ESP Design Specifications............. 11

3 Exxon Miniplant Operating Conditions....................... 16

4 Specifications for W.W. Criswell Woven Glass Bags.......... 20

5 Shake-Cleaning Parameters.................................. 20

6 Pilot ESP Operating Conditions............................. 27

7 Pilot ESP Electrical Characteristics....................... 29

8 Pilot ESP Average V-I Characteristics...................... 31

9 *In-situ* Resistivity Data.................................. 33

10 Chemical Analysis of ESP Ash Samples....................... 39

11 Pilot ESP Inlet and Outlet Loadings........................ 40

12 Summary of Average ESP Performance......................... 42

13 Pilot Baghouse Cleaning Cycles and Pressure Drop Characteristics........................................ 54

14 Pilot Baghouse Inlet and Outlet Loadings................... 57

15 Summary of Average Baghouse Performance.................... 59

16 Chemical Analyses of Pilot Baghouse and Miniplant Ash Samples.................................................. 68

17 Tertiary Cyclone Average Outlet Loadings................... 70

18 Comparison of Empirical and Predicted ESP Performance...... 73

## TABLES (continued)

Number Page

19 Summary of Baghouse Performance Modeling.................. 78

20 Summary of Scrubber Performance Modeling.................. 79

21 Basis for ESP Design and Cost Estimation.................. 81

22 Basis for Baghouse Design and Cost Estimation............. 82

23 Basis for Scrubber Design and Cost Estimation............. 83

24 Summary of Costs of Control............................... 84

25 Summary of Costs of Control versus Emission Levels......... 87

Appendix

Exxon Miniplant Run Summaries.............................A-1

# CONVERSION FACTORS FOR BRITISH AND SI UNITS

| To convert from | To | Multiply by |
|---|---|---|
| Btu | joule | 1055 |
| °F | °C | °C=(°F - 32)/1.8 |
| ft | m | 0.3048 |
| gpm | $m^3/s$ | $6.309 \times 10^{-5}$ |
| inch | cm | 2.54 |
| inch $H_2O$ | pascal | 248.8 |
| lb/hr | kg/s | $1.259 \times 10^{-4}$ |
| $lb/ft^3$ | $kg/m^3$ | 16.01 |

## ACKNOWLEDGEMENTS

This program was sponsored by the U.S. Environmental Protection Agency (EPA), with participation by the Exxon Research and Engineering Company and Acurex/Aerotherm.

The authors wish to express their sincere appreciation to and acknowledge the contributions of James H. Turner, EPA project officer for the EPA mobile collectors, and D. Bruce Henschel, EPA project officer for the EPA/Exxon miniplant at Linden, New Jersey.

The cordial assistance and support of Ron Hoke, Mike Ernst, and Vince Siminski of the Exxon Research and Engineering Company contributed greatly to the successful completion of this study.

The authors also wish to thank the following Acurex/Aerotherm personnel:

- Hal Buck, Mike Griffin, Randy Page, Evelyn Rice, Kenny Case, Danny Ashley, Don Fraser, Cliff Cox, Regan Best, Jerry Bault, Paul Jarman, and Ron Davis, for their skilled technical assistance, without which timely execution of the field-testing programs would not have been possible; and
- Dan Buedel and Bill Jones, for their data reduction and analysis.

# SECTION 1

# INTRODUCTION AND OBJECTIVES

Fluidized-bed combustion (FBC) systems being developed for steam and electrical power generation and process heating employ a number of concepts, including atmospheric and pressurized combustion, temperature control by fuel-to-air ratio, heat transfer surface, and particulate circulation. These FBC systems offer attractive advantages over conventional combustion in costs, resource utilization, and environmental impact.

Current FBC development programs use calcium-based sorbents (limestones and dolomites) for in-situ control of sulfur oxides ($SO_x$) in the combustor, while lower combustion temperatures limit to some degree the formation of thermal nitrogen oxides ($NO_x$). Particulate matter (PM) emissions from an atmospheric FBC system are controlled by conventional technology. In contrast, the pressurized fluidized-bed combustion (PFBC) process uses the hot, high-pressure flue gas exiting the combustor to drive a gas turbine to generate additional power, and conventional technology for control of PM emissions is not applicable.

There has been considerable discussion of the degree of PM removal required ahead of the gas turbine to prevent excessive corrosion and/or erosion of the turbine. High-pressure, high-temperature PM control technology (e.g., ceramic filters) has been investigated to provide a flue gas cleansed of PM to ensure acceptable turbine operating and maintenance costs and life expectancy. Recently, turbine designers have reduced the limitations on PM concentration and size distribution required so that a secondary or tertiary cyclone system can achieve the required level of PM control. The residual particulates, while acceptable for the gas turbine, must be further controlled to meet environmental standards.

The purpose of this study was to assess a pilot-scale application of conventional PM control technology, i.e., an electrostatic precipitator (ESP) and a fabric filter (baghouse), to a PFBC cyclone-cleaned exhaust. The program's objectives were accomplished using the EPA mobile ESP and baghouse slipstreamed from the 630 kW EPA/Exxon Research and Engineering Company miniplant in Linden, New Jersey.

The mobile ESP pilot assessment was conducted during April and May 1979, and the mobile fabric filter program was accomplished in June 1979.

Specific program objectives were to:

- test the applicability of conventional PM control technology to cyclone-cleaned PFBC emissions,
- evaluate respective control device operating characteristics and performance levels,
- exercise the EPA Industrial Environmental Research Laboratory (IERL) control device performance models to establish a basis for cost analysis, and
- generate cost-of-control estimates for an ESP, a baghouse, and a venturi scrubber.

The results presented in this report are specific to the Exxon miniplant and the slipstreamed mobile ESP and baghouse; extrapolation to other systems may be risky.

## SECTION 2

## CONCLUSIONS

- Conventional PM control technology appears applicable to cyclone-cleaned PFBC emissions.
- ESP operating characteristics and performance were influenced by PFBC operating conditions and sorbent type.

  Cold-sided ESP performance was better than hot-side performance on a normalized gas treatment basis.
- Fabric filtration affords an appreciably higher degree of control at approximately the same costs as an ESP.
- This PFBC process is apparently subject to peaking sulfur dioxide ($SO_2$) /sulfur trioxide ($SO_3$) emission levels, which cause acid dew-point excursions and seriously impact control hardware specifications and operating conditions.
- There were both similarities and differences in conventional control device operating characteristics for the PFBC process and for conventional coal-fired boilers.

# SECTION 3

# RECOMMENDATIONS

- Conduct further pilot-scale control evaluations of the PFBC process to optimize control device design and operating conditions.
- Address the extent of and resolution of the apparent $SO_2/SO_3$ excursions associated with this and possibly other PFBC processes.

# SECTION 4

# DESCRIPTION OF FACILITIES

## EPA/EXXON MINIPLANT

The EPA/Exxon miniplant, located at the Exxon Research and Engineering Company research complex in Linden, New Jersey, is a 630 kW PFBC and $SO_2$ sorbent regenerator facility. The miniplant combustor is a refractory-lined vessel 10 m (33 ft) high, with an inside diameter of 32 cm (12.5 in). It is capable of operating at pressures up to 1000 kPa (10 atm), at a temperature up to the ash agglomeration of coal (usually less than 980°C), at superficial velocities up to 3 m/s (10 ft/s), and with expanded beds up to 6.1 m (20 ft).

The maximum design coal feed rate is 220 kg/hr (485 lb/hr). Detailed design and operating specifications and performance results are given in References 1, 2, and 3. A schematic of the miniplant is shown in Figure 1.

During the pilot-scale test programs, miniplant runs were made with an Eastern bituminous Pittsburgh seam coal (Champion) containing 2.0 percent sulfur and an Illinois no. 6 coal containing 4.2 percent sulfur, each screened to a particle size distribution of 200 to 2400 )m. Two sorbents were also used: a Virginia high-calcium limestone (Grove no. 1359) and an Ohio dolomite (Pfizer no. 1337), both screened to a size range of 840 to 2400 )m. Table 1 provides more detailed specifications for the coals and sorbents.

## PILOT ESP

The EPA mobile ESP facility consists of two separate units mounted on freight trailers 12.2 m long. Figure 2 is a floor plan of the two units.

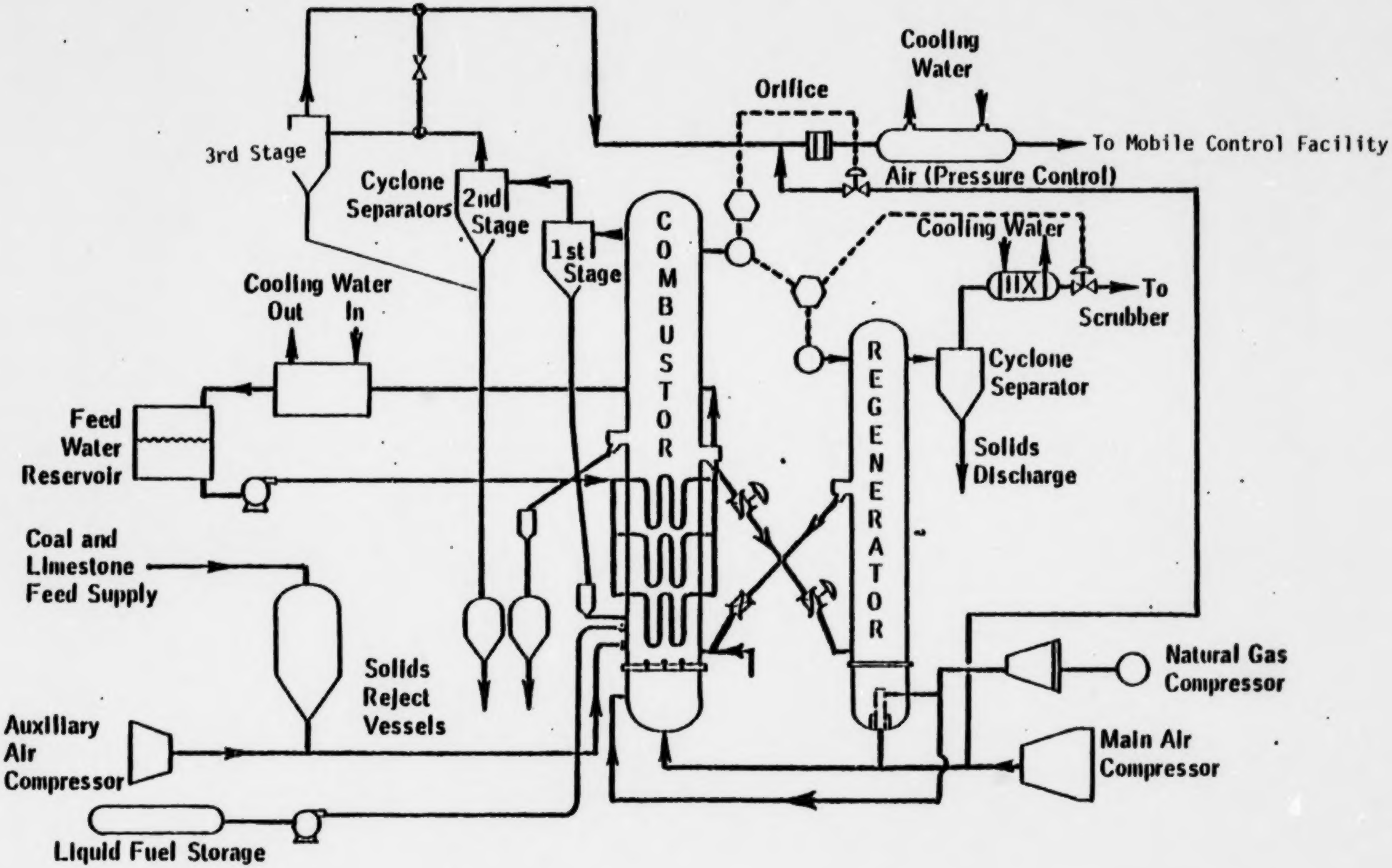
3rd Stage
Cyclone Separators
2nd Stage
1st Stage
Cooling Water Out
In
Feed Water Reservoir
Coal and Limestone Feed Supply
Solids Reject Vessels
Auxiliary Air Compressor
Liquid Fuel Storage
COMBUSTOR
Orifice
Cooling Water
To Mobile Control Facility
Air (Pressure Control)
Cooling Water
IIX
To Scrubber
REGENERATOR
Cyclone Separator
Solids Discharge
Natural Gas Compressor
Main Air Compressor

Figure 1. Exxon pressurized fluidized-bed combustion miniplant schematic.

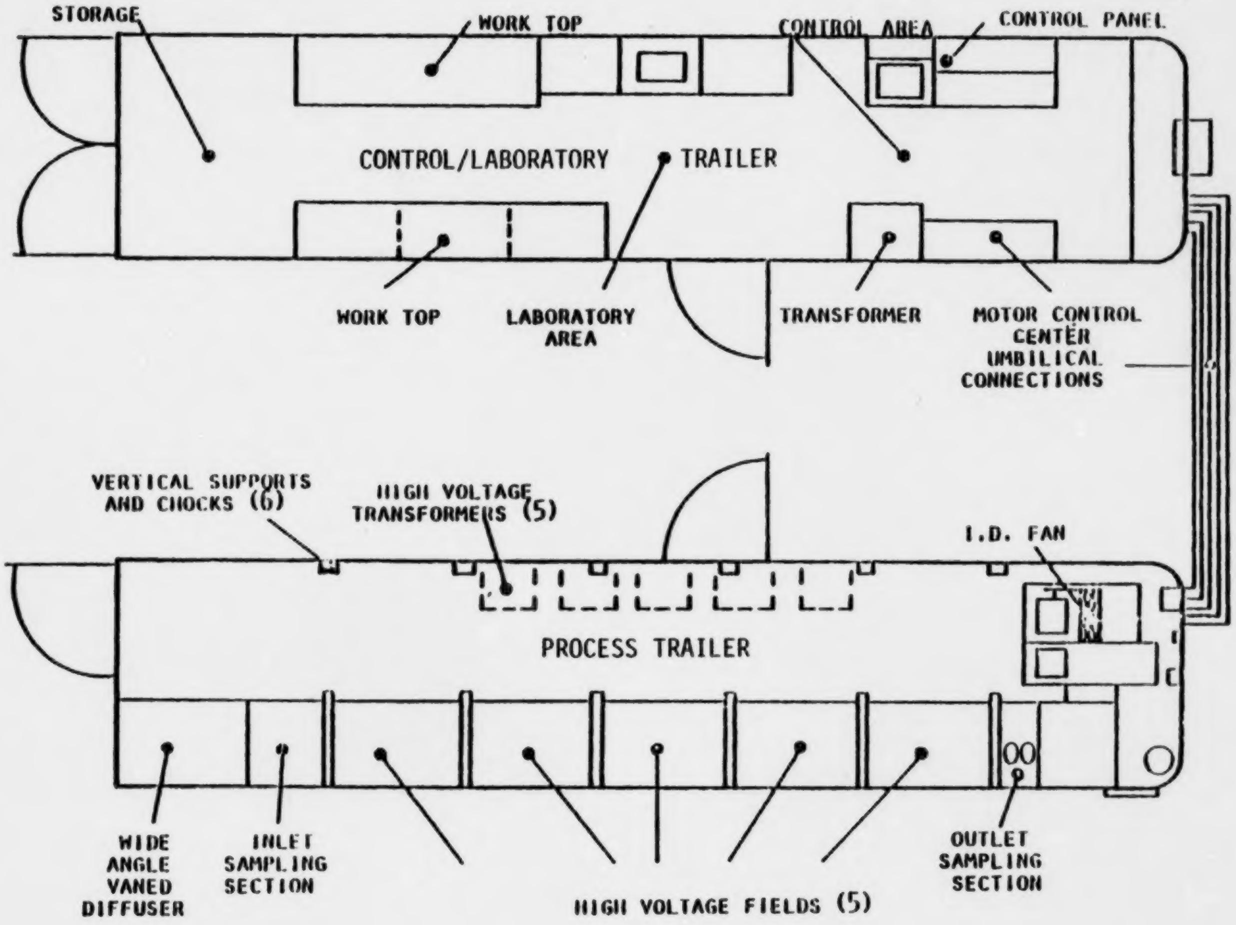

STORAGE
WORK TOP
CONTROL AREA
CONTROL PANEL
CONTROL/LABORATORY TRAILER
WORK TOP
LABORATORY AREA
TRANSFORMER
MOTOR CONTROL CENTER
UMBILICAL CONNECTIONS
VERTICAL SUPPORTS AND CHOCKS (6)
HIGH VOLTAGE TRANSFORMERS (5)
I.D. FAN
PROCESS TRAILER
WIDE ANGLE VANED DIFFUSER
INLET SAMPLING SECTION
HIGH VOLTAGE FIELDS (5)
OUTLET SAMPLING SECTION

Figure 2. Plan view of mobile ESP facility.

TABLE 1. PFBC COAL AND SORBENT SPECIFICATIONS

Ultimate analysis, %

| Coal type | Moisture | Ash | Total Carbon | H | S | N | Cl | $O_2$ | Heating value, kJ/kg |
|---|---|---|---|---|---|---|---|---|---|
| Champion | 2.83 | 8.03 | 70.38 | 5.01 | 1.96 | 1.36 | 0.09 | 10.43 | 31,025 |
| Illinois | 3.01 | 9.95 | 67.71 | 4.77 | 4.20 | 1.17 | 0.05 | 9.19 | 28,470 |

Weight, %

| Sorbent | CaO | MgO | $SiO_2$ | $Al_2O_3$ | $Fe_2O_3$ |
|---|---|---|---|---|---|
| Grove limestone | 97.0 | 1.2 | 1.1 | 0.3 | 0.2 |
| Pfizer dolomite | 54.0 | 44.0 | 0.9 | 0.2 | 0.3 |

The first unit is the process trailer, which houses a five-section ESP and the following auxiliary equipment:

- a diffuser section for flow rectification,
- a screw conveyor and rotary airlock to allow removal of collected material during ESP operation,
- electromagnetic vibrators for rapping the collection plates,
- pneumatic impactors for rapping the corona wires, and
- five transformer-rectifiers, each with a rated capacity of 50 kV and 10 MA DC.

The system is designed to operate up to 540°C over a flow range of 28-85 $m^3$/min (1000-3000 afcm). It is connected to the plant process by sections of heat-treated, insulated 25.4 cm (10 in) stainless steel duct. Additional vaned elbows are placed between the duct and the ESP entrance to ensure a uniform velocity profile. Details of the high voltage field design are shown in Figure 3.

The second unit is a control/laboratory trailer containing all process controls, monitors, and recorders, as well as analytical laboratory facilities and spare equipment storage.

Table 2 compares design specifications of the mobile ESP with those typical of full-scale. The following comparisons are apparent:

- Fixed design parameters on the pilot unit lie midway in the normal range for full-scale installations.
- Operational parameters may be varied as necessary to cover the spectrum typical of commercial units.
- Plate area is the only parameter that does not compare, being the inherent concession of pilot-scale methodology.

Reference 4 contains a more detailed discussion of the ESP design specifications and operating characteristics.

## PILOT BAGHOUSE

The EPA mobile baghouse, which is contained in a 2.4 m x 12.2 m freight trailer, consists of a single compartment containing three bags 14.1 cm (5 9/16 in) in diameter by 1.83 m (6 ft) long. Designed to determine the effects of dust properties, fabric media, cleaning parameters, and other operating parameters on fabric filter performance, the system has the following capabilities:

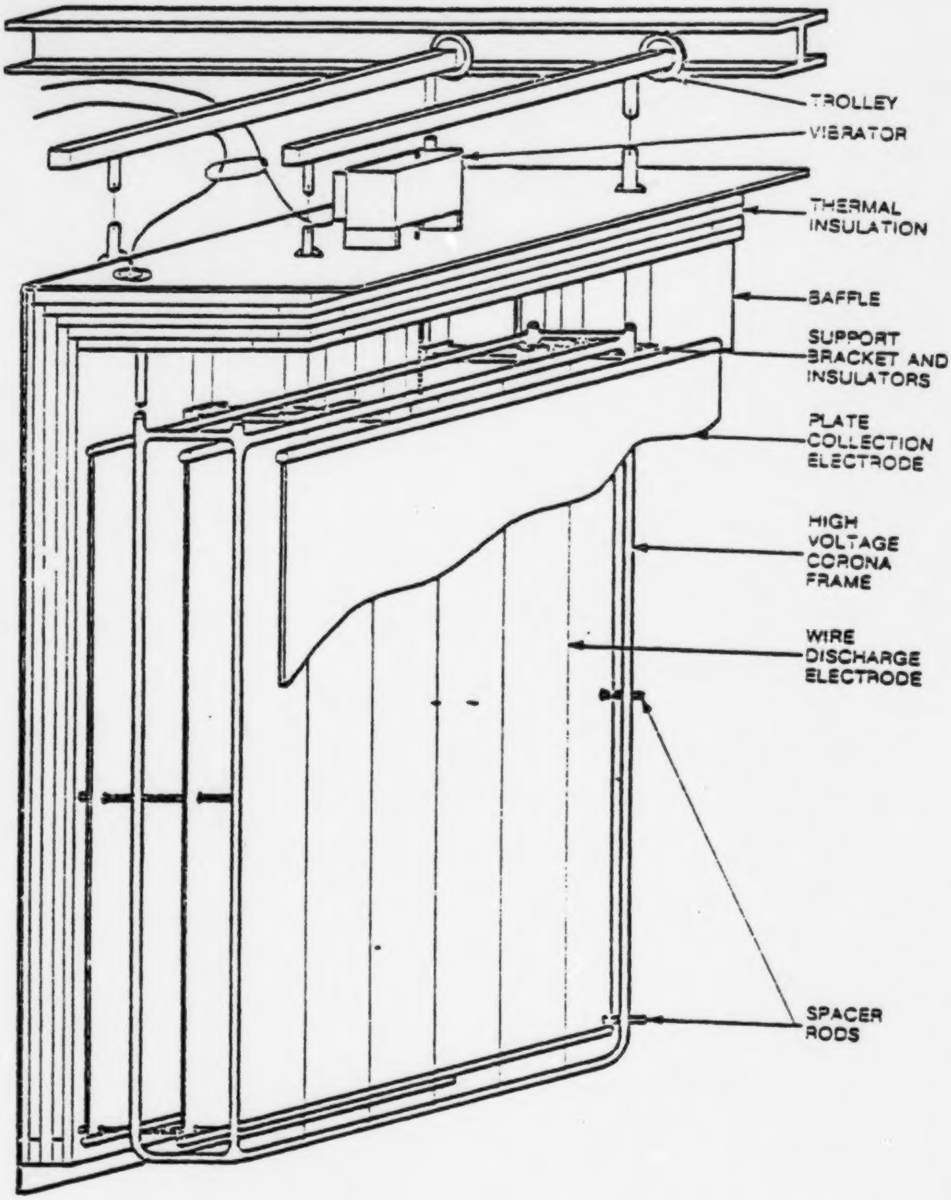
TROLLEY
VIBRATOR
THERMAL INSULATION
BAFFLE
SUPPORT BRACKET AND INSULATORS
PLATE COLLECTION ELECTRODE
HIGH VOLTAGE CORONA FRAME
WIRE DISCHARGE ELECTRODE
SPACER RODS

Figure 3. Removable high voltage field.

TABLE 2. FULL-SCALE AND PILOT ESP DESIGN SPECIFICATIONS

| | Full-scale ESP | PILOT ESP |
|---|---|---|
| Discharge wire diameter, cm | 0.25 | 0.25 |
| Wire-wire spacing, cm | 10-30 | 18 |
| Wire-plate spacing, cm | 10-15 | 13 |
| Specific collection area, $m^2/m^3/s$ | 20-150 | 20-100 |
| Collection area/T-R set, $m^2$ | 50-750 | 9 |
| Aspect ratio | 0.5 - 1.5 | 0.67 |
| Specific corona power, $W/m^3/s$ | 100 - 1000 | 100 - 1000 |
| Current density, $nA/cm^2$ | 5-70 | 5-100 |
| Gas velocity, m/s | 1.0 - 5.0 | 0.5 - 2.0 |
| No. of fields in series | 2 - 8 | 2 - 5 |

- filtration at cloth velocities as high as 6 m/min, with a pressure differential up to 50 cm of water and at gas temperatures up to 260°C;
- adaptability of the mobile system to cleaning by mechanical shake, pulse jet, or low-pressure reverse flow, with cleaning parameters varying over a wide range; and
- continuous 24-hour operation, with use of automatic instruments and controls.

The mobile fabric filter is shown schematically in Figure 4. More detailed design specifications and operating characteristics may be found in Reference 5.

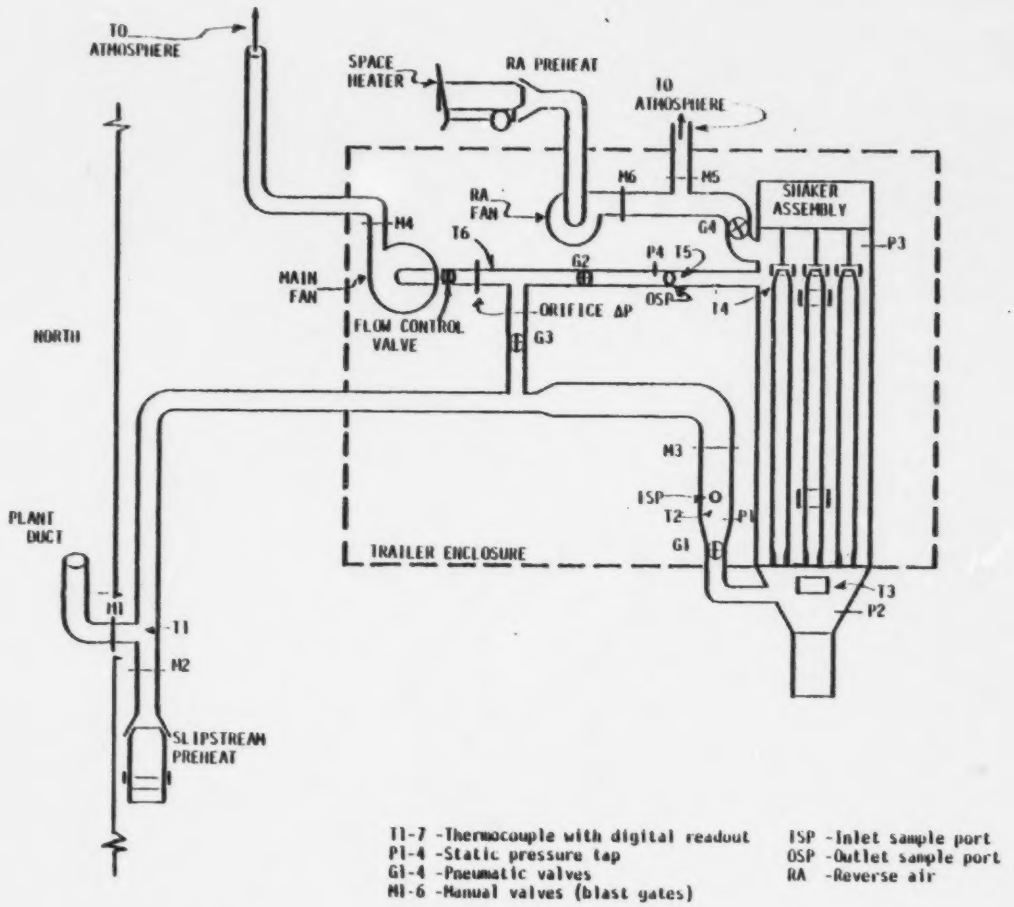
TO ATMOSPHERE
SPACE HEATER
RA PREHEAT
TO ATMOSPHERE
RA FAN
M6
M5
SHAKER ASSEMBLY
M4
T6
G2
P4
T5
G4
P3
MAIN FAN
OSP
T4
ORIFICE ΔP
FLOW CONTROL VALVE
G3
NORTH
M3
ISP
T2
P1
PLANT DUCT
G1
TRAILER ENCLOSURE
T3
P2
M1
T1
M2
SLIPSTREAM PREHEAT
T1-7 -Thermocouple with digital readout
P1-4 -Static pressure tap
G1-4 -Pneumatic valves
M1-6 -Manual valves (blast gates)
ISP -Inlet sample port
OSP -Outlet sample port
RA -Reverse air

Figure 4. Mobile baghouse schematic.

## SECTION 5

## PROGRAM METHODOLOGY

### GENERAL

The mobile ESP and baghouse were slipstreamed from the Exxon miniplant downstream of the tertiary cyclone. The temperature and pressure of the flue gas were reduced within the miniplant to provide a slipstream representative of that exiting a combined-cycle turbine.

The specific methodology and test conditions employed during this program were selected to provide (1) an assessment of conventional PM control technology applied to a PFBC process and (2) a comparison of control device operating characteristics and performance for the PFBC process and for pulverized coal-fired boilers. This comparison was accomplished by selecting operating conditions, such as specific collection area (SCA) for the ESP, and bag type, filtration velocity, and cleaning parameters for the baghouse, representative of control systems for conventional coal-fired boilers.

### INSTALLATION

#### Pilot ESP

The mobile ESP process and lab trailers were spotted adjacent to and connected to the Exxon miniplant via 30 m of 25.4 cm schedule 5 stainless steel pipe. The slipstream was heated (82 W/m), insulated, and clad. Connection to the miniplant was made downstream of the tertiary cyclone. An orifice was used to maintain back pressure in the PFBC process, and a heat exchanger located downstream from the orifice reduced the gas stream temperature to the level required for the ESP test conditions. A pair of pneumatic gate valves were used to direct the PFBC exhaust either to the mobile ESP or to the miniplant scrubber (when the ESP was not in operation).

### Pilot Baghouse

The pilot baghouse installation was similar to that for the ESP and is shown schematically in Figure 5. The slipstream was 7.6 cm schedule 5 stainless steel pipe heated and insulated to maintain reasonably constant operating temperatures at the baghouse. It was connected to the miniplant downstream of the tertiary cyclone via a remotely activated 7.6 cm I.P.S. automatic valve installed by Exxon. Operational problems encountered with this valve will be discussed later. Ultimate valve failure required installation of a 1.55 cm diameter orifice plate (for flow control) at one of the slipstream flanged joints. The baghouse slipstream split off approximately 10 percent of the miniplant flue gas flow, with the remainder following the normal process flow through the miniplant scrubber. This necessitated operation of the mobile baghouse under positive pressure.

## OPERATION

### EPA/Exxon Miniplant

Two coal types, two sorbent types, and runs with and without sorbent regeneration were used during the mobile ESP and baghouse test programs (miniplant runs 103-108) at the Exxon miniplant (see Table 3). Only Champion coal was fired during the ESP test program (runs 103-105), but Grove limestone and Pfizer dolomite were both used as sorbents and runs 103 and 105 were conducted with sorbent regeneration. During the baghouse test program, Illinois coal was fired during miniplant run 106 and Champion coal was fired during runs 107 and 108. Only Pfizer dolomite was used as a sorbent during these runs, and there was no sorbent regeneration. A more detailed summary of the miniplant operating conditions and performance characteristics for miniplant runs 103-108 is presented in Table 3 and in Appendix A.

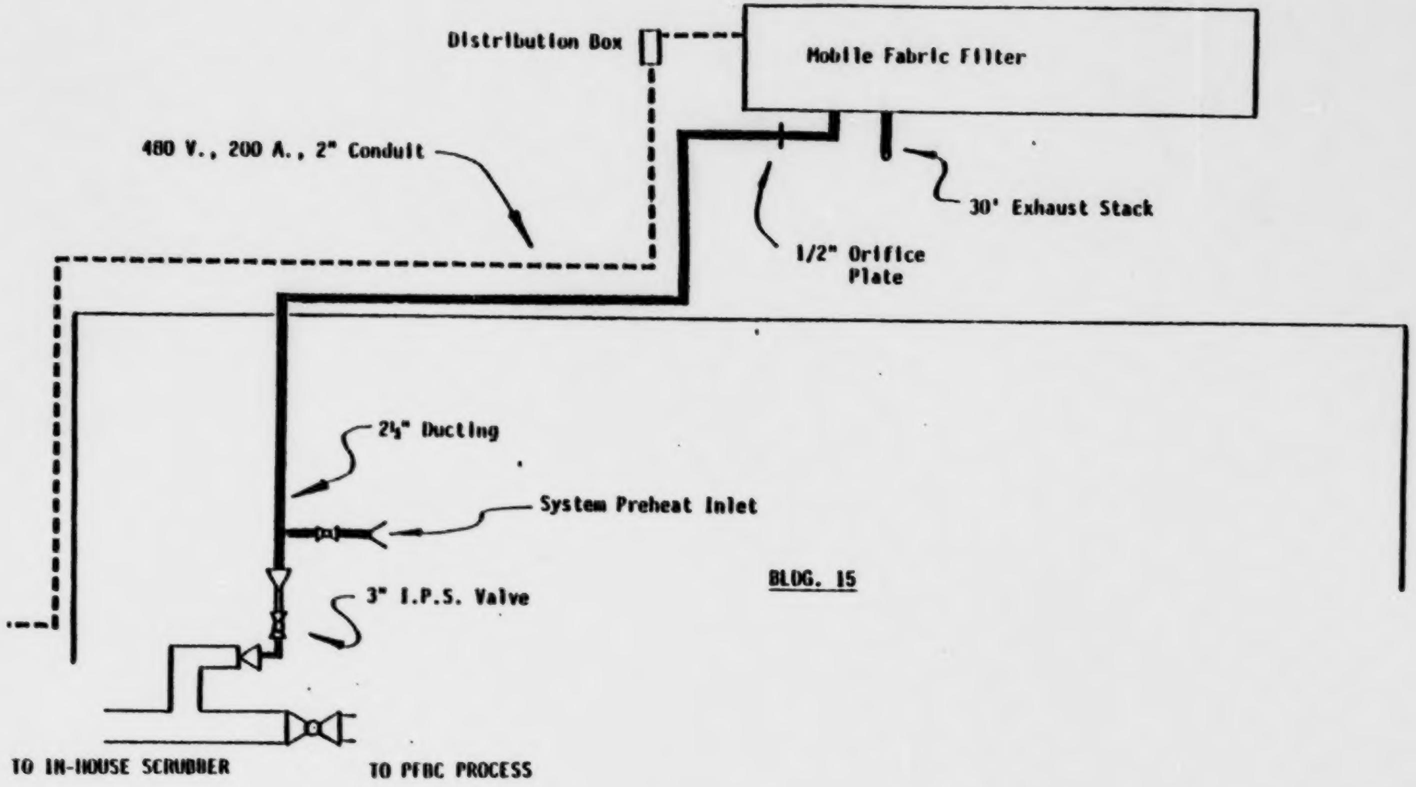
Distribution Box
Mobile Fabric Filter
480 V., 200 A., 2" Conduit
30' Exhaust Stack
1/2" Orifice Plate
2½" Ducting
System Preheat Inlet
BLDG. 15
3" I.P.S. Valve
TO IN-HOUSE SCRUBBER
TO PFBC PROCESS

Figure 5. Schematic of the mobile baghouse installation at the Exxon miniplant.

## TABLE 3. EXXON MINIPLANT OPERATING CONDITIONS

| | Miniplant run no. | | | | | |
|---|---|---|---|---|---|---|
| | 103 | 104 | 105 | 106 | 107 | 108 |
| ESP test no. | 1-9 | 10-13 | 14-17 | - | - | - |
| Baghouse test no. | - | - | - | 1-7 | 8-11 | 12-14 |
| Run time, days | 12 | 4 | 4 | 11 | 4.5 | 4 |
| Coal[a] | CH | CH | CH | ILL | CH | CH |
| Sorbent[b] | GR | PF | GR | PF | PF | PF |
| Regeneration run | Yes | No | Yes | No | No | No |
| Excess air, % | - | 42.1 | - | 5.8-15.6 | 31.4 | 23 |
| Superficial gas velocity, m/s | 1.3-1.4 | 1.62 | 1.5 | 1.62-1.71 | 1.31 | 1.31 |
| Pressure, kPa | 710 | 850 | 710 | 902-912 | 912 | 912 |
| Bed temperature, °C | 890-910 | 899 | 890-914 | 904-914 | 872 | 877 |
| Flue gas $SO_2$, ppm | 0-70 | 5-160 | 30-90 | 21-91 | 41.5 | 27.8 |
| Flue gas $O_2$, ppm | 3 | 3.8 | 3-4 | 1.1-3.1 | 5.1 | 4.0 |
| Dilution air, %[c] | 50 | 20 | 50 | 10-30 | 50-70 | 50-70 |

[a] CH =Champion coal; ILL = Illinois no. 6 coal.

[b] GR = Grove no. 1359 limestone; PF = Pfizer no. 1337 dolomite.

[c] Dilution air introduced downstream of the miniplant combustor for control of combustor pressure.

## Pilot ESP

The pilot ESP could handle the entire miniplant exhaust stream; therefore, the ESP flow rate was determined by the PFBC operating conditions. The butterfly valve at the ESP inlet was left fully open to avoid high back pressure in the inlet duct.

The mobile ESP was operated as a hot-side unit (340-370°C) during tests 6-9 (parts of miniplant run 103) and as a cold-side unit (170-200°C) during all other runs. These two temperature ranges were chosen to simulate hot- and cold-side ESP applications.

The inlet duct was designed to maintain an isothermal gas stream up to 370°C. Temperature changes were effected by adjusting the water flow rate through the heat exchanger and by injecting methane and oxygen into the FBC exhaust stream.

Water flow through the heat exchanger was reduced to raise gas temperature, but temperature control was difficult due to the high efficiency of the heat exchanger and the lack of precise control of cooling water flow rate. Temperature of the gas fluctuated between 340 and 410°C.

Miniplant process gas flow rate was expected to range from 16 to 20 $Nm^3$/min, but averaged 26-38 $Nm^3$/min due to dilution from an air supply used to control combustion pressure (see Table 3). Two separate orifices were made for the cold- and hot-side runs in an attempt to maintain a constant back pressure and flow rate with minimal dilution of the miniplant exhaust stream.

A full-scale ESP designed to reduce emissions from the levels in the Exxon PFBC cyclone exhaust to coal-fired utility boiler new source performance standard (NSPS) levels would probably require fewer cells than a conventional ESP (80 percent versus 98 plus percent design efficiency, respectively). Therefore, the pilot

ESP was operated with only three of its five cells (cells 2, 3, and 4) energized during all tests. No appreciable effect was anticipated from particulate fallout in cell 1 via mechanical settling due to the fineness of the inlet particle size distribution.

Pilot Baghouse

In contrast to the pilot ESP, the baghouse treated less than 10 percent of the miniplant's flue gas. This presented an operating problem due to positive static pressure in the slipstream. The mobile baghouse was designed for and previously operated in a negative static pressure mode, utilizing its own blower on the clean-gas side of the bag compartment.

The mobile baghouse was connected to the miniplant duct via an Exxon remotely operated pneumatic valve, which had to be fully open or closed. The initial startup indicated that the gas flow through the slipstream without the baghouse blower operating was roughly an order of magnitude greater than that desired for a face velocity of 0.61 m/s (2 ft/min). A series of successively smaller stops was installed on the Exxon valve to limit gas flow to the pilot baghouse. The final stop used limited the Exxon valve to an estimated 10 percent open position.

Problems related to this valve continued. After several days of operation, the valve appeared to be partially blocked, limiting gas flow. To solve this problem, the valve was scheduled to be opened and closed every 8 hours to clear any accumulated PM upstream of the valve. This solution, while satisfactory, did not last, because the valve ultimately failed in the open position and could not be repaired without shutting down the miniplant.

This problem was solved by installing an orifice in the slipstream line. The orifice was sized to limit gas flow to the desired level. The first orifice installed (1.4 cm in diameter) was too small and was replaced with a larger one (1.55 cm in diameter) that was satisfactory for the duration of the program.

Initial startup and subsequent operation of the mobile baghouse revealed a series of operational problems relating to both the mobile unit and the PFBC facility. Some of these problems were significant and severely affected the pilot baghouse program. Consequently, they are documented and presented chronologically in Appendix B.

Typical baghouse startup and operating procedures were originally employed and included a preheat procedure for the slipstream and baghouse to minimize acid dew-point condensation. After failure of the Exxon valve on the slipstream and installation of the orifice for flow control, the normal baghouse preheat procedure could not be implemented. Startup was accomplished by by-passing the bag compartment for sufficient time to preheat the slipstream and internal baghouse ducting. At the same time, the baghouse compartment electricial strip heaters were energized to preheat that chamber as much as possible before the introduction of flue gas.

## TEST CONDITIONS

The limited availability of both the EPA mobile control facilities and the Exxon miniplant prevented a comprehensive evaluation of control device performance over a range of PFBC operating conditions during this test program.

The mobile ESP was operated in both hot- and cold-side modes over an SCA range of 26.2-37.4 $m^2/m^3/s$.

The mobile baghouse was operated in one constant mode throughout the test schedule. Silicone-graphite coated fiberglass bags were employed with shake cleaning. Manufacturers' specifications for the glass bags and the cleaning parameters employed are presented in Tables 4 and 5, respectively.

## TABLE 4. SPECIFICATIONS FOR W. W. CRISWELL WOVEN GLASS BAGS

(Style 445-04)

| | |
|---|---|
| Fabric | woven glass |
| Weight, oz/yd$^2$ | 10.5 |
| Weave | 3 x 1 twill (right hand) |
| Thread count | 65 x 33 |
| Permeability, cfm/ft$^2$ at 0.5 in $H_2O$ | 45-65 |
| Finish | silicone and graphite, 1% by weight total |
| Warp yarn | 150 1/2 |
| Fill yarn | 37/S textured |

## TABLE 5. SHAKE-CLEANING PARAMETERS

| | |
|---|---|
| Amplitude | 0.95 cm (0.375 in) |
| Frequency | 6.4 cps |
| First delay | 30 s |
| Shake duration | 10 s |
| Final delay | 60 s |
| Acceleration | 1.56 g (15.2 m/s$^2$) |
| Bag tension | 6.8 kg (15 lb) |

## DATA ACQUISITION

Mass and particle size distribution sampling required long outlet sampling times due to the low inlet grain loading. Outlet mass and impactor sample durations were generally 10-12 and 18-20 hours for the ESP and baghouse, respectively. Pertinent operating data were logged semi-hourly and evaluated on a daily basis, along with results of the particulate sampling, to ensure data quality and provide feedback for quality assurance and test plan evaluation.

Specific data logged for the mobile ESP included:

- inlet/outlet gas temperatures
- individual field voltages
- individual field currents

Specific data logged for the mobile baghouse included:

- pressure drop across the bags, continuously recorded
- system flow, continuously recorded
- static pressure profile across the system
- temperature profile across the system
- cleaning cycle parameters (terminal pressure drop and flow, residual pressure drop and flow, and number of shakes)

### Particulate Measurements

Brink and Andersen impactors were used to measure size distribution at the baghouse inlet and outlet, respectively. Brink and University of Washington impactors were used for the ESP inlet and outlet size distributions. Total mass and impactor measurements were conducted isokinetically at the pilot facilities' inlet and outlet sampling points, with the exception of the ESP Brink sampler, which had to be run at subisokinetic conditions.

Reeve Angel 934AH glass-fiber substrates were employed for all samples. All substrates were preconditioned for 12-20 hours, dependent on sample time for the respective pilot units, by exposing them to PFBC process gas at the pilot facility outlet sampling point.

All samples were obtained with extractive probes fitted with interchangeable nozzles at average velocity locations. Sampling trains were similar to those of EPA Method 5 (FEDERAL REGISTER, Volume 42, Number 160).

There were considerable difficulties with the mobile baghouse outlet sampling due to contamination of the samples with foreign debris. The contamination was apparently due to corrosion and/or condensation experienced on an intermittent basis. A significant part of the outlet sampling effort was affected and had to be disregarded during data reduction and analysis.

## Resistivity Measurements

A point-to-plane type of probe capable of operating at 370°C was used for making *in-situ* resistivity measurements. Maintenance and operation were conducted in accordance with procedures outlined in Reference 6. The measurements were performed in the reduced velocity (3-5 m/s) area immediately upstream from the first field of the mobile ESP. The low inlet grain loading, combined with the low flow rate through the probe, dictated sampling periods of about 20 hours. This reduced the amount of data but improved its quality due to averaging effects.

Resistivity values were calculated from the available test data by two different methods: the spark method and the V-I method. All resistivity values were calculated as the ratio of electric field to current density. A complete discussion of the equipment, procedure, and significance of resistivity measurements is contained in Reference 6.

## DATA REDUCTION

The impactor and mass data generated during the two test programs offered a substantial analytic task. Rapid and statistically reliable methods were needed to reduce the data and maintain consistency in the analytic procedure. This was accomplished through the use of three different computer programming stages. The computations were aided and supplemented by manual graphic procedures, algorithms, and engineering judgment as necessary. The analytic technique is described in greater detail below.

The first computation step involved calculation of impactor stage cutpoints, PM size distributions, and overall PM loading for inlet and outlet impactors. Impactor calibration constants developed by Southern Research Institute[7] (SRI) were used to calculate impactor stage cutpoints. Mass loadings were calculated using the standard algorithm described in EPA Method 5. Mass concentration and size distribution data showed normal scatter. Engineering judgment dictated abortion of apparent fluke runs.

The objective of the second computation step was to obtain inlet and outlet differential size distributions and fractional penetrations. This was accomplished using the program described in Reference 8, which performs linear least square, quadratic least square and spline fits to log-normal transformed inlet and outlet cumulative size distribution data. Differential size distributions and fractional penetrations are then calculated by the program through analytical differentiation.

Mathematical performance modeling for each control device constituted the third computation stage. EPA's primary objective in generating performance models for an ESP, baghouse, and venturi scrubber is to develop control device performance predictive capability that can be used as a design tool. The ESP and baghouse models were exercised to evaluate and compare their performance in controlling emissions from the PFBC process. The venturi scrubber model was exercised to obtain an estimate of pressure drop requirements for PFBC emission control. The three performance models are described in greater detail below.

## ESP Performance Modeling

The computer program for the EPA/SRI ESP performance model, as described in Reference 9, was used to predict ESP operation and performance characteristics.

The ESP model offers a range of input options, depending upon the number of empirical parameters available for performance prediction and the desired accuracy level. Typically, the input included the following information:

- flue gas characteristics: flow rate, temperature, pressure, viscosity, PM concentration, particle size distribution histogram, and fly ash resistivity;
- pilot ESP design specifications: cell-plate and wire geometry, size of cell plate area, and number of baffles;
- empirical cell voltage-current characteristics and collection efficiency;
- one ideal and two nonideal gas velocity distributions; and
- programming instructions to minimize computation cost for the first modeling iteration.

## Baghouse Performance Modeling

The EPA/GCA fabric filter performance model for coal fly ash with glass fabrics[10] was used to predict baghouse operation and performance characteristics. The following input parameters were estimated, based on performance of the mobile baghouse at the Exxon miniplant:

- effective residual drag, $S_E$

- specific resistance coefficient, $K_2$
- residual fabric loading, $W_R$
- fractional area cleaned, $A_C$

The baghouse performance model predicts operating pressure drop and penetration as a function of cleaning cycle number, and determines the magnitude of these parameters at equilibrium conditions.

### Scrubber Performance Modeling

The computer program for the EPA/A.P.T., Inc., venturi scrubber performance model described in Reference 11 was used to predict the scrubber pressure drop requirement for control of PFBC emissions.

The model input requirements include seven parameters to define scrubber design and operating conditions and appropriate description of the influent PM stream. With these specifications, the model:

- determines droplet size formation
- determines pressure drop across the venturi section
- determines the fractional penetration relationship
- relates the influent size distribution with the fractional penetration
- integrates the influent distribution/fractional penetration relationship to determine the effluent PM concentration

# SECTION 6

# RESULTS AND DISCUSSION

## PILOT ESP PERFORMANCE

A summary of the pilot ESP operating conditions is presented in Table 6. Tables 7 and 8 list the operating voltages and current densities for the mobile ESP, which are given for each cell, then averaged for each test. There were changes in these values within each of the four test conditions.

Tests 1-5 (run 103, low temperature) showed no changes in voltages and currents with time. Voltages and currents were inexplicably spark-limited during test 3 but returned to normal afterward.

Voltages were reduced but fairly steady and currents dropped with time during tests 6-9 (run 103, high temperature).

Voltages began slightly higher but decreased slightly with time during tests 10-13 (run 104). Currents were much lower and cotinued to decline with time. The electrical data for test 12 was unusual. Current dropped markedly on cell 2 and increased on cells 3 and 4 for a 24-hour period. All voltages dropped during this time. Electrical characteristics returned to normal afterward, with current continuing to decrease with time.

Voltage and current values rose initially, but voltage dropped with time and currents increased substantially during tests 14-17.

Apparently a change in test conditions (temperature, $SO_x$ concentration, or bed material) caused an initial change in both voltage and current levels. The change in current density continued in the initial direction. A change from low temperature to high temperature with limestone steadily reduced voltage and current values after an initial decrease. Changing to dolomite

## TABLE 6. PILOT ESP OPERATING CONDITIONS

| Exxon PFBC run no. | Acurex test no. | 1979 date | Sample time | Inlet temp., $^oC$ | Flow, $am^3/min$ |  |  | SCA $m^2/m^3/s$ | Flow, $Nm^3/min$ |  | Run average |  |
|---|---|---|---|---|---|---|---|---|---|---|---|---|
|  |  |  |  |  | Inlet | Outlet | Average |  | Inlet | Outlet | Inlet temp., $^oC$ | SCA, $m^2/m^3/s$ |
| 103 | 1 | 3/29 | 1800 | 177 | 47.3 | 44.1 | 45.7 | 35.1 | 31.5 | 26.3 | 184 | 31.8 |
| 103 | 2 | 3/30 | 1100 | 171 | 51.4 | 50.5 | 50.9 | 31.6 | 32.4 | 31.8 | 184 | 31.8 |
| 103 | 3 | 3/31 | 1230 | 164 | 54.5 | 50.0 | 52.2 | 30.8 | 33.8 | 33.9 | 184 | 31.8 |
| 103 | 4 | 4/1 | 930 | 176 | 51.7 | 53.5 | 52.6 | 30.6 | 32.2 | 32.7 | 184 | 31.8 |
| 103 | 5 | 4/2 | 1800 | 232 | 52.4 | 52.0 | 52.2 | 30.8 | 31.9 | 31.5 | 184 | 31.8 |
| 103 | 6 | 4/3 | 1400 | 358 | 58.3 | 50.4 | 54.4 | 29.5 | 25.9 | 27.4 | 354 | 26.6 |
| 103 | 7 | 4/4 | 1600 | 371 | 60.0 | 62.9 | 61.5 | 26.1 | 27.0 | 28.9 | 354 | 26.6 |
| 103 | 8 | 4/5 | 1200 | 338 | 63.7 | 61.9 | 62.8 | 25.6 | 28.8 | 32.5 | 354 | 26.6 |
| 103 | 9 | 4/6 | 1600 | 348 | 65.0 | 63.4 | 64.2 | 25.0 | 29.1 | 29.5 | 354 | 26.6 |
| 104 | 10 | 4/17 | 1600 | 209 | 38.2 | 46.4 | 42.3 | 38.0 | 22.0 | 31.7 | 210 | 36.2 |
| 104 | 11 | 4/18 | 1200 | 201 | 42.7 | 45.1 | 43.9 | 36.6 | 24.1 | 30.3 | 210 | 36.2 |
| 104 | 12 | 4/19 | 930 | 209 | 46.5 | 46.6 | 46.6 | 34.5 | 26.4 | 31.6 | 210 | 36.2 |
| 104 | 13 | 4/20 | 930 | 221 | 42.3 | 48.3 | 45.3 | 35.5 | 22.8 | 32.2 | 210 | 36.2 |

(continued)

TABLE 6. (Continued)

| Exxon PFBC run no. | Acurex test no. | 1979 date | Sample time | Inlet temp., $^{\circ}C$ | Flow, $am^3/min$ |  |  | SCA, $m^2/m^3/s$ | Flow, $Nm^3/min$ |  | Run average |  |
|---|---|---|---|---|---|---|---|---|---|---|---|---|
|  |  |  |  |  | Inlet | Outlet | Average |  | Inlet | Outlet | Inlet temp., $^{\circ}C$ | SCA, $m^2/m^3/s$ |
| 105 | 14 | 5/1 | 1500 | 167 | 40.0 | 43.8 | 41.9 | 38.4 | 25.1 | 31.6 | 195 | 37.4 |
| 105 | 15 | 5/2 | 1130 | 208 | 39.8 | 46.5 | 43.3 | 37.1 | 23.7 | 32.8 | 195 | 37.4 |
| 105 | 16 | 5/3 | 1200 | 205 | 41.1 | 45.6 | 43.4 | 37.0 | 24.1 | 27.8 | 195 | 37.4 |
| 105 | 17 | 5/4 | 1200 | 198 | 41.5 | 45.6 | 43.5 | 36.9 | 24.2 | 31.3 | 195 | 37.4 |

## TABLE 7. PILOT ESP ELECTRICAL CHARACTERISTICS

| Exxon PFBC run no. | Acurex test no. | 1979 date | Outlet sampling times |  |  | Temp., °C | Cell[a] voltages, kV |  |  |  | Cell current densities, nA/$cm^2$ |  |  |  |
|---|---|---|---|---|---|---|---|---|---|---|---|---|---|---|
|  |  |  | Start | Stop | Duration, min |  | #1 | #2 | #3 | Avg. | #1 | #2 | #3 | Avg. |
| 103 | 1 | 3/29 | 1845 | 2445 | 360 | 177 | 31.8 | 33.5 | 34.4 | 33.2 | 37.1 | 45.6 | 50.3 | 44.3 |
| 103 | 2 | 3/30 | 1140 | 2340 | 720 | 171 | 36.8 | 34.0 | 36.5 | 35.8 | 39.1 | 47.1 | 46.4 | 44.2 |
| 103 | 3 | 3/31 | 1345 | 2330 | 585 | 164 | 19.4 | 20.9 | 23.5 | 21.3 | 15.2 | 17.2 | 19.4 | 17.3 |
| 103 | 4 | 4/1 | 1010 | 2210 | 720 | 176 | 34.4 | 34.5 | 34.8 | 34.6 | 18.5 | 61.8 | 53.6 | 44.6 |
| 103 | 5 | 4/2 | 1830 | 2230 | 240 | 232 | 37.0 | 34.0 | 38.0 | 36.3 | 32.5 | 44.8 | 53.8 | 43.7 |
| 103 | 6 | 4/3 | 1450 | 2150 | 420 | 358 | 26.0 | 22.4 | 26.5 | 25.0 | 24.0 | 50.2 | 46.1 | 40.1 |
| 103 | 7 | 4/4 | 1645 | 2345 | 420 | 371 | 22.9 | 22.6 | 21.9 | 22.5 | 13.1 | 18.9 | 60.5 | 30.8 |
| 103 | 8 | 4/5 | 1235 | 2220 | 585 | 338 | 26.2 | 29.0 | 26.1 | 27.1 | 14.6 | 36.6 | 28.1 | 26.4 |
| 103 | 9 | 4/6 | 1640 | 2100 | 260 | 348 | 27.0 | 26.0 | 27.0 | 26.7 | 7.8 | 24.6 | 14.4 | 15.6 |
| 104 | 10 | 4/17 | 1635 | 2300 | 385 | 209 | 32.7 | 31.1 | 30.6 | 31.5 | 6.2 | 7.0 | 12.3 | 8.5 |
| 104 | 11 | 4/18 | 1300 | 2300 | 600 | 201 | 31.8 | 28.3 | 21.8 | 30.6 | 2.4 | 4.2 | 11.1 | 5.9 |
| 104 | 12 | 4/19 | 1015 | 2450 | 855 | 209 | 26.1 | 23.9 | 24.5 | 24.8 | 0.2 | 33.0 | 30.6 | 21.3 |
| 104 | 13 | 4/20 | 1010 | 2210 | 600 | 221 | 26.9 | 31.4 | 31.5 | 29.9 | 0.9 | 3.4 | 9.9 | 4.7 |

(continued)

TABLE 7. (Continued)

| Exxon PFBC run no. | Acurex test no. | 1979 date | Outlet sampling times |  |  | Temp., $^{o}C$ | Cell[a] voltages, kV |  |  |  | Cell current densities, $nA/cm^2$ |  |  |  |
|---|---|---|---|---|---|---|---|---|---|---|---|---|---|---|
|  |  |  | Start | Stop | Duration, min |  | #1 | #2 | #3 | Avg. | #1 | #2 | #3 | Avg. |
| 105 | 14 | 5/1 | 1525 | 2325 | 480 | 167 | 35.0 | 37.0 | 37.5 | 36.5 | 7.1 | 11.7 | 18.2 | 12.3 |
| 105 | 15 | 5/2 | 1217 | 2317 | 660 | 208 | 33.6 | 33.4 | 32.0 | 33.0 | 11.8 | 39.2 | 20.5 | 23.8 |
| 105 | 16 | 5/3 | 1240 | 2300 | 620 | 205 | 27.5 | 29.1 | 27.1 | 27.9 | 40.6 | 40.6 | 47.8 | 43.0 |
| 105 | 17 | 5/4 | 1230 | 2130 | 540 | 198 | 24.2 | 26.0 | 37.0 | 29.1 | 76.2 | 50.4 | 48.2 | 58.3 |

[a] Cell numbers 1, 2 and 3 correspond with cells 2, 3 and 4, respectively, in the EPA mobile ESP.

## TABLE 8. PILOT ESP AVERAGE V-I CHARACTERISTICS

| Exxon PFBC run no. | Average inlet temp., °C | Cell voltages,[a] kV | | | | Cell current densities, nA/cm$^2$ | | | |
|---|---|---|---|---|---|---|---|---|---|
| | | #1 | #2 | #3 | Avg. | #1 | #2 | #3 | Avg. |
| 103 | 184 | 35.0 | 34.0 | 35.9 | 35.0 | 28.5 | 43.3 | 44.7 | 41.0 |
| 103 | 354 | 25.5 | 25.0 | 25.4 | 25.3 | 14.9 | 32.6 | 37.3 | 28.3 |
| 104 | 210 | 29.4 | 28.8 | 29.6 | 29.3 | 4.3 | 11.9 | 15.9 | 10.7 |
| 105 | 195 | 30.1 | 31.4 | 33.4 | 31.6 | 33.9 | 35.5 | 33.7 | 34.4 |

[a] Cell numbers 1, 2 and 3 correspond with cells 2, 3 and 4, respectively, in the EPA mobile ESP.

and lower temperature initially increased the voltage slightly and decreased the current, but both parameters gradually decreased afterward. A return to limestone caused voltages and currents to increase initially. Voltages decreased with time, but currents rapidly increased.

The overall average voltages and current densities for each cell are shown in Table 8 for each PFBC run. Here the effects of hot-side operation are depressed values for both cell voltage and current density. Also, the current density is considerably lower during the PFBC run 104 with no regeneration and dolomite sorbent.

## Resistivity Measurements

Table 9 summarizes all of the in-situ resistivity test results. Nearly all values were in the range of $10^{11}$ Ω-cm, so no correlation could be made between resistivity and the changes in ESP electrical parameters. The field resistivity data were reviewed in depth, and electric breakdown strenghts were calculated, then divided by the respective resistivities to obtain current densities in the resistivity probe at breakdown. The purpose of this exercise was to correlate current densities in the probe with those in the precipitator fields. However, the probe values often exceeded the field values by factors of 10-15, and correlation was poor. None of the effects of process stream changes (temperature and bed material) on voltage and current density could be linked to changes in dust resistivity.

Figures 6, 7, and 8 show representative V-I curves for Acurex tests 2, 8, and 14, respectively.

The laboratory resistivity values of ESP ash samples (determined by SRI) are presented in Figure 9.

## TABLE 9. IN-SITU RESISTIVITY DATA

| Acurex test no. | Exxon PFBC run no. | Start time | Duration, hr | Temperature, $^{o}C$ | Resistivity, $\Omega$-cm | |
|---|---|---|---|---|---|---|
| | | | | | Spark | V-I |
| 6,7 | 103 | 1345 | 47 | 343 | $4.9 \times 10^{11}$ | $3.1 \times 10^{11}$ |
| 8 | 103 | 1430 | 21 | 330 | $1.7 \times 10^{11}$ | $2.5 \times 10^{10}$ |
| Average | | | | 337 | $1.6 \times 10^{11}$ | |
| 10 | 104 | 1405 | 21 | 186 | $9.8 \times 10^{11}$ | - |
| 11 | 104 | 1200 | 24 | 217 | $2.7 \times 10^{9}$[a] | - |
| 12 | 104 | 1600 | 22 | 210 | $3.2 \times 10^{11}$ | $1.1 \times 10^{11}$ |
| 14 | 105 | 1545 | 23 | 166 | $2.1 \times 10^{11}$ | $1.3 \times 10^{11}$ |
| 15 | 105 | 1545 | 24 | 188 | $6.5 \times 10^{10}$ | $6.3 \times 10^{11}$ |
| Average | | | | 193 | $2.3 \times 10^{11}$ | |

[a] Not included in the average.

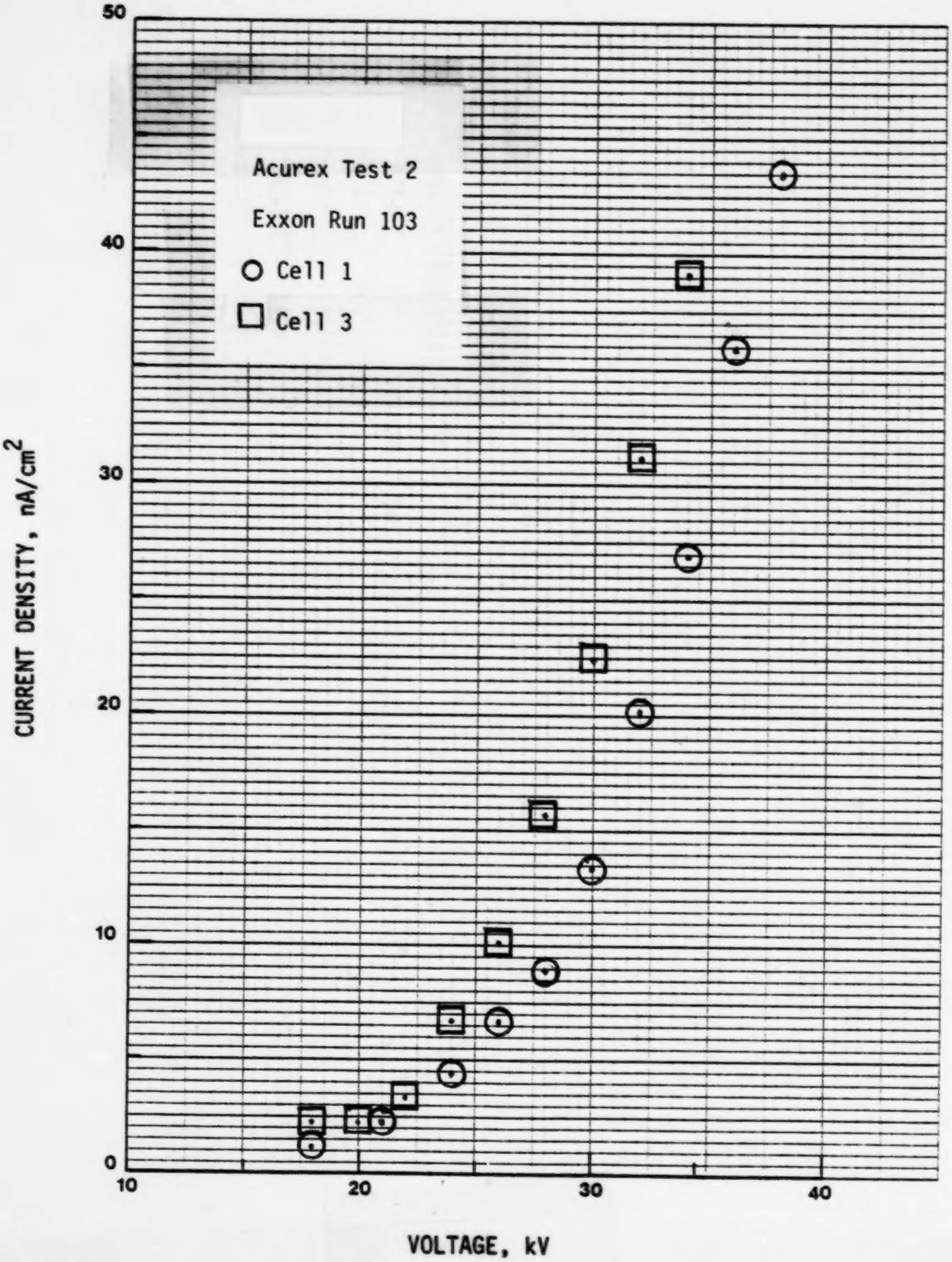

Figure 6. Representative ESP V-I curve for miniplant run 103.

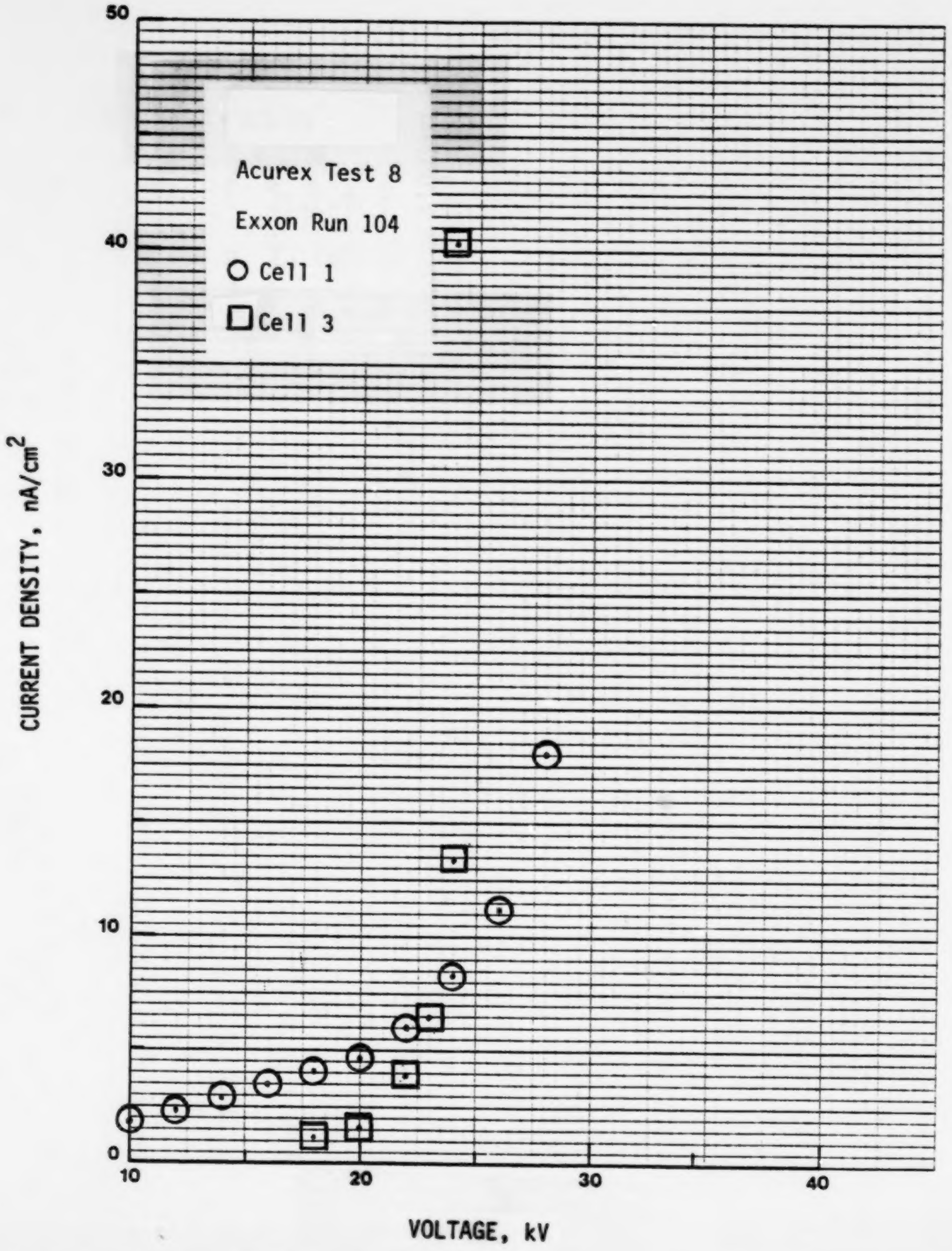

Figure 7. Representative ESP V-I curve for miniplant run 104.

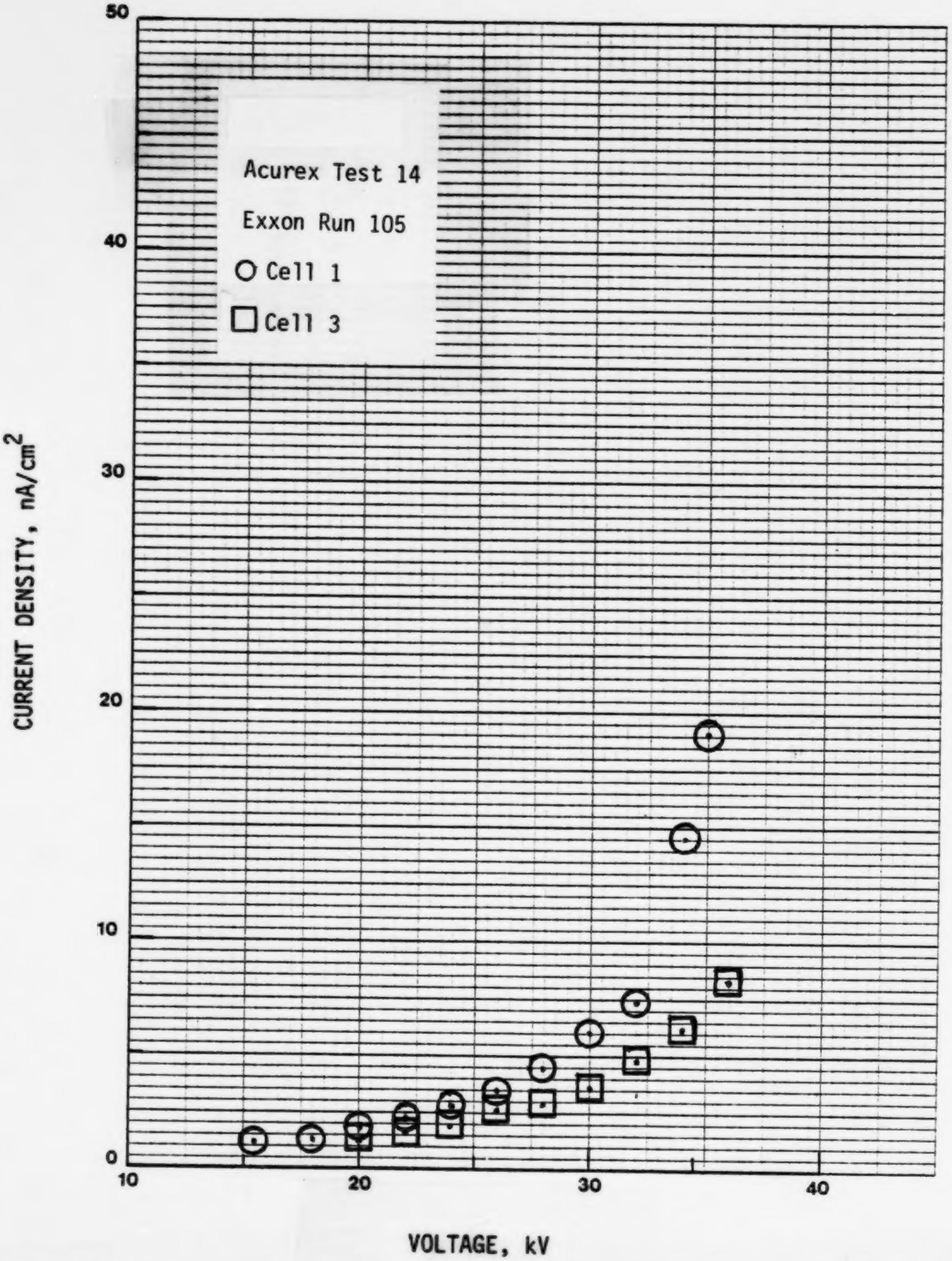

Figure 8. Representative ESP V-I curve for miniplant run 105.

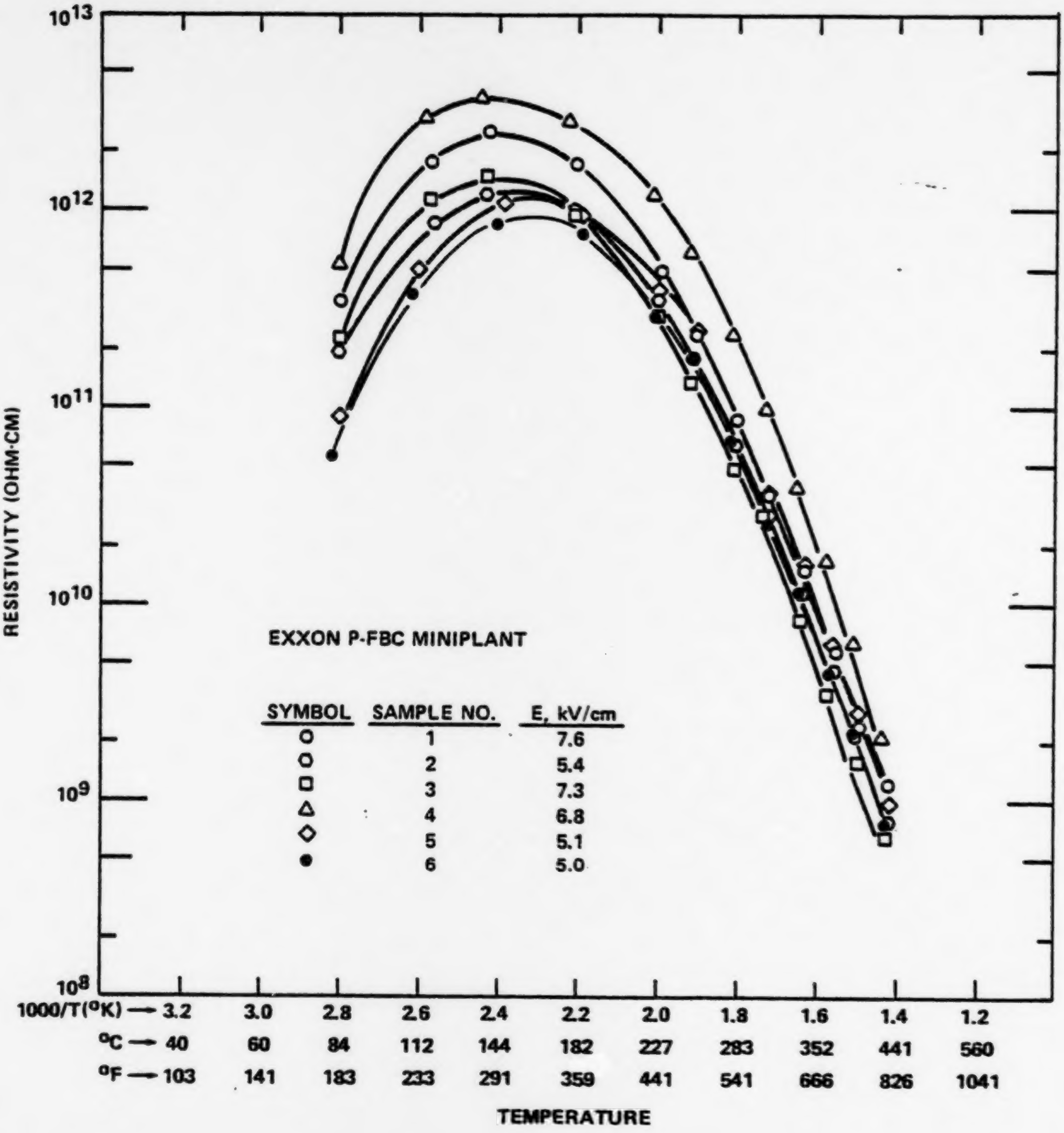

Figure 9. Laboratory resistivity for ash samples from pilot ESP.

Table 10 shows a chemical analysis of fly ash samples from the ESP. The first four samples were obtained from the wires and plates of the inlet and outlet cells. An average of these values was used to compare these samples with the two subsequent hopper samples. The ash analysis gives no clues to explain the poor precipitability of emissions from a dolomite bed. Sample no. 5 does show a slightly lower sodium and higher silica content than the others, but there is not enough difference in the values to explain the sharp drop in cell current densities.

## Mass Efficiency

The ESP inlet and outlet grain loadings for mass and impactor sampling are shown in Table 11, along with average values for each miniplant run. Acurex tests 6-9 correspond to the operation of the pilot ESP in a hot-side mode. All other tests are for cold-site operation.

Table 12 presents a summary of ESP performance parameters, listed by process stream condition. Inlet mass loading was approximately 0.11 g/Nm$^3$ in all runs, except run 104 in which a lower inlet loading (0.09 g/Nm$^3$) apparently resulted from a difference in miniplant operating conditions.

The change from low to high temperature in the ESP resulted in a 7 percent decrease in outlet grain loading, although the SCA fo the ESP was reduced by 16 percent. Thus, an increase in ESP performance was experienced at high temperature and constant SCA. However, cold-side ESP performance was better than hot-side performance on a normalized gas treatment basis. Hence, the gain in efficiency at higher temperature and constant SCA is not substantial enough to translate into an economic advantage.

Most of the test conditions of run 104 favored high efficiency. The SCA was 14 percent higher than it was with limestone at the same temperature.

## TABLE 10. CHEMICAL ANALYSIS OF ESP ASH SAMPLES (weight percent as oxides)

| Sample[a] no.: | 1 | 2 | 3 | 4 |  | 5 | 6 |
|---|---|---|---|---|---|---|---|
| Exxon PFBC run no.: | 103 | 103 | 103 | 103 | 103 | 104 | 105 |
| Acurex test no.: | 1 | 2 | 3 | 4 | avg. | 5 | 6 |
| Sample locations: | Cell #1 plate | Cell #1 wire | Cell #3 plate | Cell #3 wire | 2 avg. ESP | ESP hopper | ESP hopper |
| 1979 date: | 3/30 | 3/30 | 3/30 | 3/30 | 3/30 | 4/20 | 5/4 |
| $Li_2O$ | 0.04 | 0.04 | 0.04 | 0.04 | 0.04 | 0.04 | 0.04 |
| $Na_2O$ | 0.58 | 0.54 | 0.85 | 0.87 | 0.71 | 0.63 | 0.73 |
| $K_2O$ | 1.5 | 1.3 | 1.4 | 1.5 | 1.4 | 1.3 | 1.4 |
| MgO | 2.5 | 3.2 | 2.3 | 1.8 | 2.5 | 2.7 | 1.3 |
| CaO | 12.8 | 12.9 | 12.7 | 12.3 | 12.7 | 12.0 | 13.2 |
| $Fe_2O_3$ | 10.3 | 10.9 | 11.6 | 11.7 | 11.1 | 13.8 | 15.6 |
| $Al_2O_3$ | 22.4 | 22.3 | 22.1 | 22.7 | 22.4 | 22.3 | 20.6 |
| $SiO_2$ | 30.8 | 31.1 | 29.6 | 30.7 | 30.6 | 32.2 | 30.7 |
| $TiO_2$ | 1.8 | 1.8 | 1.8 | 1.9 | 1.8 | 1.6 | 1.6 |
| $P_2O_5$ | 0.6 | 0.5 | 0.6 | 0.7 | 0.6 | 0.5 | 0.6 |
| $SO_3$ | 12.9 | 13.6 | 16.2 | 9.6 | 13.1 | 11.6 | 10.4 |
| Total | 96.2 | 98.2 | 99.2 | 93.8 | 96.9 | 98.7 | 96.2 |
| LOI | 2.5 | 2.2 | 3.0 | 1.8 | 2.4 | 3.5 | 3.6 |

[a] All analyses were conducted on ignited samples.

TABLE 11. PILOT ESP INLET AND OUTLET LOADINGS, g/Nm$^3$

| Exxon PFBC run no. | 1979 date | Acurex test no. | Inlet | | | | Outlet | |
|---|---|---|---|---|---|---|---|---|
| | | | Impactor | | Mass | | | |
| | | | A | B | A | B | Impactor | Mass |
| 103 | 3/29 | 1 | - | - | - | - | 0.016 | 0.013 |
| | 3/30 | 2 | 0.068 | - | 0.158 | - | 0.006[a] | 0.004[a] |
| | 3/31 | 3 | 0.024 | 0.060 | 0.048 | 0.121 | 0.017 | 0.018 |
| | 4/1 | 4 | 0.048 | 0.132 | 0.104 | 0.156 | 0.007 | 0.012 |
| | 4/2 | 5 | - | - | - | - | 0.041[a] | 0.038[a] |
| Average | | | 0.066 | | 0.117 | | 0.013 | 0.014 |
| 103 | 4/3 | 6 | 0.060 | - | 0.046 | - | - | 0.025[a] |
| | 4/4 | 7 | 0.011[a] | - | 0.060 | - | 0.011 | 0.016 |
| | 4/5 | 8 | 0.015[a] | 0.093 | 0.157 | 0.580[a] | 0.015 | 0.010 |
| | 4/6 | 9 | 0.054 | 0.064 | 0.156 | 0.137 | 0.086[a] | 0.042[a] |
| Average | | | 0.068 | | 0.111 | | 0.013 | 0.013 |

See footnote at the end of the table, page 41.

(continued)

## TABLE 11. (Continued)

| Exxon PFBC run no. | 1979 date | Acurex test no. | Inlet |  |  |  | Outlet |  |
|---|---|---|---|---|---|---|---|---|
|  |  |  | Impactor |  | Mass |  |  |  |
|  |  |  | A | B | A | B | Impactor | Mass |
| 104 | 4/17 | 10 | 0.061 | 0.044 | 0.177 | 0.049 | 0.020 | 0.019 |
|  | 4/18 | 11 | 0.176[a] | 0.012[a] | 0.006[a] | 0.075 | 0.015 | 0.018 |
|  | 4/19 | 12 | 0.079 | 0.094 | 0.011[a] | 0.017[a] | 0.008 | - |
|  | 4/20 | 13 | 0.039 | 0.057 | 0.081 | 0.074 | 0.027[a] | 0.003[a] |
| Average |  |  | 0.062 |  | 0.091 |  | 0.014 | 0.019 |
| 105 | 5/1 | 14 | 0.080 | 0.091 | 0.041 | 0.084 | 0.007 | 0.016 |
|  | 5/2 | 15 | 0.114 | 0.054 | 0.107 | 0.176 | 0.015 | 0.004 |
|  | 5/3 | 16 | 0.039 | 0.516[a] | 0.130 | 0.134 | 0.008 | 0.006 |
|  | 5/4 | 17 | 0.012[a] | 0.035[a] | 0.024[a] | - | 0.070[a] | 0.017 |
| Average |  |  | 0.076 |  | 0.112 |  | 0.010 | 0.011 |

[a] Runs aborted due to process fluctuations and/or measurement errors.

### TABLE 12. SUMMARY OF AVERAGE ESP PERFORMANCE

| Exxon PFBC run no. | Average inlet temp., $^oC$ | Average inlet loading, $g/Nm^3$ |  | Average outlet loading, $g/Nm^3$ |  | Efficiency, % |  | SCA, $m^2/m^3/s$ | Emissions[a] ng/J |
|---|---|---|---|---|---|---|---|---|---|
|  |  | Impactor | Mass | Impactor | Mass | Impactor | Mass |  |  |
| 103 | Cold, 184 | 0.066 | 0.117 | 0.013 | 0.014 | 80.3 | 88.0 | 31.8 | 10.8 |
| 103 | Hot, 354 | 0.068 | 0.111 | 0.013 | 0.013 | 80.8 | 88.3 | 26.6 | 9.8 |
| 104 | 210 | 0.062 | 0.091 | 0.014 | 0.019 | 77.4 | 79.1 | 36.2 | 12.4 |
| 105 | 195 | 0.076 | 0.112 | 0.010 | 0.011 | 86.8 | 90.2 | 37.4 | 7.6 |

[a] Based on mass data.

Inlet loadings were down by over 20 percent. However, mass efficiency dropped from 90 percent to 80 percent and outlet loadings increased by 35 percent. Current densities were sharply reduced in the first two cells, suggesting an increase in resistivity or a decrease in breakdown strength of the dust layer. Neither effect was apparent in the resistivity data.

A return to limestone bed material in run 105 resulted in both higher inlet loadings and higher mass efficiencies. Current densities increased rapidly during the run. The SCA was nearly identical to that of run 104, but outlet mass emissions were reduced by almost 40 percent.

The use of dolomite in the PFBC apparently suppresses current densities and reduces ESP performance to the point where emissions from the ESP are greatly increased despite a reduction in inlet loading.

## Particle Size Measurements

The ESP inlet particle size measurements were accomplished at subisokinetic extraction velocity due to high flue gas volcity and practical constraints on the Brink impactor flow rate and nozzle size.

The recommended upper limit for Brink sampling flow rate is 1.42 liter/m. Nozzle clogging problems preclude the use of nozzles less than 2.5 mm in diameter. Thus, the maximum extraction velocity can be 4.8 m/s, which is about one-third of the 16.5 m/s duct velocities encountered at Linden.

Anisokinetic sampling does not appreciably affect concentration measurement for particles less than about 1 μm size, but substantially affects collection of larger particles. Subisokinetic sampling results in a higher measured concentration of larger particles, while superisokinetic sampling results in lower measurement. Reference 12 describes the quantitative effect of anisokinetic sampling on particulate measurement.

The Brink inlet measurements were adjusted for subisokinesis, using the following equations.

$$\frac{C}{Co} = \quad 1 + \frac{Uo}{U} - 1 \qquad 1 - \frac{1}{1-0.3\ P\ln(1-\rho)}$$

where $P = \frac{2a^2\sigma Uo}{9\ \eta\ P}$

and where $\rho$ = orifice radius, cm

$a$ = particle radius, cm

$Uo$ = duct velocity, cm/s

$\eta$ = viscosity, g/cm·s

$\sigma$ = particle density, g/cc

$U$ = extraction velocity, cm/s

$C$ = measured concentration

$Co$ = true concentration

for, $\rho$ = 0.125 μm $\quad$ $a$ = $0.5 \times 10^{-4}$ cm (1 μm dia.)

$\sigma$ = 2.6 g/cc $\quad$ $Uo$ = 1650 cm/s

$\eta$ = 0.00022 g/cm·s $\quad$ $\frac{U}{Uo}$ = 3.44

$$P = \frac{2 \times (0.5 \times 10^{-4})^2 \times 2.6 \times 1652}{9 \times 0.00022 \times 0.125} = 0.0868$$

From this, the following values for C/Co, with respect to particle diameter, were generated:

| Dia., μm | C/Co |
|---|---|
| 1.0 | 1.006 |
| 1.5 | 1.014 |
| 2.0 | 1.024 |
| 3.0 | 1.054 |
| 5.0 | 1.114 |
| 7.0 | 1.260 |
| 10.0 | 1.471 |
| 50.0 | 2.748 |

These values were then applied to the inlet cumulative and differential size distributions to adjust for subisokinesis.

The ESP average inlet cumulative size distribution curves for runs 103, 104, and 105 are shown in Figure 10 with and without the probe wash fraction.

Figures 11-13 depict the ESP average inlet differential size distribution curves, with both spline and least square fit, for runs 103, 104, and 105, respectively. Due to the limited number of inlet Brink samples available for each miniplant run, it was not possible to statistically relate differences in inlet particle size distribution between the respective runs to miniplant operating conditions (e.g., coal or sorbent type, with or without regeneration). Individual inlet differential size distribution curves are included in Appendix C.

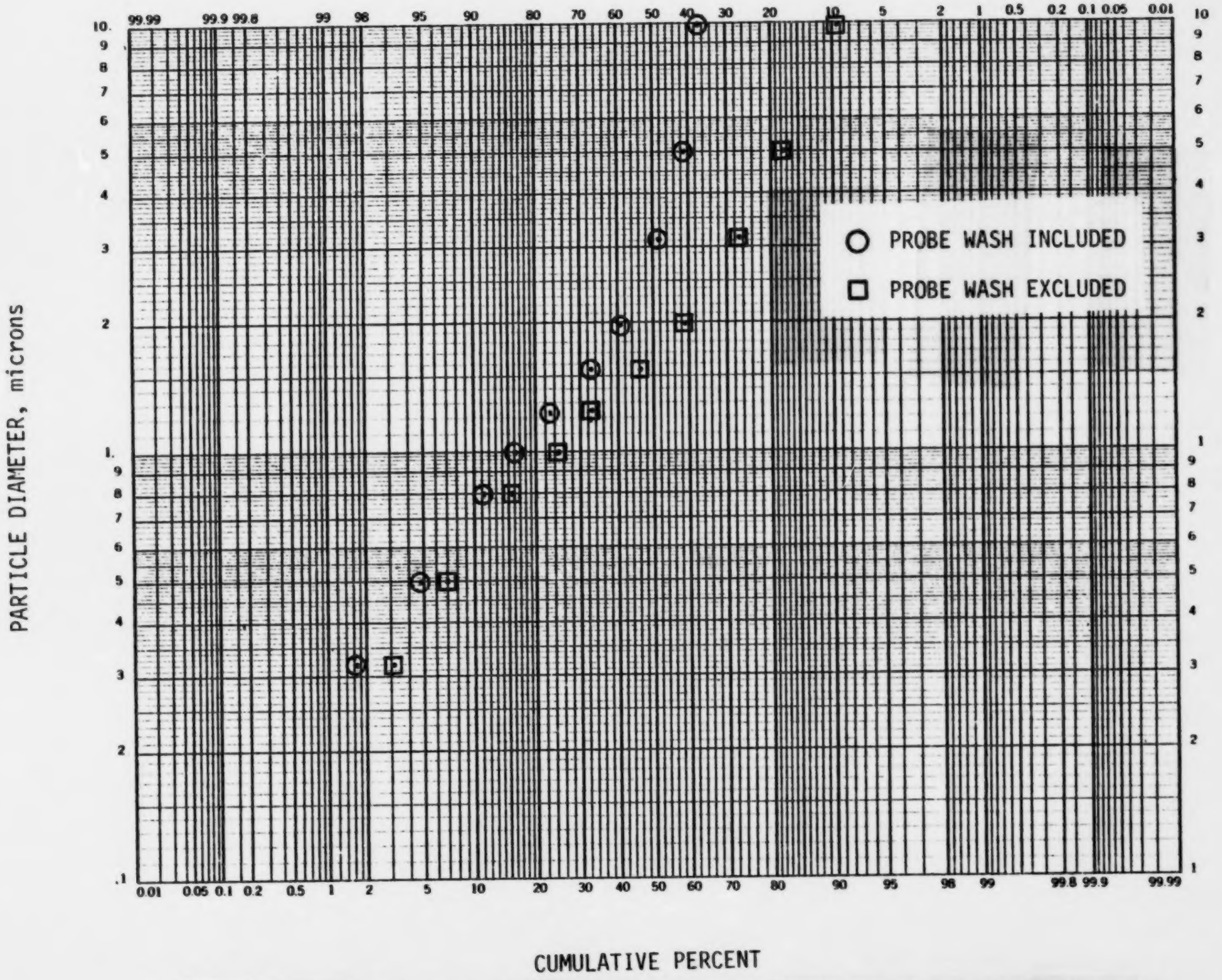

Figure 10. ESP average inlet cumulative size distribution for runs 103, 104, and 105.

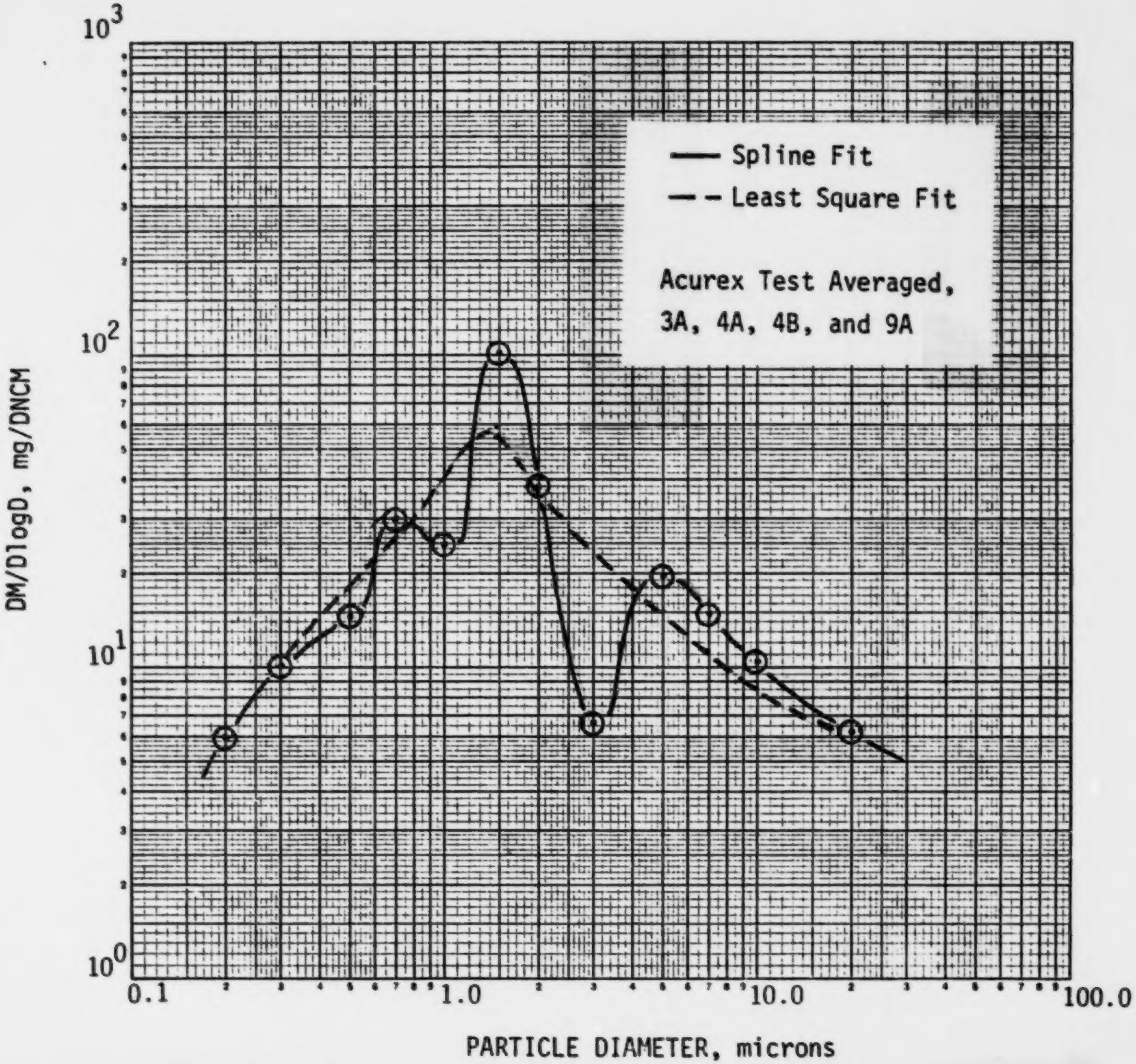

Figure 11. ESP average inlet differential size distribution for run 103.

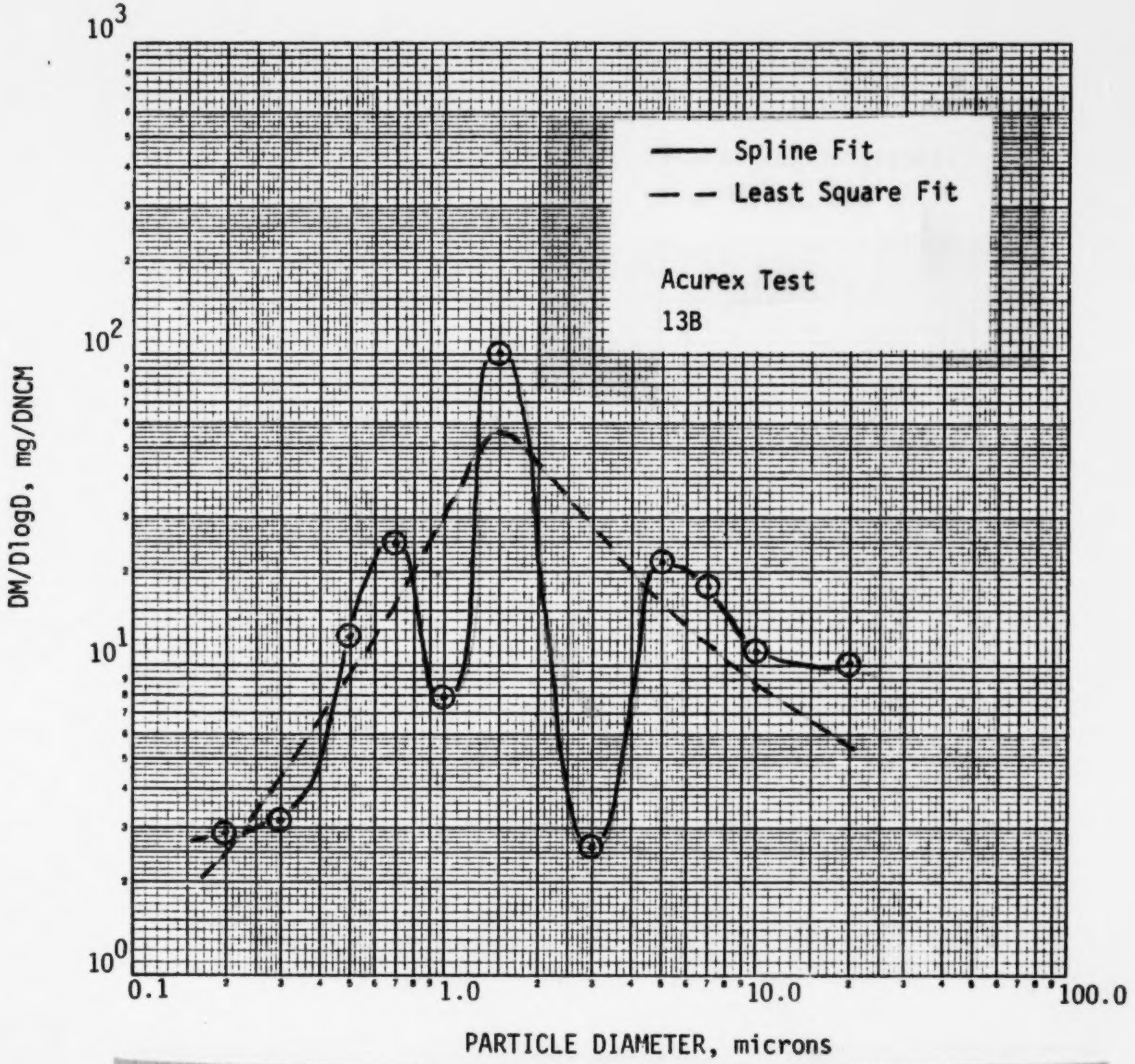

Figure 12. ESP average inlet differential size distribution for run 104.

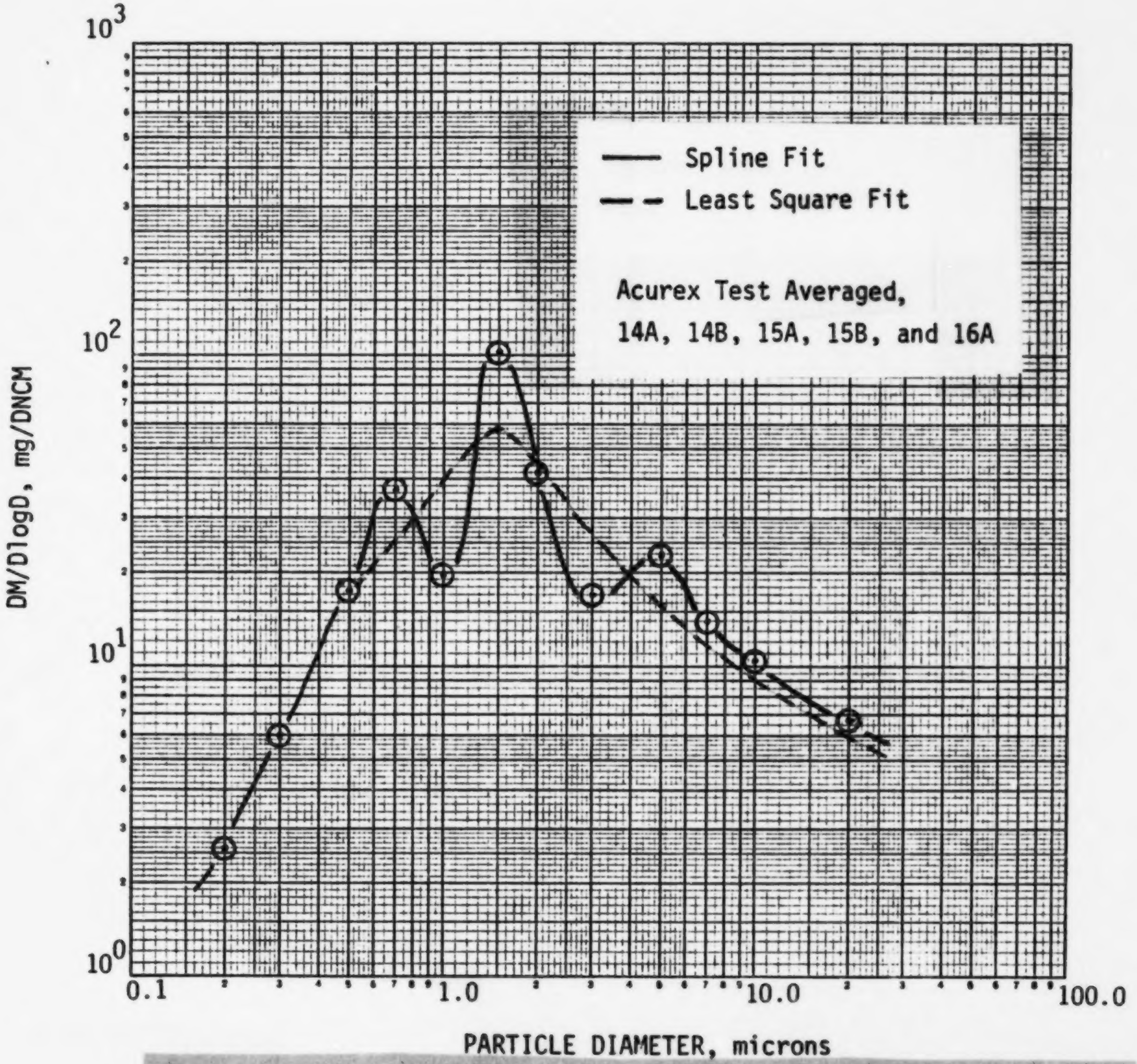

Figure 13. ESP average inlet differential size distribution for run 105.

The inlet differential size distribution curves for the three respective runs were averaged and are presented in Figure 14, with 50 percent confidence intervals.

The overall average ESP outlet differential size distribution for miniplant runs 103, 104, and 105 is shown in Figure 15, with 50 percent confidence intervals. The resultant curves for ESP average penetration as a function of particle size are presented in Figure 16. Although the shape of this curve is inverted from the typical ESP penetration curve, it is the logical result of the inlet/outlet differential distributions with their respective minima and maxima points.

## PILOT BAGHOUSE PERFORMANCE

There were a variety of operational problems, not only with the slipstream duct and pilot baghoue but also with the miniplant itself. These problems, coupled with the brevity of the baghouse test program, severely limited the amount and, possibly, the representativeness of the data collected. However, with these limitations in mind, the authors have attempted to present a reasonable evaluation of fabric filtration applied to a PFBC cyclone precleaned exhaust stream.

The cleaning cycle pressure drop data and filtration time presented in Table 13 demonstrate the erratic nature of the pilot baghouse operation. The initial cleaning cycle occurred at a terminal pressure drop ($\Delta P_T$) of 1000 pascals (Pa), after an extended period of bag conditioning and initial cake formation. The residual pressure drop ($\Delta P_R$) across the bags immediately after cleaning was 570 Pa. Successive cleaning cycles were initiated at the same $\Delta P_T$ of 1000 Pa; however, the $\Delta P_R$ incrementally decreased to 250 Pa.

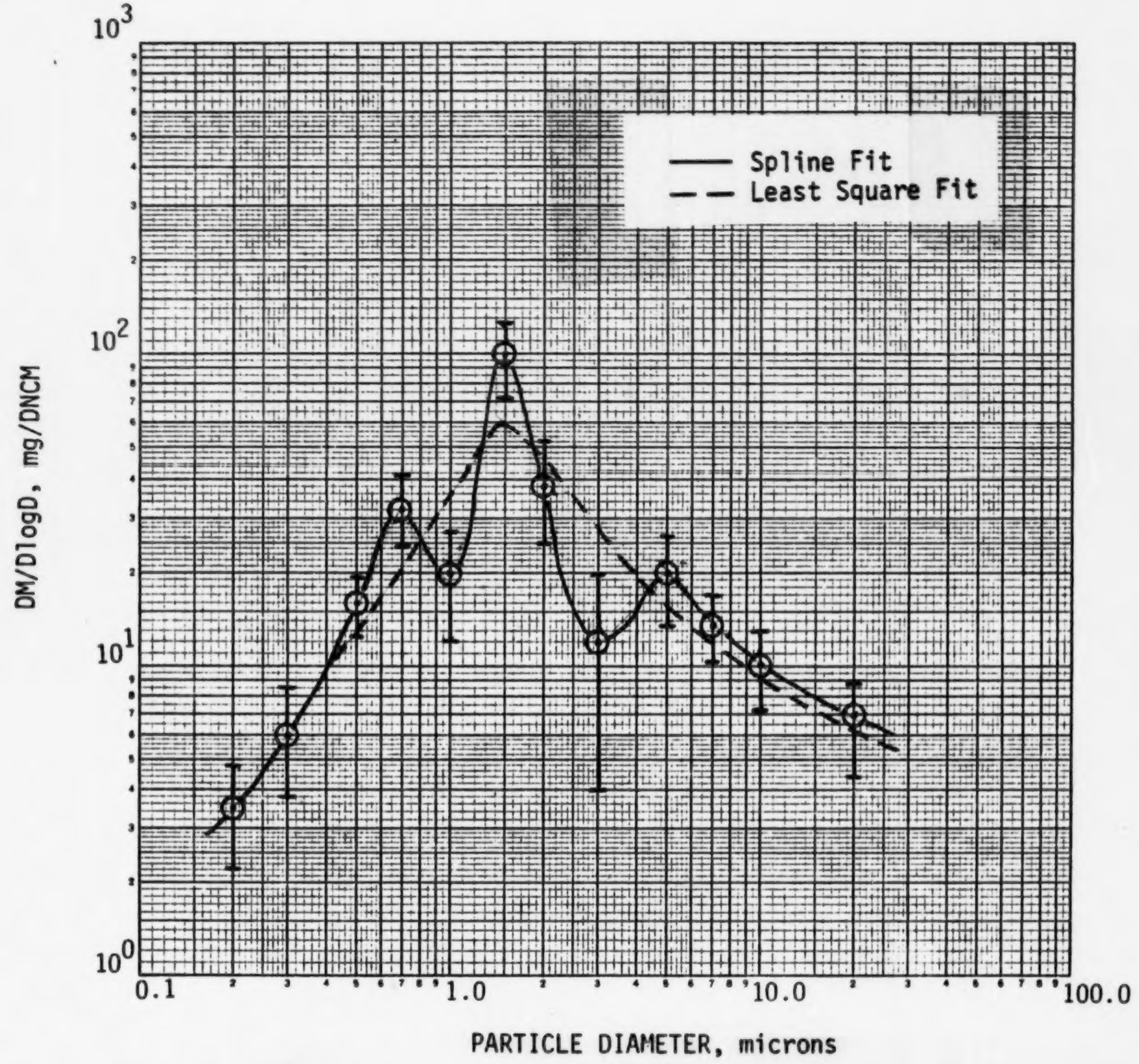

Figure 14. ESP average inlet differential size distribution for runs 103, 104, and 105, with 50 percent confidence intervals.

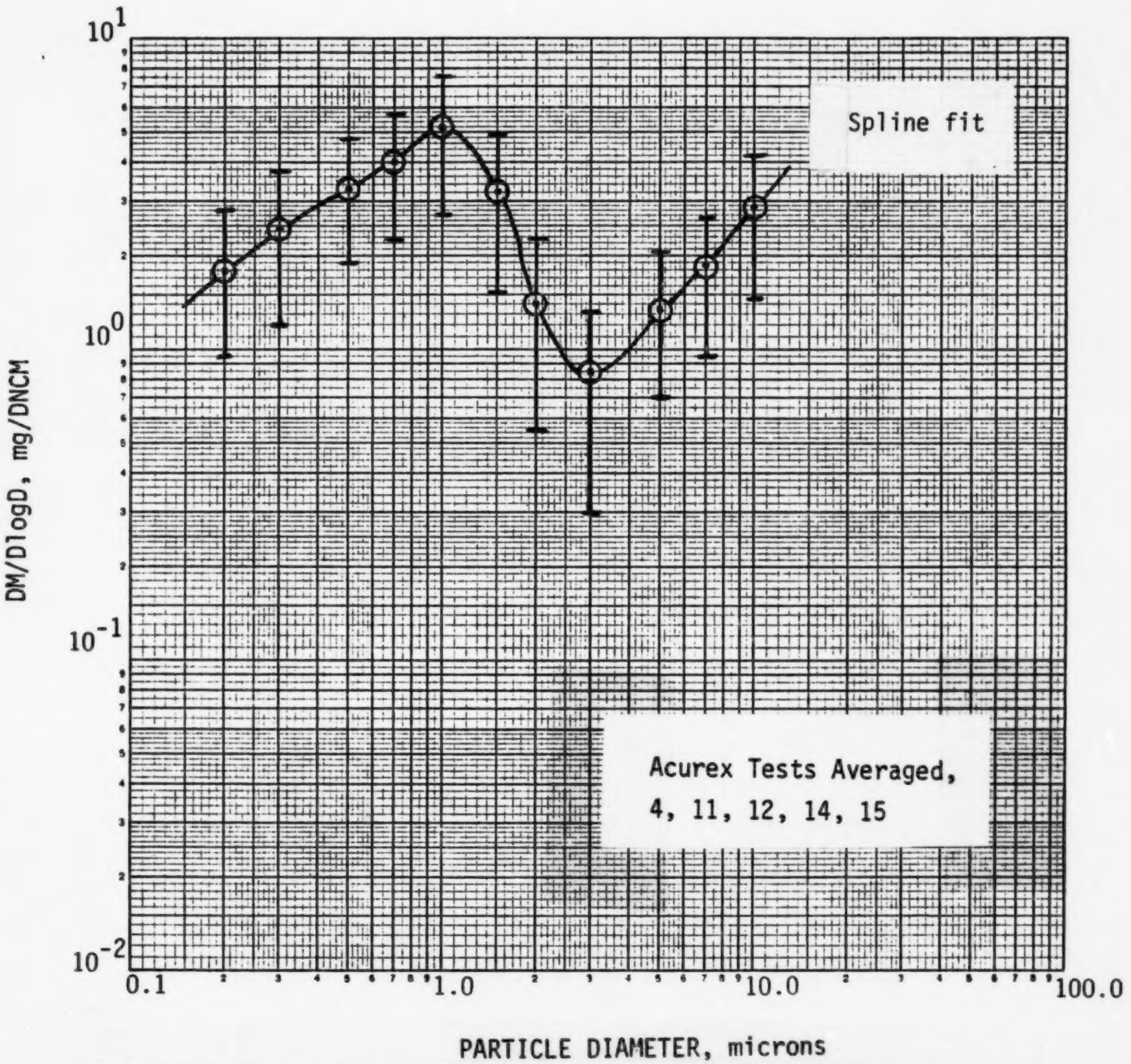

Figure 15. ESP average outlet differential size distribution for runs 103, 104, and 105, with 50 percent confidence intervals.

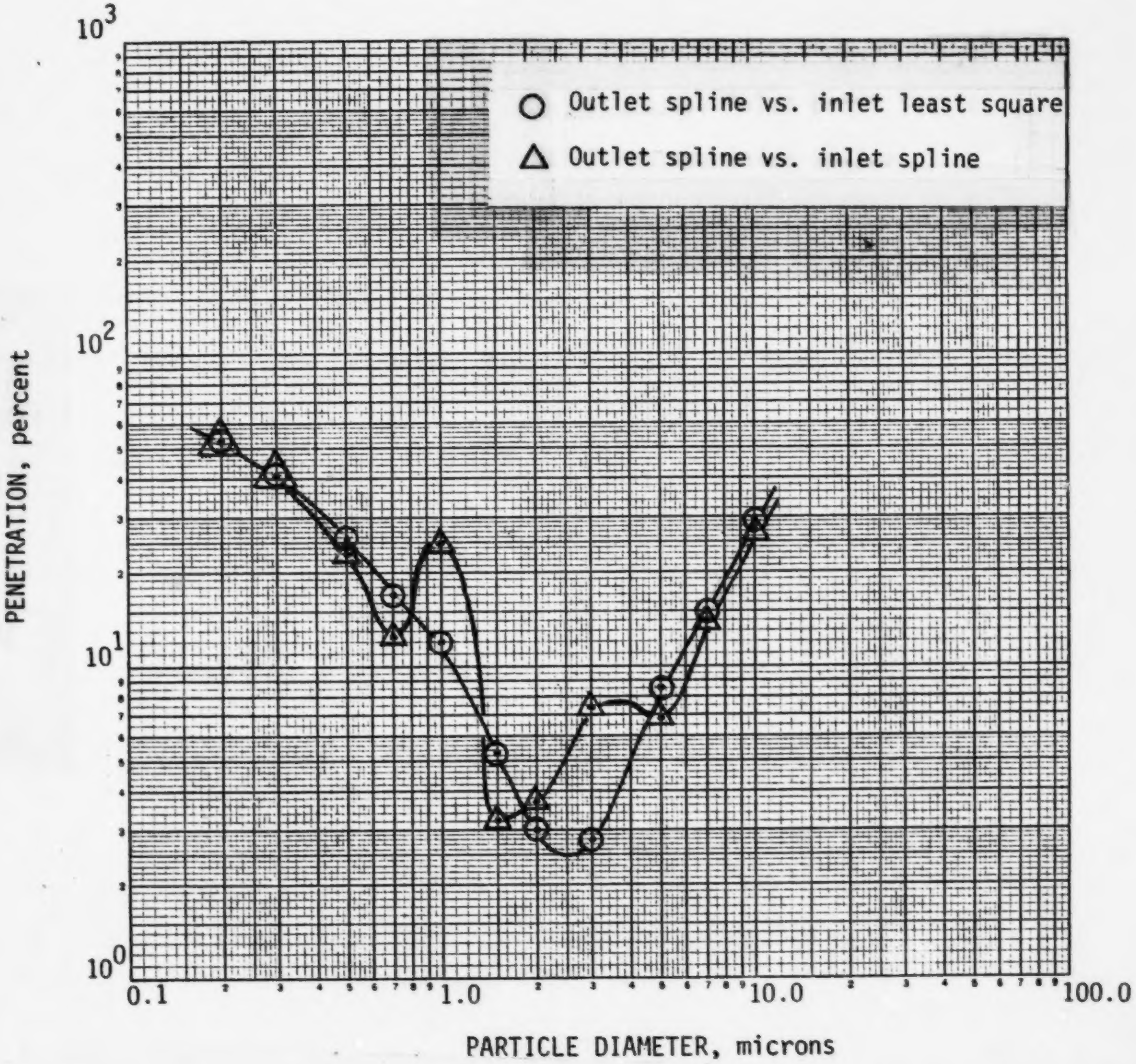

Figure 16. ESP average penetration characteristics for runs 103, 104, and 105.

TABLE 13. PILOT BAGHOUSE CLEANING CYCLES AND PRESSURE DROP CHARACTERISTICS

| Exxon PFBC run no. | Acurex test no. | 1979 date(s) | Avg. inlet flow, $m^3/min$ | Air/cloth ratio, m/min | (ft/min) | Pressure drops, Pa Terminal | Residual | Filtration time, min |
|---|---|---|---|---|---|---|---|---|
| 106 | 1-5 | 6/2-6/7 | 2.11 | 0.87 | (2.85) | 1000 | 570 | 8640 |
| 106 | 5 | 6/7 | 2.11 | 0.87 | (2.85) | 1070 | 770 | 360 |
| 106 | 5 | 6/7 | 2.11 | 0.87 | (2.85) | 1000 | 570 | 360 |
| 106 | 6,7 | 6/8-6/9 | 2.21 | 0.91 | (3.0) | 1000 | 350 | 1140 |
| 106 | 7 | 6/9 | 2.21 | 0.91 | (3.0) | 650 | 375 | 70 |
| 106 | 7 | 6/9 | 2.21 | 0.91 | (3.0) | 1000 | 250 | 900 |
| 106 | 7 | 6/10 | 2.21 | 0.91 | (3.0) | 725 | - | 420 |
| 107 | 8-11 | 6/19-6/22 | 1.80 | 0.74 | (2.4) | 1000 | 250 | 4200 |
| 107 | 11 | 6/23 | 1.80 | 0.74 | (2.4) | 800 | 375 | 915 |
| 108 | 12-14 | 6/26-6/29 | 1.92 | 0.79 | (2.6) | 1000 | 185 | 3480 |
| 108 | 14 | 6/29 | 1.92 | 0.79 | (2.6) | 375 | 185 | 240 |

The variation in on-line time required to reach a $\Delta P_T$ of 1000 Pa cannot readily be explained. The inlet loading and flow rate both remained reasonably constant, which would lead one to expect insignificant variation in online filtering time. The filtration times for cleaning cycles 4, 6, 8, and 10, however, are extremely long in comparison to the others. Cleaning cycles 8 and 10 correspond to initial startup and formation of a dust cake after the pilot baghouse was shutdown for a weekend.

The condensation problems discussed earlier certainly may have been a contributing factor. However, the limited data do not allow an assessment of this effect.

One attempt made to clarify the nature of the condensation/corrosion problems that plagued the baghouse test programs was a qualitative spectrographic emission analysis of a sample of the unknown material found in the system. The sample was collected from the bottom rear panel of the baghouse compartment on June 18, when the entire baghouse and hopper sections were dismantled for cleaning (see Appendix B).

The sample consisted of several grams of light green powdery material taken from the stainless steel panel. Qualitative spectrographic emission analysis yielded the following:

- major constituents: Fe, Ni, Cr
- minor constituents: Ca, Al, K
- trace constituents: Mg, Mn, Ti
- less than trace constituents: Ba, Ge, Mo, Sn, Cd, Cu, Zn, Zr, and Co.

Thus, it would indeed appear that the green powdery material is the result of sulfuric acid attack on the stainless steel. However, it is not known if this is the same material that contaminated outlet samples and, in some cases, appeared to result from deposition of a condensable material. It is also reasonable to assert that the pilot baghouse never achieved a state of equilibrium with respect to cake formation and release.

## Mass Efficiency

The inlet and outlet mass loadings for the pilot baghouse are shown in Table 14. While the inlet loadings are quite simlar for PFBC runs 106-108, the outlet loadings show the effect of condensation product contamination of the outlet samples. Due to the nature of operational and sampling problems experienced, the data for Acurex tests 1-9 were rejected and not used for performance evaluation. Data for these tests will be presented, but extreme caution is advised when attempting to evaluate them.

Table 15 shows a summary of average baghouse performance. The significance of the high outlet loadings for PFBC run 106 and the first half of run 107 is evident from the difference in emission levels. It is felt that the 0.5 ng/J emission level, attained at an operating efficiency of 99.3 percent, is a realistic indication of fabric filter performance.

## Particle Size Measurements

The average inlet and outlet cumulative size distribution curves for runs 106-108 are presented in Figures 17 and 18. Figure 17 includes the probe wash fraction, while Figure 18 depicts the effect of excluding the probe wash fraction on the overall curve.

## TABLE 14. PILOT BAGHOUSE INLET AND OUTLET LOADINGS, g/Nm$^3$

| Exxon PFBC run no. | Acurex test no. | 1979 date | Inlet | | Outlet | | Stack temp., °C | Air/cloth ratio m/min |
|---|---|---|---|---|---|---|---|---|
| | | | Impactor | Mass | Impactor | Mass | | |
| 106 | 1 | 6/2 | 0.120 | 0.060 | - | - | 182 | 0.07 |
| | 2 | 6/3 | 0.098 | 0.066 | - | 0.0029 | 172 | 1.12 |
| | 3 | 6/4 | 0.062 | 0.062 | 0.004[a] | 0.0051 | 159 | 0.64 |
| | 4 | 6/5 | 0.015 | 0.050 | 0.0017 | 0.0062[a] | 163 | 0.60 |
| | 5 | 6/7 | 0.065 | 0.123 | 0.0079 | - | 179 | 0.87 |
| | 6 | 6/8 | 0.167 | - | 0.0039 | 0.0056 | 176 | 0.93 |
| | 7 | 6/9 | 0.094 | 0.203 | - | 0.0060 | 180 | 0.91 |
| Average | | | 0.089 | 0.094 | 0.0045 | 0.0052 | 173 | 0.83 |

See footnote at end of table, page 58.

(continued)

TABLE 14. (continued)

| Exxon PFBC run no. | Acurex test no. | 1979 date | Inlet |  |  | Outlet |  | Stack temp., $^{\circ}C$ | Air/cloth ratio, m/min |
|---|---|---|---|---|---|---|---|---|---|
|  |  |  |  | Mass |  |  |  |  |  |
|  |  |  | Impactor | A | B | Impactor | Mass |  |  |
| 107 | 8 | 6/19 | 0.070 | 0.053 | 0.093 | 0.0005 | 0.0030 | 176 | 0.58 |
|  | 9 | 6/20 | 0.164 | 0.100 | - | 0.0010 | 0.0048 | 182 | 0.64 |
|  | 10 | 6/21 | 0.081 | 0.089 | 0.099 | 0.0006 | 0.0010 | 182 | 0.60 |
|  | 11 | 6/22 | 0.135 | 0.119 | 0.128 | 0.0005 | 0.0008 | 193 | 0.79 |
| Average |  |  | 0.112 | 0.097 |  | 0.0006 | 0.0024 | 183 | 0.65 |
| 108 | 12 | 6/26 | 0.076 | 0.075 | 0.095 | 0.0006 | 0.0004 | 193 | 0.85 |
|  | 13 | 6/27 | 0.086 | 0.093 | 0.077 | 0.0006 | 0.0008 | 169 | 0.78 |
|  | 14 | 6/28 | 0.087 | 0.107 | - | 0.0006 | 0.0006 | 176 | 0.79 |
| Average |  |  | 0.083 | 0.089 |  | 0.0006 | 0.0006 | 179 | 0.81 |

[a] Excluded from the average.

TABLE 15. SUMMARY OF AVERAGE BAGHOUSE PERFORMANCE

| Exxon PFBC run no. | Average temperature, °C | Air/cloth ratio, m/min | Average inlet loading, g/Nm$^3$ |  | Average outlet loading, g/Nm$^3$ |  | Efficiency, % |  | Emissions,[a] ng/J |
|---|---|---|---|---|---|---|---|---|---|
|  |  |  | Impactor | Mass | Impactor | Mass | Impactor | Mass |  |
| 106[b] | 173 | 0.83 | 0.088 | 0.094 | 0.0045 | 0.0049 | 94.9 | 94.8 | 3.5 |
| 107[b] | 181 | 0.64 | 0.112 | 0.097 | 0.0006 | 0.0024 | 99.5 | 97.5 | 1.7 |
| 108 | 179 | 0.81 | 0.083 | 0.089 | 0.0006 | 0.0006 | 99.3 | 99.3 | 0.5 |

[a] Based on mass data.

[b] Outlet samples contaminated with corrosion/condensation material.

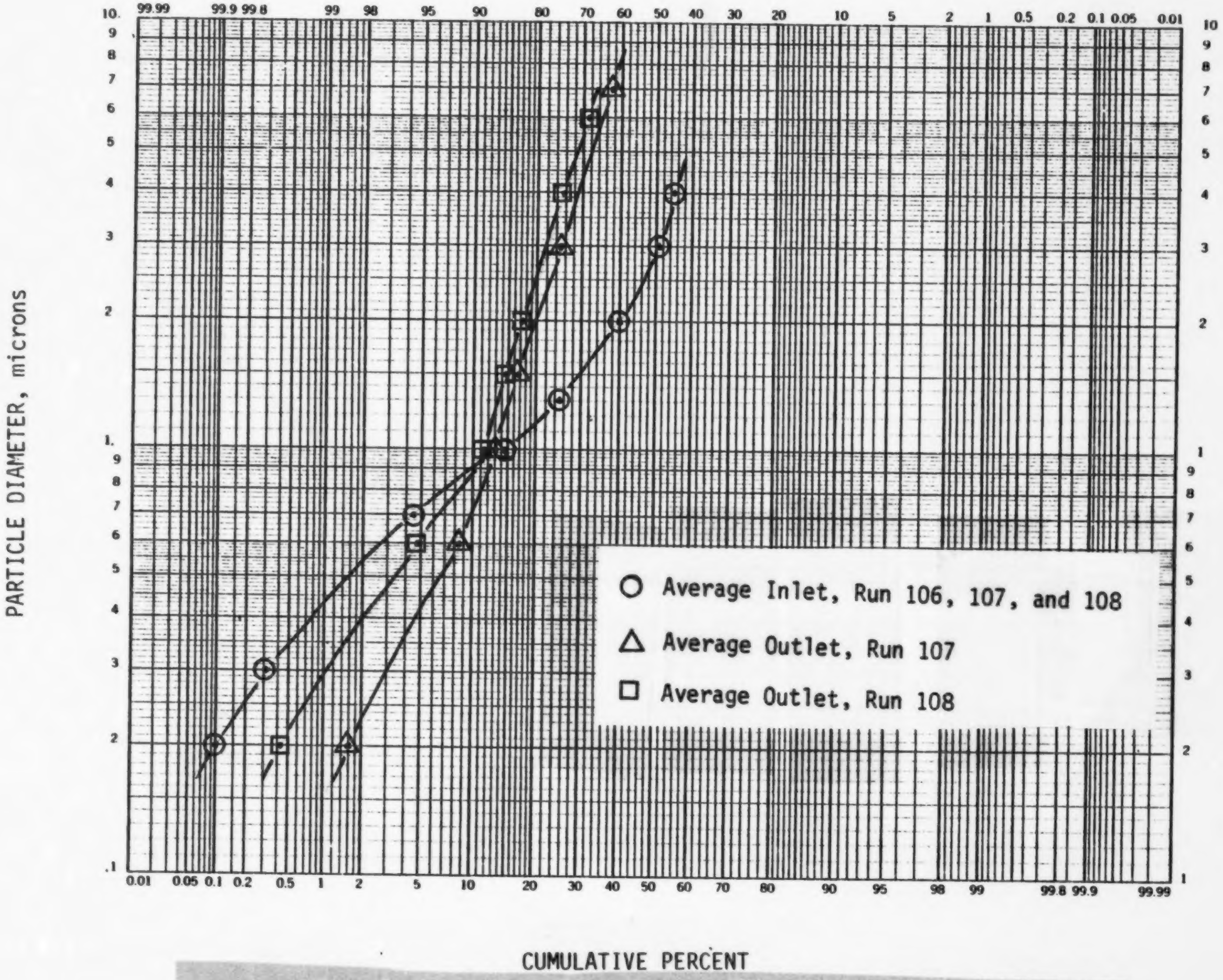

**Figure 17.** Baghouse inlet and outlet cumulative size distributions, including probe wash.

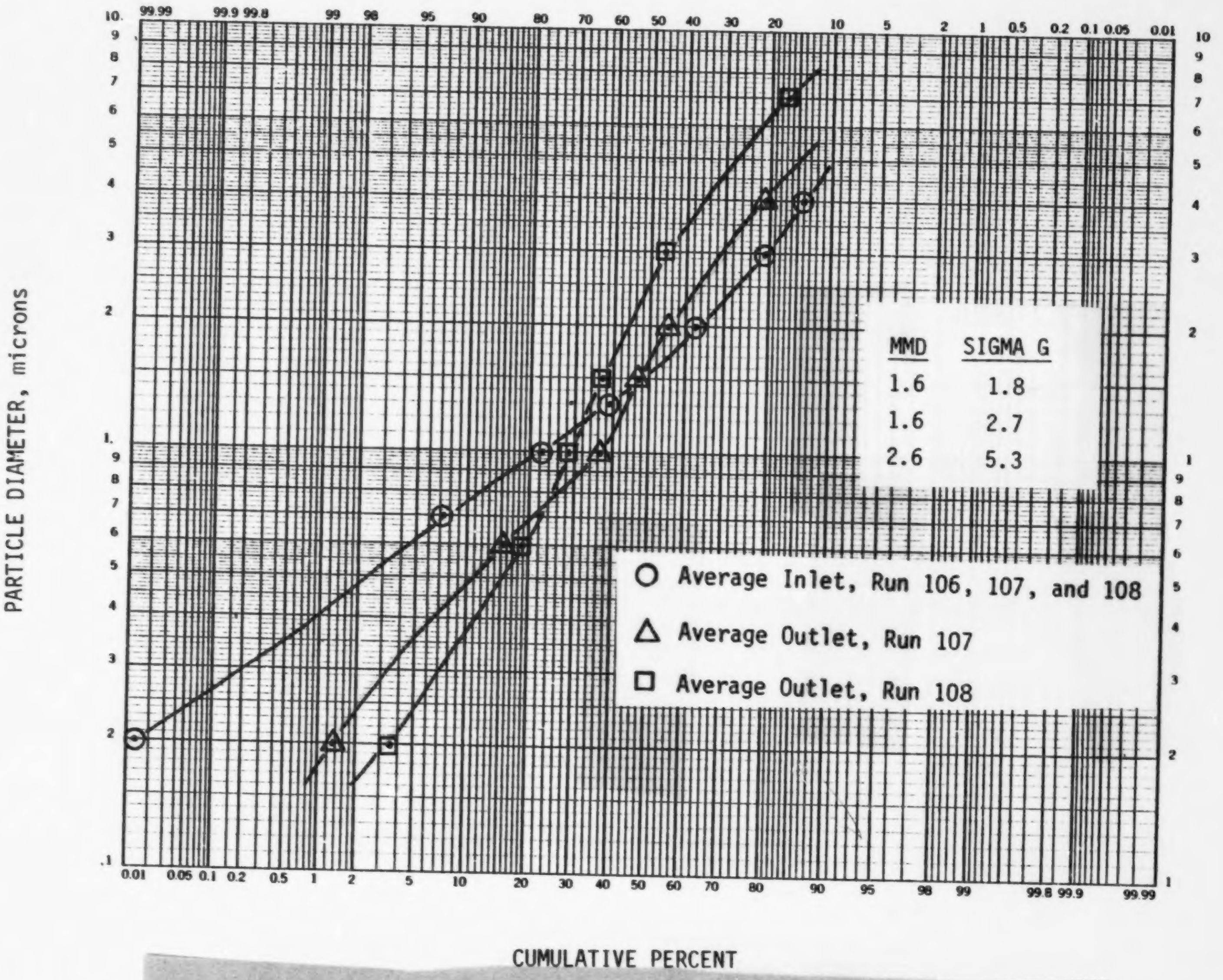

Figure 18. Baghouse inlet and outlet cumulative size distributions, excluding probe wash.

The overall average inlet differential size distribution curve for runs 106-108 is shown in Figure 19, with both spline and least-square curve fits.

Figures 20 and 21 show the average outlet differential size distributions for runs 107 and 108, respectively. These curves, in conjunction with the average inlet differential size distribution, yield the fractional penetration curves presented in Figures 22 and 23.

Again it is cautioned that these figures represent the performance characteristics of the pilot baghouse under non-equilibrium operating conditions. It is felt that the inlet size distribution curves realistically portray the PFBC cyclone effluent. However, the outlet distribution curves and resulting fractional penetration curves may have been influenced by operating problems discussed earlier.

### Analysis of Ash Samples

Results of chemical analyses (conducted by SRI) of baghouse ash samples are shown in Table 16. The corresponding laboratory resistivity values shown in Figure 24 are comparable to those presented earlier for ESP ash samples.

## MINIPLANT TERTIARY CYCLONE EMISSIONS

The high performance of the miniplant tertiary cyclone has been the subject of much discussion. Table 17 presents a comparison of the average inlet grain loadings for the mobile control facilities for runs 103-108. These are compared with Balston filter outlet loading data from the miniplant tertiary cyclone. The ESP and baghouse inlet grain loadings were derived from dilution air estimates for the respective miniplant runts (see Table 5).

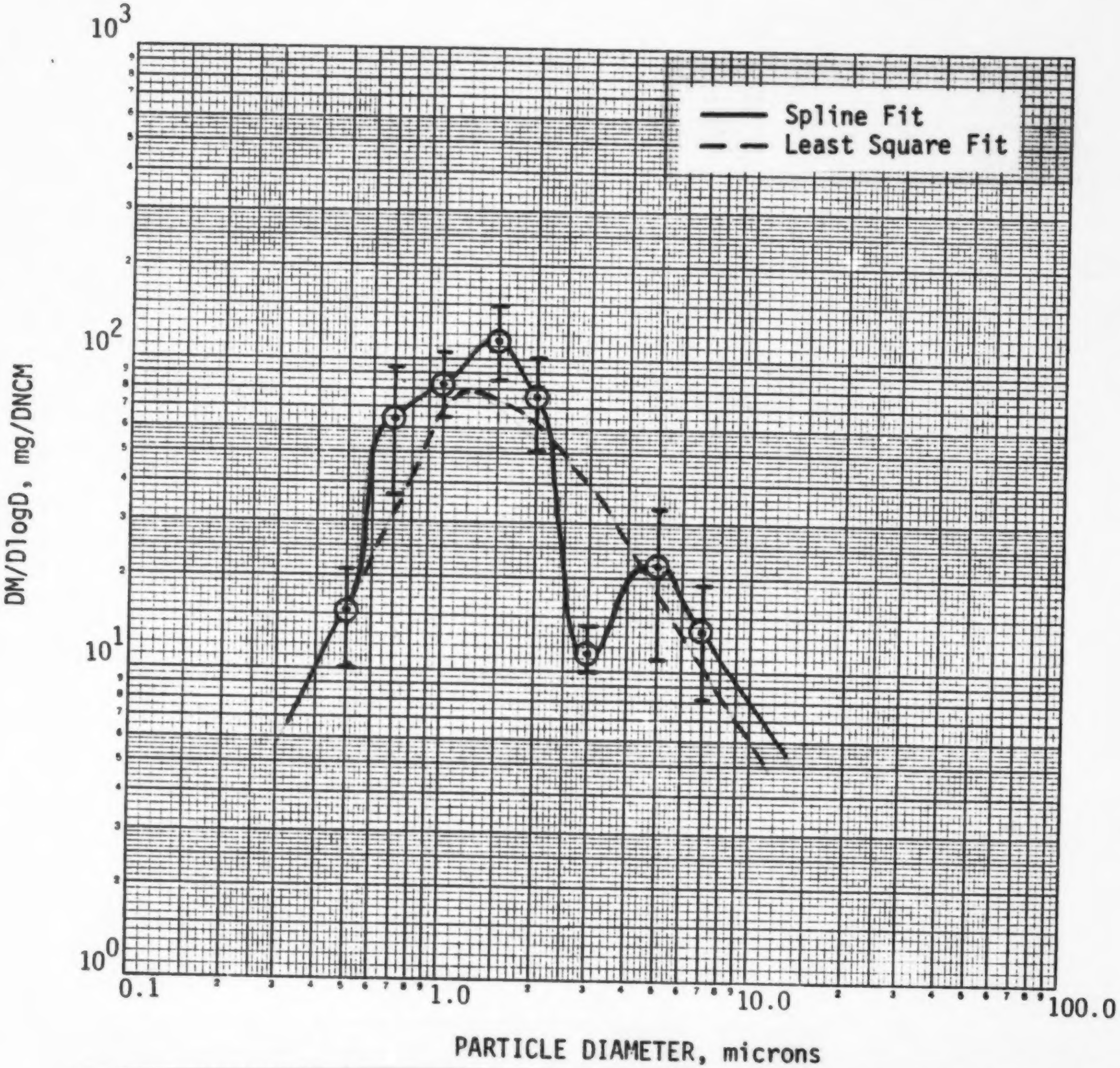

Figure 19. Baghouse average inlet differential size distribution for runs 106, 107, and 108, with 50 percent confidence intervals.

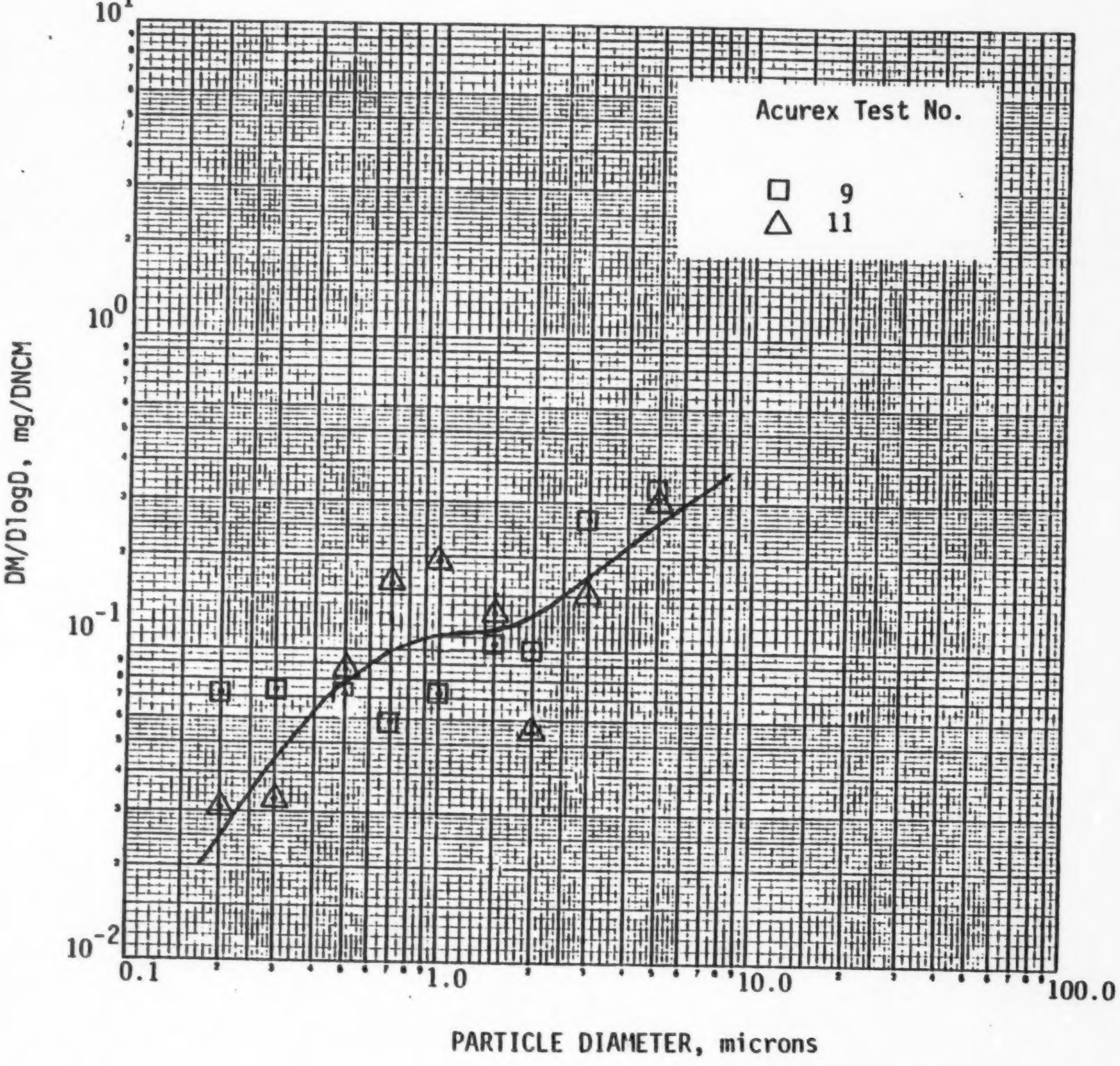

Figure 20. Baghouse outlet differential size distributions for run 107.

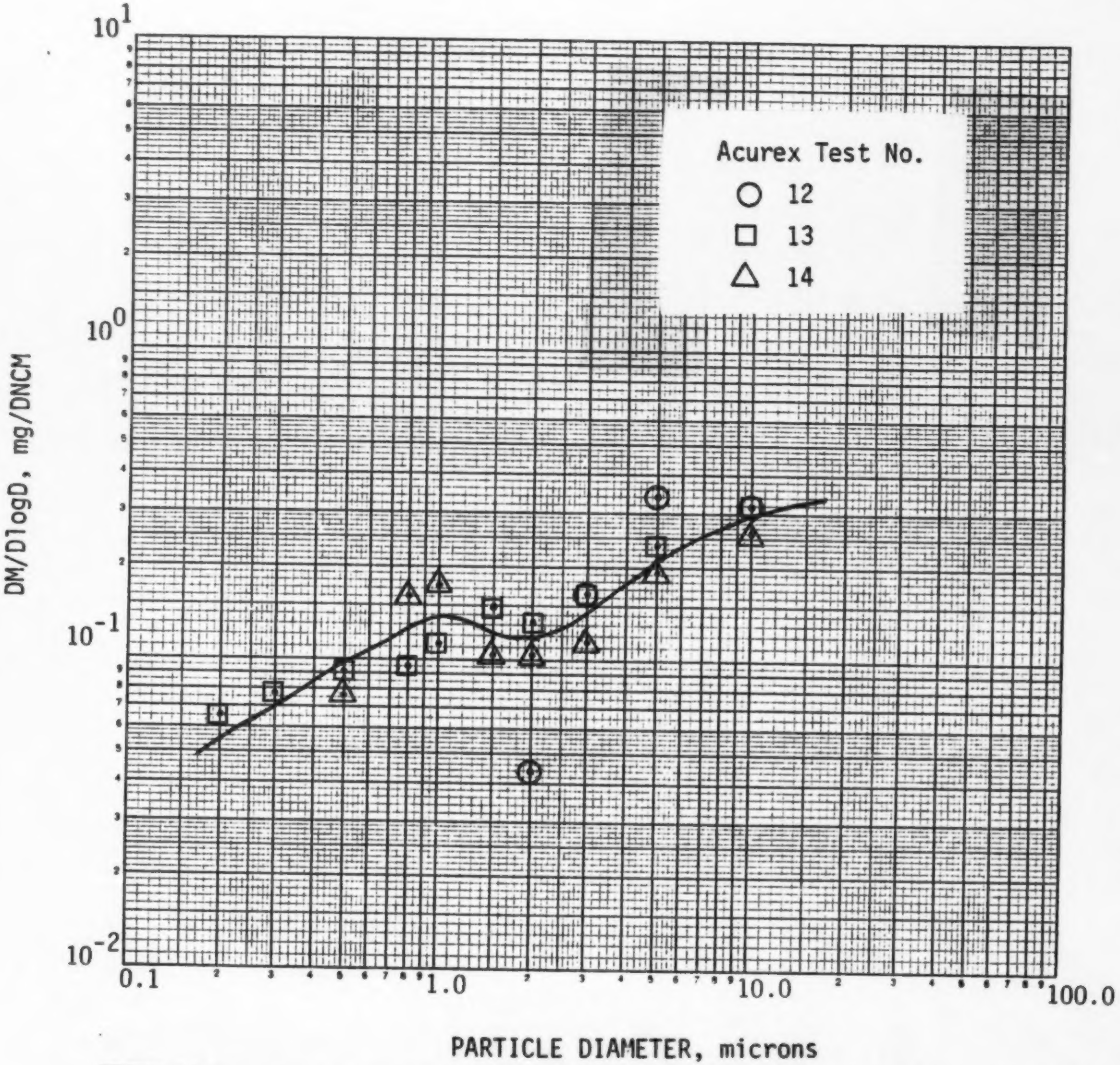

Figure 21. Baghouse outlet differential size distributions for run 108.

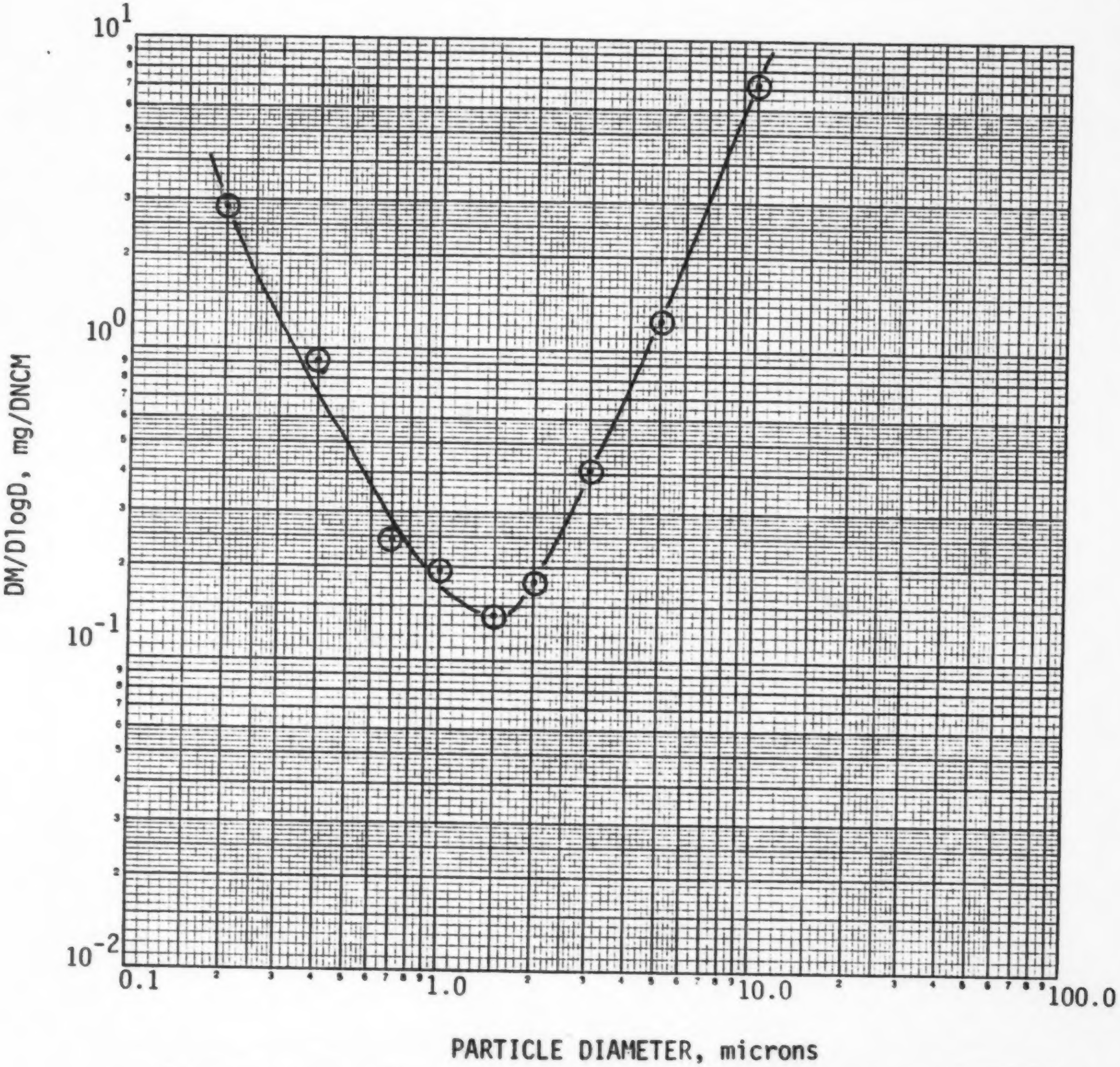

Figure 22. Baghouse average penetration characteristics for run 107.

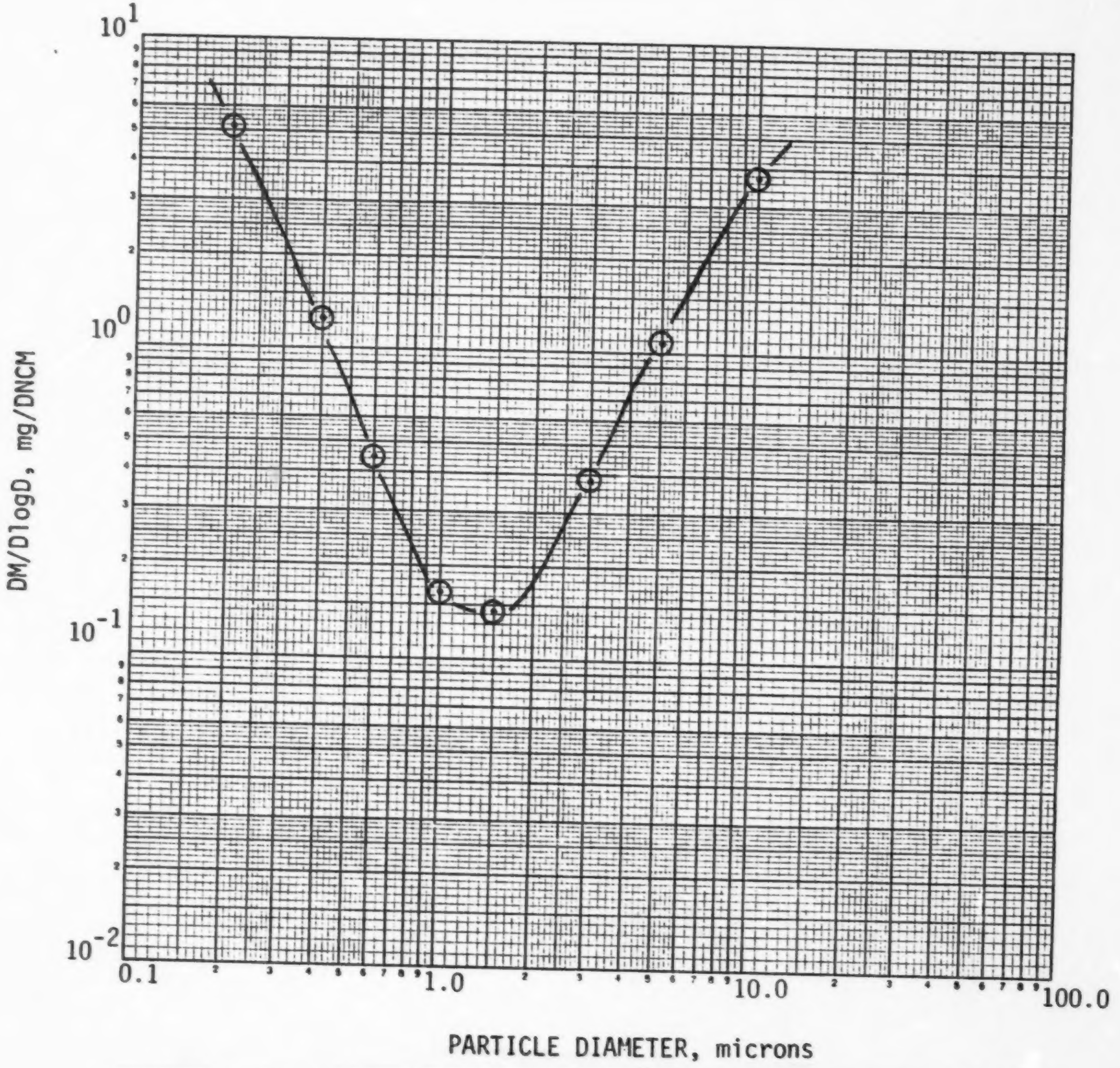

Figure 23. Baghouse average penetration characteristics for run 108.

## TABLE 16. CHEMICAL ANALYSES OF PILOT BAGHOUSE AND MINIPLANT ASH SAMPLES (weight percent as oxides)[a]

| Sample no.: | 7 | 8 | 9[b] | 10 |
|---|---|---|---|---|
| Exxon PFBC run no.: | 107 | 108 | 106 | 106 |
| Sample location: | FF hopper | FF hopper | FF hopper | PFBC tertiary cyclone |
| 1979 date: | 6/18 | 6/25 | 6/7 | 6/7 |
| $Li_2O$ | 0.03 | 0.03 | 0.01 | 0.01 |
| $Na_2O$ | 0.52 | 0.57 | 0.73 | 1.13 |
| $K_2O$ | 1.30 | 1.30 | 0.94 | 2.60 |
| MgO | 4.0 | 3.7 | 2.7 | 4.5 |
| CaO | 10.6 | 9.1 | 12.7 | 8.9 |
| $Fe_2O_3$ | 13.6 | 18.8 | 20.6 | 12.1 |
| $Al_2O_3$ | 20.8 | 17.7 | 9.8 | 16.3 |
| $SiO_2$ | 29.0 | 25.8 | 23.5 | 39.8 |
| $TiO_2$ | 1.8 | 1.6 | 0.8 | 0.9 |
| $P_2O_5$ | 0.5 | 0.4 | 0.4 | 0.1 |
| $SO_3$ | 16.6 | 17.7 | 14.8 | 9.8 |
| Total | 99.0 | 96.7 | 87.0 | 96.1 |
| LOI | 8.6 | 14.4 | 1.7 | 0.9 |

[a] All analyses were conducted on ignited samples.

[b] Analyses for calcium, iron, silicon, and aluminum were repeated with results similar to those shown for sample #9. The qualitative test for carbonate was negative for sample #9.

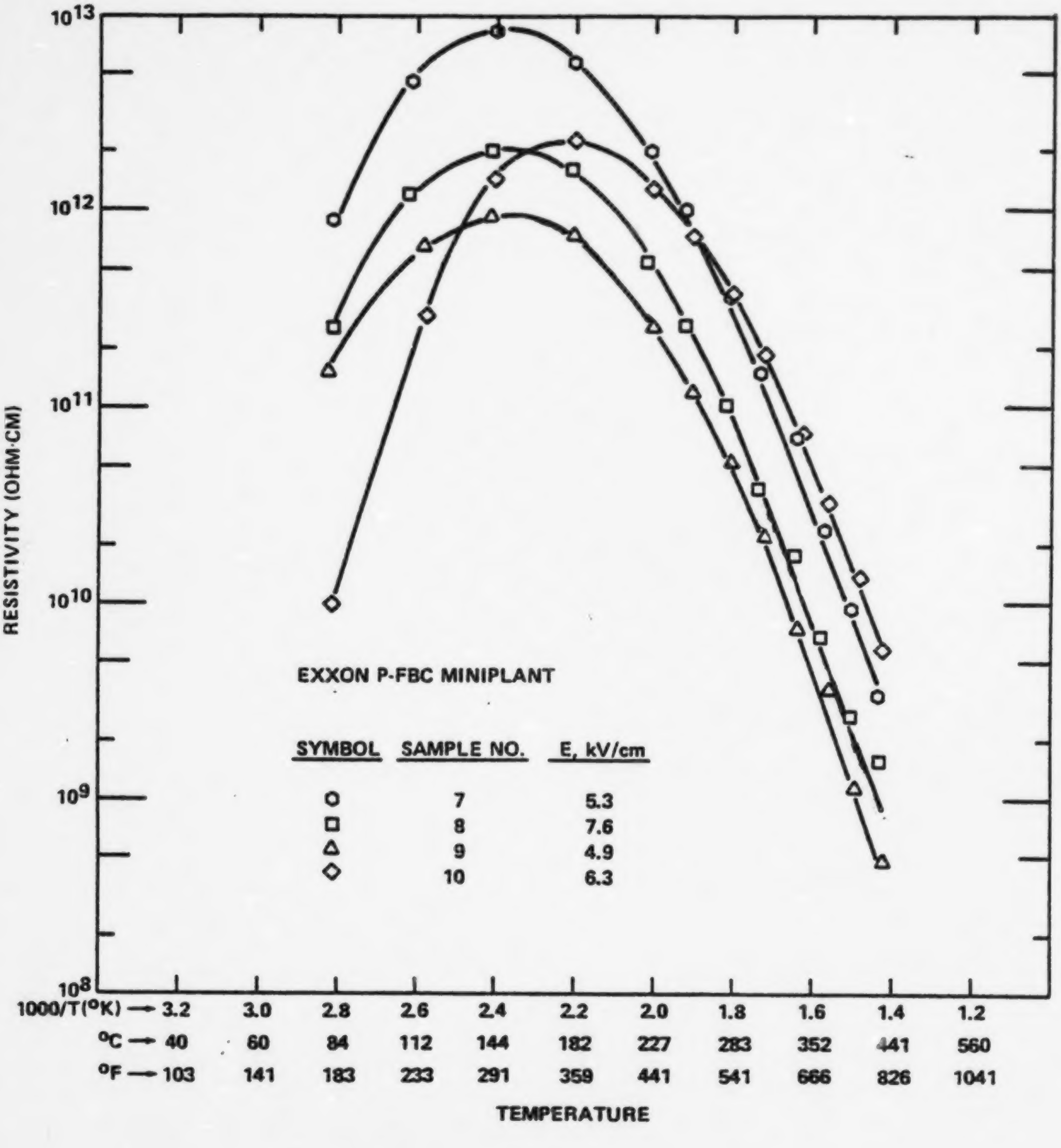

Figure 24. Laboratory resistivity for ash samples from the pilot baghouse and miniplant.

TABLE 17. TERTIARY CYCLONE AVERAGE OUTLET LOADINGS

| Exxon PFBC run no. | Acurex Method 5[a] data, $g/Nm^3$ | Exxon Balston filter data, $g/Nm^3$ |
|---|---|---|
| 103 | 0.22 | 0.15 |
| 104 | 0.16 | 0.23 |
| 105 | 0.20 | 0.18 |
| 106 | 0.18 | 0.15 |
| 107 | 0.18 | 0.23 |
| 108 | 0.16 | 0.28 |
| Average | 0.18 | 0.20 |

[a] Estimated from PM loadings at the vans that were lower by 20-70 percent due to pressure control dilution air (see Table 3.)

Figure 25 compares the miniplant tertiary cyclone outlet particle size distribution with the average ESP and baghouse inlet distribution.

## PERFORMANCE MODELING

The EPA particulate control device performance models were used for comparison and prediction purposes to gain further insight into the application of conventional control technology to the PFBC process. Some degree of assumption and engineering judgment were necessary due to program constraints and field-testing problems. Nevertheless, the results of the modeling effort support and enhance this initial assessment.

### ESP Modeling

The purpose of the ESP modeling exercise was to compare empirical with predicted control-device performance. The results of this effort are tabulated in Table 18. Three cases were generated for modeling: (1) ideal, (2) nonideal A, and (3) nonideal B. The model input parameters that varied for the three cases were cell bypass fraction, or sneakage, and the normalized standard deviation of inlet velocity. The footnote to Table 18 identifies the values assigned to each variable for the three cases. The nonideal A case is asserted to be the one most representative of the mobile ESP.

The predicted efficiencies are quite similar to the empirical values for the ideal case. Nonideal cases A and B result in lower predicted efficiencies. The lower predicted efficiencies for the part of run 103 in the hot-side mode indicate that the model does not account for the improved performance realized during hot-side operation.

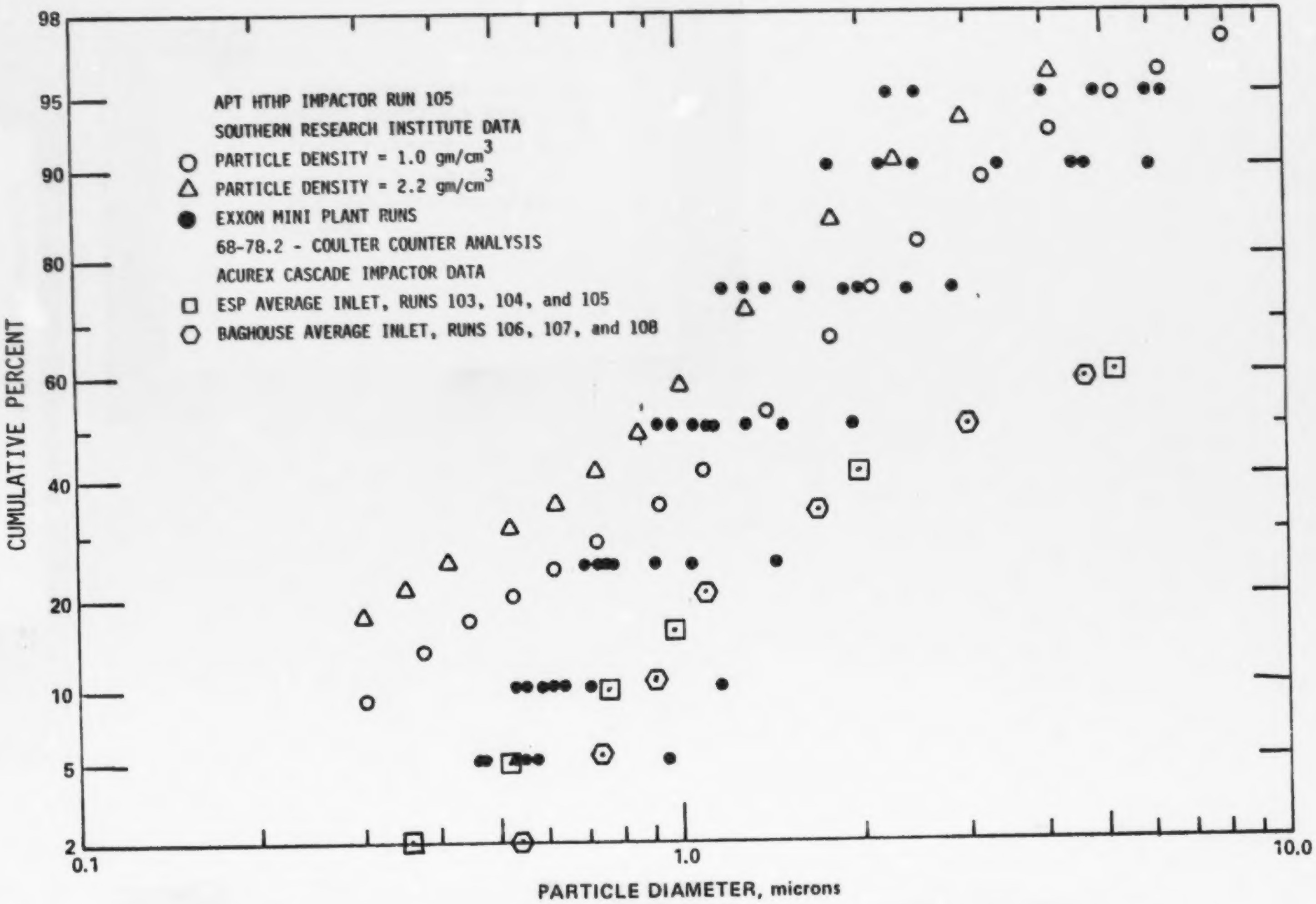

Figure 25. Tertiary cyclone outlet particle size distributions from Coulter Counter and cascade impactors.

TABLE 18. COMPARISON OF EMPIRICAL AND PREDICTED ESP PERFORMANCE

| Exxon PFBC run no. | SCA, $m^2/m^3/s$ | Temperature, $^oC$ | Empirical efficiency, mass | Predicted efficiency[a] | | |
|---|---|---|---|---|---|---|
| | | | | Ideal | Nonideal A | Nonideal B |
| 103 | 31.8 | 184 | 88.0 | 86.3 | 82.1 | 79.1 |
| 103 | 26.6 | 354 | 88.3 | 59.2 | 54.5 | 51.5 |
| 104 | 36.2 | 210 | 79.1 | 76.9 | 72.4 | 69.5 |
| 105 | 37.4 | 195 | 90.2 | 85.3 | 81.1 | 78.1 |

[a] Ideal: ASNUCK = 0.0, AZIGGY = 0.0; nonideal A: ASNUCK = 0.1, AZIGGY = 0.25; nonideal B: ASNUCK = 0.1, AZIGGY = 0.50
ASNUCK = cell bypass fraction (sneakage);
AZIGGY = normalized standard deviation of inlet velocity.

The ESP performance model also predicts fractional penetration. Figure 26 is a comparison of empirical and predicted fractional penetration. The model overpredicts penetration in the 0.3-6.0 µm size range.

## Baghouse Modeling

The baghouse performance model was used to predict emission levels and operating pressure drop as a function of air/cloth (A/C) ratio. A critical input parameter required for the performance model is the specific cake resistance coefficient, $K_2$. The model has the capability of determining $K_2$, if the following are known: inlet particle size mass mean diameter (MMD), geometric standard deviation ($\sigma_G$), bulk particle density, and discrete particle density. Because there were no experimental values for bulk and discrete particle density, this means of establishing a $K_2$ value could not be used.

The $K_2$ value was estimated by a graphical procedure discussed in Reference 10, which involves construction of a fabric loading versus drag curve. Figure 27 shows the relationship for typical drag versus loading curves as a function of the degree of cleaning. The drag versus loading curve constructed for the mobile baghouse at the Exxon miniplant is shown in Figure 28. This curve is similar to curve 4 in the previous figure, which indicates an average cleaning range for reverse flow with bag collapse.

Since shake cleaning was the cleaning mode employed, this indicates a relatively low degree of cleaning or area-cleaned ($a_c$) fraction. The actual $a_c$ value was estimated to be 22 percent.

A summary of the predicted performance and average pressure drop is shown in Table 19. Emission levels and operating pressure drop are both

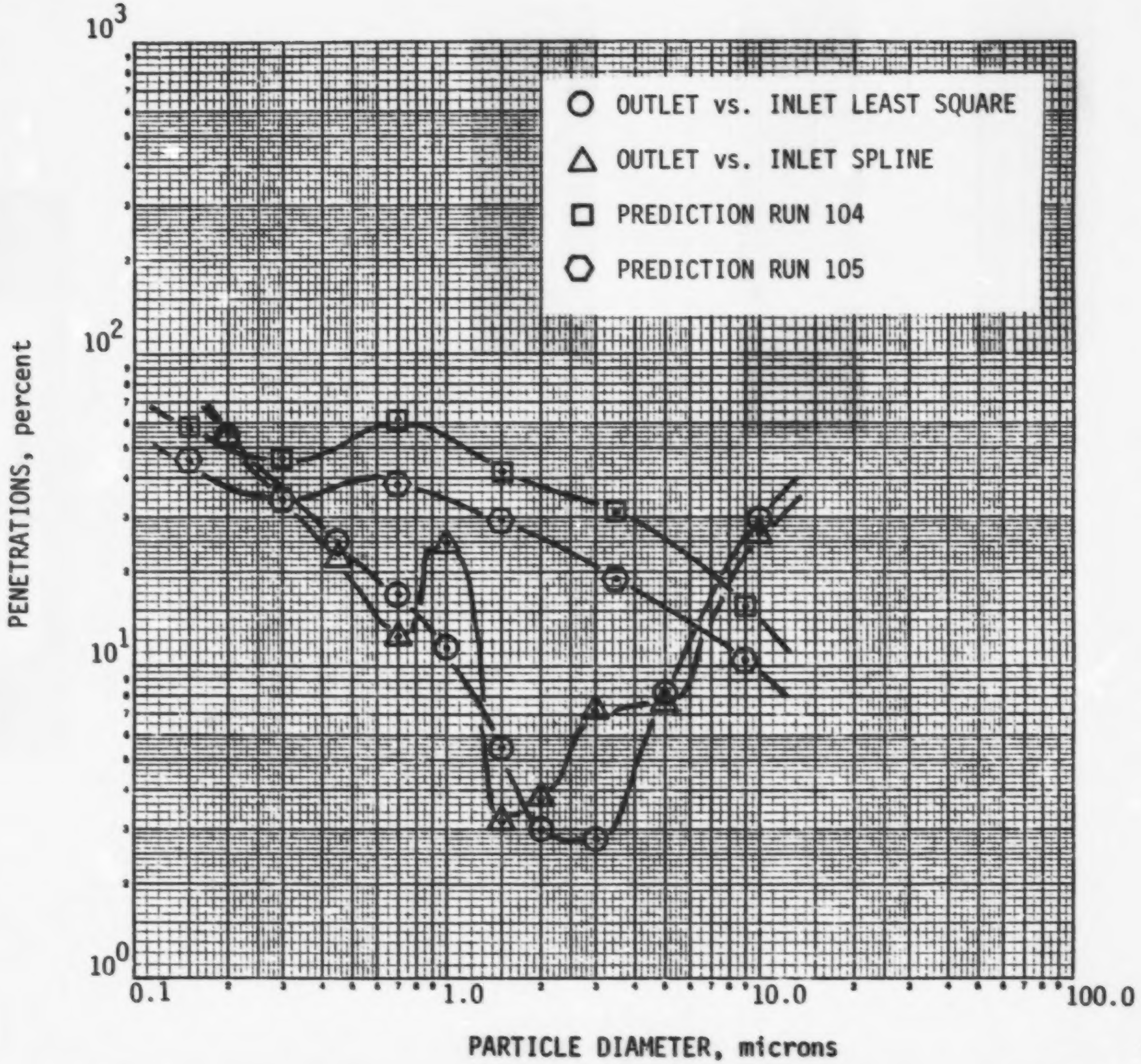

Figure 26. Comparison of ESP empirical and predicted fractional penetrations.

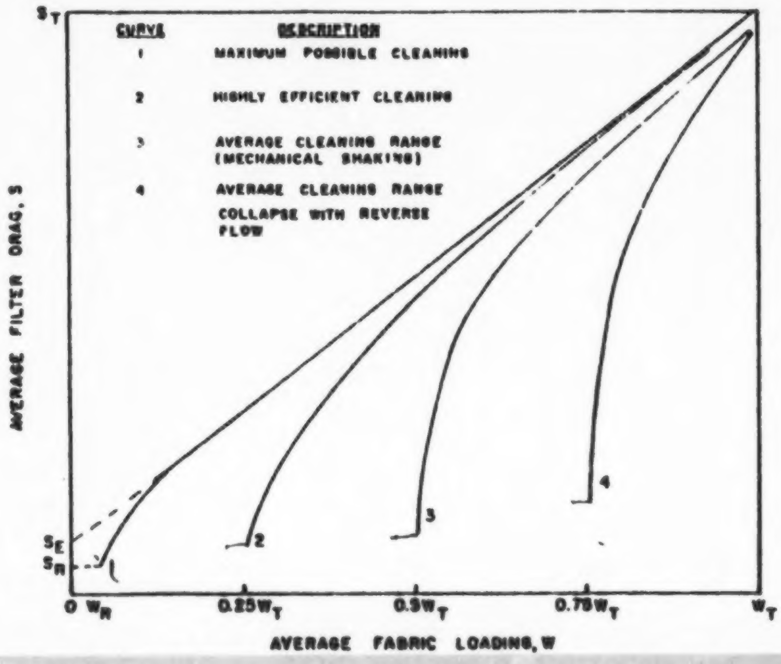

Figure 27. Typical drag versus loading curves (for filters with different degrees of cleaning and a maximum allowable level for terminal drag, $S_T$, and terminal fabric loading, $W_T$).

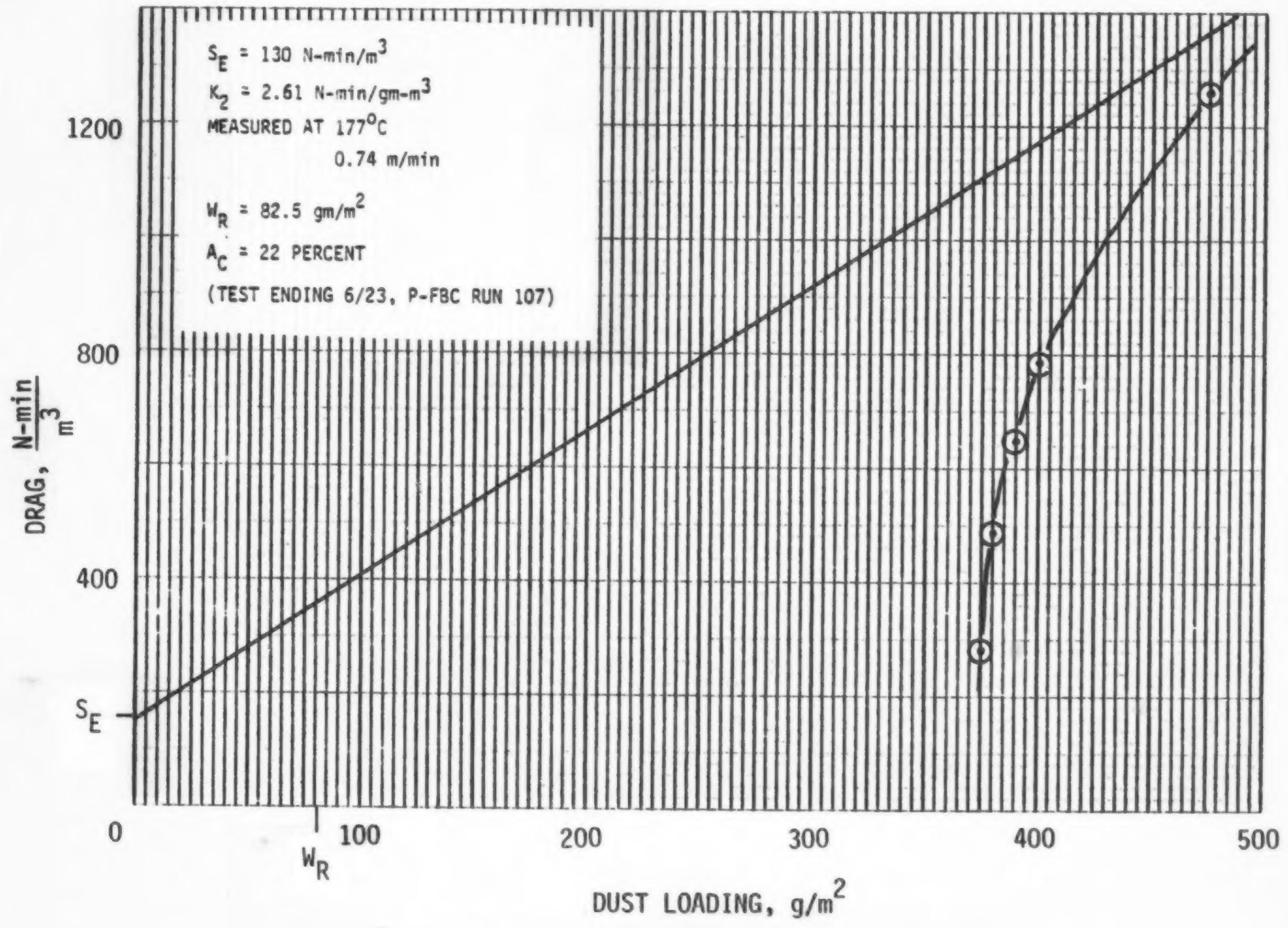

Figure 28. Estimation of $K_2$ and $S_E$ values.

TABLE 19. SUMMARY OF BAGHOUSE PERFORMANCE MODELING

| Velocity, m/min (ft/min) | | Time, min | | Average penetration, % | Average pressure drop, $N/m^2$ (in WC) |
|---|---|---|---|---|---|
| Face velocity | Reverse flow | Cleaning cycle | Total cycle | | |
| 0.79 (2.6) | 1.0 (3.3) | 28 | 530 | 0.64 | 900 (3.6) |
| 1.52 (5.0) | 2.0 (6.6) | 28 | 80 | 1.63 | 1050 (4.2) |
| 2.50 (8.2) | 3.0 (9.8) | 28 | 28 | 4.1 | ~2000 (8.0) |

Face velocity

proportional to A/C ratio. However, A/C ratio and operating pressure drop have opposite effects on annualized costs, because increasing the A/C ratio reduces the size of the baghouse and the associated installation costs. On the other hand, an increase in operating pressure drop increases annual operating costs.

## Scrubber Modeling

The venturi scrubber performance model was used to predict emission levels as a function of pressure drop across the venturi. Definitions of these were necessary to establish design specifications, which in turn were used to estimate the costs of control for a venturi scrubber.

Table 20 shows the venturi scrubber efficiency and emission levels predicted by the model for a pressure drop range from 7 to 20 cm water column (WC).

TABLE 20. SUMMARY OF SCRUBBER PERFORMANCE MODELING
(liquid/gas ratio = 0.0013 liter/$m^3$;
inlet loading = 0.22 g/DNCM)

| Pressure drop, cm WC | Efficiency, % | Outlet loading, g/$Nm^3$ | Emissions ng/J |
|---|---|---|---|
| 7 | 88.85 | 0.0245 | 10.1 |
| 10 | 90.87 | 0.0200 | 8.2 |
| 13 | 92.89 | 0.0156 | 6.4 |
| 20 | 95.11 | 0.0108 | 4.4 |

## COST OF CONTROL ANALYSIS

A preliminary cost of control analysis for conventional PM control technology applied to a 350 MW PFBC system was performed. The modeling results were used as the basis for ESP, baghouse, and venturi scrubber design. The design parameters for the respective control systems are presented in Tables 21-23.

The methodology used to generate the cost estimates was in accordance with References 13 and 14. The capital costs were annualized, assuming an equipment life of 10 years and an annual discount rate of 8 percent. Annualized capital cots were added to annual operating and maintenance costs to obtain costs of control per kilowatt hour (kWh) energy. These costs are summarized in Table 24. The ESP and baghouse control costs are comparable, while the venturi scrubber costs are significantly higher.

The achievable emission levels with the ESP and baghouse differ considerably, with the baghouse performing at 98.5 percent efficiency and the ESP at only 82.0 percent efficiency. To compare costs of control for more equivalent performance levels, control costs were generated for the baghouse as a function of A/C ratio and operating pressure drop as predicted by the modeling effort. Also, ESP control costs as a function of SCA were generated. These relationships are depicted in Figures 29 and 30 for an ESP and baghouse, respectively, and summarized in Table 25.

TABLE 21. BASIS FOR ESP DESIGN AND COST ESTIMATION

| | |
|---|---|
| Plant capacity | 350 MW |
| Flue gas flow rate | 36,400 acm/min at 177°C,<br>104 acm/min/MW at 177°C |
| Design SCA[a] | 43.5 $m^2/m^3/s$ |
| Plate area | 26,400 $m^2$ |
| Performance level | 13.0 ng/J |
| Precipitator configuration | 8 parallel chambers, thermally insulated cold side |

[a] Based on worst performance case, i.e., run 104 at 20 percent safety factor for SCA (25 percent safety factor for emission level).

## TABLE 22. BASIS FOR BAGHOUSE DESIGN AND COST ESTIMATION

| | |
|---|---|
| Plant capacity | 350 MW |
| Flue gas flow rate | 36,400 acm/min at 177°C,<br>104 acm/min/MW at 177°C |
| A/C ratio | 1.52 $m^2/m^3$/min (5.0 ft/min) |
| Reverse A/C ratio | 2.0 $m^2/m^3$/min (6.6 ft/min) |
| Total net cloth area | 23,900 $m^2$ |
| System pressure drop | 1394 $N/m^2$ (1046 $N/m^2$ across the fabric)<br>5.6 in WC (4.2 in across the fabric) |
| Emission level | 0.5 ng/J |
| Number of chambers | 14 |
| Cleaning cycle time | 28 min |
| Total cycle time | 80 min |
| Thermal insulation | Yes |

## TABLE 23. BASIS FOR SCRUBBER DESIGN AND COST ESTIMATION

| | |
|---|---|
| Plant capacity | 350 MW |
| Flue gas flow rate | 36,400 acm/min at 177°C,<br>104 acm/min/MW at 177°C |
| Scrubber configuration | Three parallel modular venturi scrubbers |
| Sludge treatment | Clarification, filtration, and landfill |
| System pressure drop[a] (required for emission level of 13 ng/J) | 10 cm WC |
| Material of construction | Carbon steel |

[a] Based on 100 percent safety factor for system pressure drop (35 percent safety factor for emission level).

## TABLE 24. SUMMARY OF COSTS OF CONTROL (in 1000's of December 1979 dollars)

| Item | ESP | Baghouse | Scrubber |
|---|---|---|---|
| 1. Equipment cost (control device plus auxiliaries) | 3325 | 2172 | 1892 |
| 2. Tax and freight at 7% of 1 | 233 | 152 | 132 |
| 3. Installation costs at 75%[a] of 1 | 2494 | 1629 | 2649[a] |
| 4. Subtotal (1 + 2 + 3) | 6052 | 3953 | 4673 |
| 5. Engineering at 10% of 4 | 605 | 395 | 467 |
| 6. Subtotal (4 + 5) | 6657 | 4348 | 5140 |
| 7. Contingencies at 10% of 6 | 666 | 435 | 514 |
| 8. Total capital costs | 7323 | 4783 | 5654 |
| 9. Annual Operating costs | 115 | 261 | 983 |
| 10. Annual maintenance cost at 2% of 1[b] | 67 | 43 | 100 |
| 11. Annual cost of bag replacement (at 2 years life) | - | 43 | - |
| 12. Present worth of 8-11 at 20 years life and 8% discount rate | 9110 | 8195 | 16,287 |
| 13. Uniform annual equivalent of 12 | 928 | 835 | 1660 |
| 14. Control costs, mils/kWh | 0.37 | 0.33 | 0.66 |
| 15. SCA ($m^2/m^3/s$)<br>A/C ($m^3/min/m^2$)<br>$\Delta P$ cm WC | 43.5 | 1.52 | 10.0 |

[a] At 140 percent of 1 for scrubber

[b] For ESP and baghouse only. At 5 percent of 1 for scrubber.

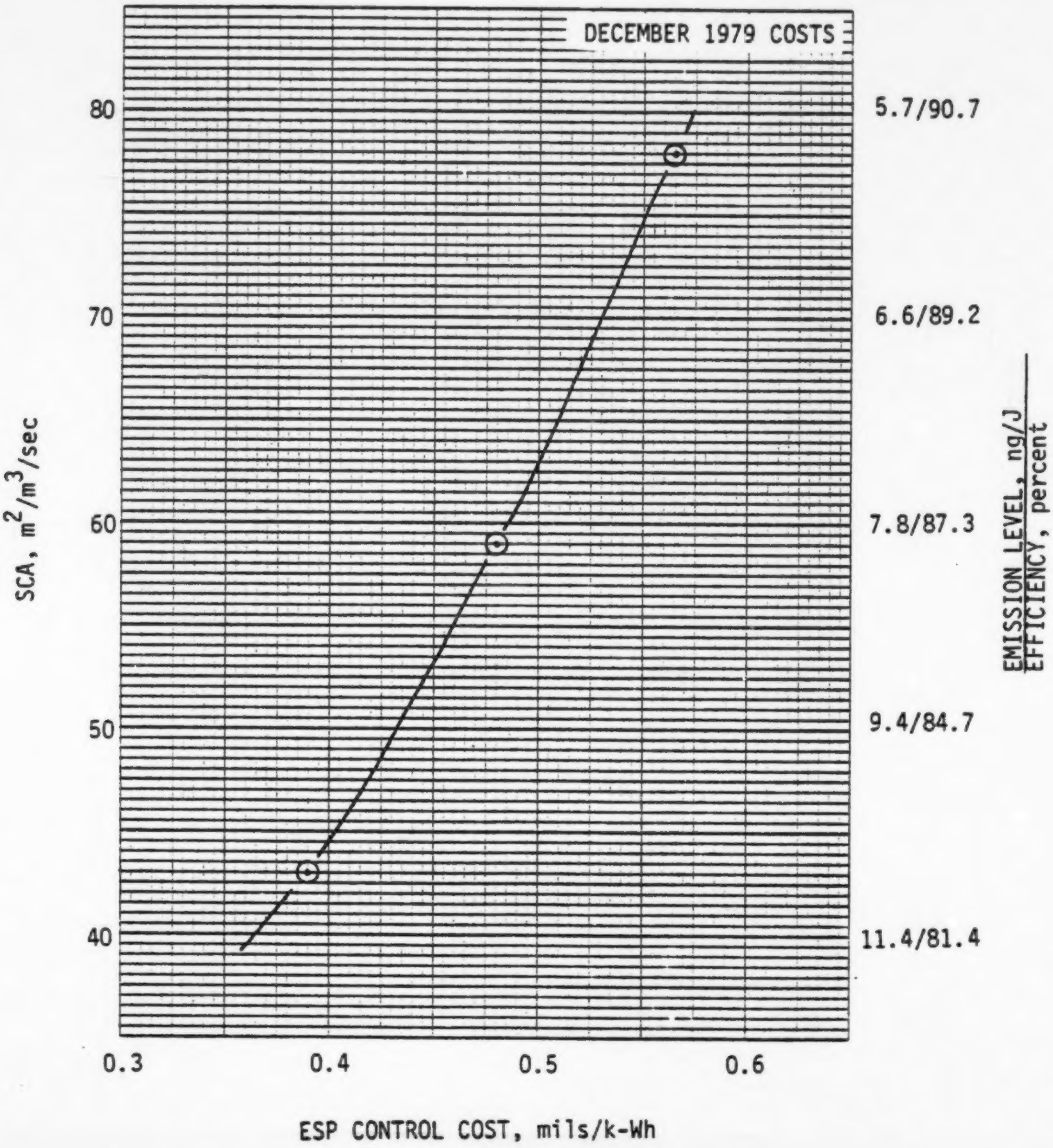

Figure 29. ESP costs versus SCA and emission level (emissions based on run 104 data and Matts-Ohnfeldt correlation).

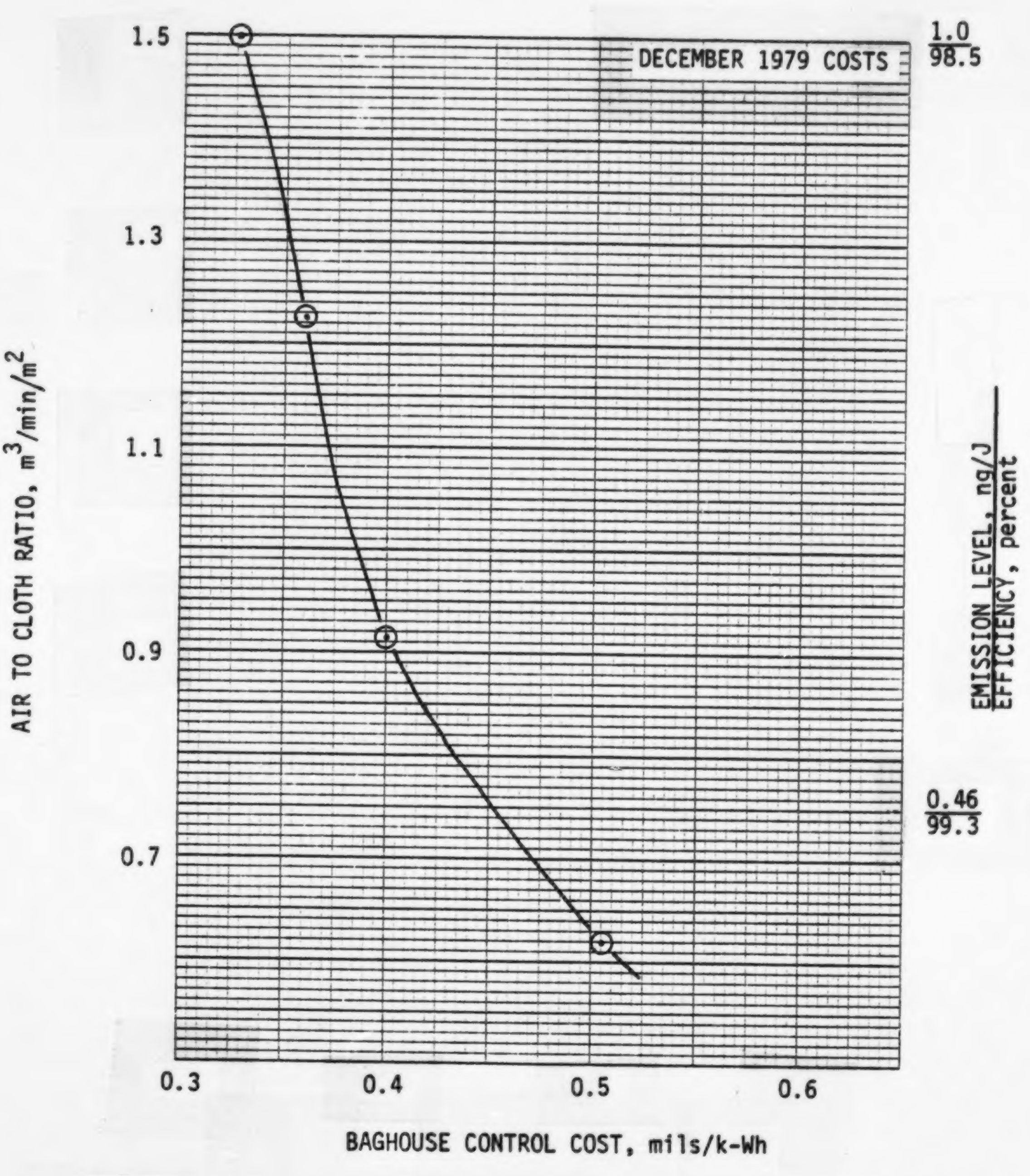

Figure 30. Baghouse costs versus air/cloth ratio and emission level.

TABLE 25. SUMMARY OF COSTS OF CONTROL VS. EMISSION LEVELS

ESP

| SCA $m^2/m^3/s$ | Efficiency, % | Emissions, ng/J | Costs, mils/kWh |
|---|---|---|---|
| 43 | 81.7 | 11.1 | 0.37 |
| 59 | 87.0 | 7.9 | 0.48 |
| 78 | 90.4 | 5.9 | 0.565 |

Baghouse

| A/C ratio | | Efficiency, % | Emissions, ng/J | Costs, mils/kWh |
|---|---|---|---|---|
| $m^2/m^3/min$ | (ft/min) | | | |
| 1.52 | (5.0) | 98.5 | 1.0 | 0.325 |
| 1.40 | (4.6) | 98.8 | 0.8 | 0.36 |
| 0.91 | (3.0) | 99.2 | 0.6 | 0.40 |
| 0.79 | (2.6) | 99.3 | 0.5 | 0.44 |
| 0.62 | (2.0) | 99.4 | 0.4 | 0.505 |

# REFERENCES

1. Hoke, R. C., et al. Miniplant Studies of Pressurized Fluidized-Bed Combustion, Third Annual Report. EPA-600/7-78-069, April 1978.

2. Hoke, R. C., et al. Studies of the Presurized Fluidized-Bed Coal Combustion Process. EPA-600/7-77-107, September 1977.

3. Hoke, R. C., et al. Studies of the Pressurized Fluidized-Bed Coal Combustion Process. EPA-600/7-76-011, September 1976.

4. Mobile Electrostatic Precipitator Specification, Operation and Maintenance. Operating Manual prepared for U.S. Environmental Protection Agency, Research Triangle Park, NC, by Environmental Sciences Group, Naval Surface Weapons Center, Dahlgren, Virginia, October 1976.

5. Hall, R. R. Mobile Fabric Filter System: Design Report. U.S. Environmental Protection Agency Contract No. 68-02-1075. NTIS No. PB 246-287/7BA. GCA/Technology Division, Bedford, Massachusetts, October 1974. 73 pp.

6. Nichols, G. N. Test Methods and Apparatus for Conducting Resistivity Measurements. U.S. Environmental Protection Agency, Contract no. 68-02-1083, Final Report No. 3121 - III, September 1977.

7. Cushing, K. M., G. E. Lacey, J. D. McCain, and W. B. Smith. Particulate Sizing Techniques for Control Device Evaluation: Cascade Impactor Calibrations. EPA-600/2-76-280, NTIS No. PB 262-849, U.S. Environmental Protection Agency, Research Triangle Park, NC, October 1976. 79 pp.

8. Lawless, P. A. Analysis of Cascade Impactor Data for Calculating Particle Penetration. EPA-600/7-78-189, U.S. Environmental Protection Agency, Industrial Environmental Research Laboratory, Research Triangle Park, NC, September 1978. 39 pp.

9. McDonald, J. R. A Mathematical Model of Electrostatic Precipitation (Revision 1): Volume I. Modeling and Programming. EPA-600/7-78-111a, U.S. Environmental Protection Agency, Research Triangle Park, NC, June 1978. 637 pp.

10. Dennis, R., and H. A. Klemm. Fabric Filter Model, Format Change: Volume I. Detailed Technical Report and Volume II. User's Guide. EPA-600/7-79-043a and EPA-600/7-79-043b, U.S. Environmental Protection Agency, Industrial Environmental Research Laboratory, Research Triangle Park, NC, February 1979.

11. Yung, S. C., S. Calvert, and H. F. Barbarika. Venturi Scrubber Performance Model. EPA-600/7-79-172, NTIS No. PB 271-515, U.S. Environmental Protection Agency, Research Triangle Park, NC, August 1977. 197 pp.

12. Davies, C. N. The entry of Aerosols into Sampling Tubes and Heads. British Journal of Applied Physics, 1(2):921-932, 1968.

13. Kinkley, M. L., and R. B. Neveril. Capital and Operating Costs of Selected Air Pollution Control Systems. EPA-450/3-76-014, NTIS No. PB 258-484, U.S. Environmental Protection Agency, Research Triangle Park, NC, May 1976. 208 pp.

14. Barrier, J. W., H. L. Faucett, and L. J. Henson. Economics of Disposal of Lime/Limestone Scrubbing Wastes: Untreated and Chemically Treated Wastes. TVA Bull. Y-123, EPA-600/7-78-023a, NTIS No. PB 218-391, U.S. Environmental Protection Agency, Research Triangle Park, NC, February 1978. 416 pp.

# APPENDIX A

## Exxon Miniplant Run Summaries

## TABLE A-1. MINIPLANT PRESSURIZED FLUIDIZED-BED COAL COMBUSTION RUN SUMMARY

| Exxon PFBC run no.: | 102 | 103.0 | 103.1 | 103.2 | 103.3 |
|---|---|---|---|---|---|
| 1979 date: | 3/13-17 | 3/30-4/1 | 4/1-3 | 4/3-4 | 4/4-6 |
| Operating conditions | | | | | |
| Length, hr | 106.5 | 54 | 48 | 20 | 56.5 |
| Pressure, kPa | 710 | 710 | 710 | 710 | 710 |
| Averaged bed temperature, °C | 890-910 | 890-910 | 890-910 | 890-910 | 890-910 |
| Superficial gas velocity, m/s | 1.3-1.4 | 1.3-1.4 | 1.3-1.4 | 1.3-1.4 | 1.3-1.4 |
| Expanded bed height, m | ~2.4 | ~2.5 | ~2.5 | ~2.5 | ~2.5 |
| Coal feed rate, kg/hr | ~75 | ~80 | ~85 | ~85 | ~85 |
| Ca/S ratio[a] - set | 1.0 | 1.0 | 0.5 | 0.5 | 0.5 |
| Ca/S ratio - calculated | 1.45 | 1.24 | 0.62 | 0.62 | 0.93 |
| Coal | CH[b] | CH | CH | CH | CH |
| Sorbent | GL[c] | GL | GL | GL | GL |
| Combustor flue gas emissions | | | | | |
| $SO_2$, ppm | 0-30 | 0-60 | 0-60 | 0-60 | 0-70 |
| $No_x$, ppm | 50-75 | 50-75 | 50-75 | 50-75 | 50-75 |
| CO, ppm | ~60 | ~60 | ~60 | ~60 | ~60 |
| $CO_2$, % | 15-16.3 | 15-16.3 | 15-16.3 | 15-16.3 | 15-16.3 |
| $O_2$, % | 2.5-3 | ~3 | ~3 | ~3 | ~3 |

See footnotes at end of table, page A-3.

(continued)

TABLE A-1. (Continued)

| Exxon PFBC run no.: | 102 | 103.0 | 103.1 | 103.2 | 103.3 |
|---|---|---|---|---|---|
| 1979 date: | 3/13-17 | 3/30-4/1 | 4/1-3 | 4/3-4 | 4/4-6 |
| Regenerator operating conditions | | | | | |
| Pressure, kPa | 714 | 714 | 714 | 714 | 714 |
| Bed temperatures, °C | | | | | |
| Reducing zone | 980-1040 | 980-1040 | 980-1040 | 980-1040 | 980-1040 |
| Oxidizing zone | 1025-1065 | 1025-1065 | 1025-1065 | 1025-1065 | 1025-1065 |
| Superficial gas velocity, m/s | 0.8-0.9 | 0.8-0.9 | 0.8-0.9 | 0.8 | 0.7-0.8 |
| Air-to-fuel equivalence ratio, ϕ | 1.4 | 1.4 | 1.4 | 1.4 | 1.4 |
| Expanded bed height, m | 1.5 | 1.5-1.7 | 1.5-1.7 | 1.5-1.7 | 1.5-1.6 |
| Solids recirculation rate, kg/hr | 88.5 | 22.7 | 22.7 | 12.3 | 12.3 |
| Average regenerator flue gas emissions | | | | | |
| $SO_2$, % | ~0.4 | ~0.3 | ~0.39 | ~0.3 | ~0.27 |
| CO, ppm | 500-2000 | 500-2000 | 500-2000 | 500-2000 | 500-2000 |
| $CO_2$, % | 10-12 | 10-12 | 10-12 | 10-12 | 10-12 |

[a] Assuming 2 percent sulfur coal.

[b] CH = Champion coal.

[c] GL = Grove limestone.

## TABLE A-2. MINIPLANT PRESSURIZED FLUIDIZED-BED COAL COMBUSTION RUN SUMMARY

| Exxon PFBC run no.: | 104 | 105 |
|---|---|---|
| 1979 date: | 4/17-20 | 4/30-5/5 |
| Operating conditions | | |
| Run length, hr | 83.5 | 98.5 |
| Pressure, kPa | 850 | 710 |
| Air flow rate, $m^3$/min | 11.5 | - |
| Temperature gradient, °C/m | - | - |
| Avg. bed temperature, °C | 899 | 890-910 |
| Superficial velocity, m/s | 1.62 | 1.5 |
| Settled bed height, m | - | - |
| Initial | 2.10 | - |
| Final | 1.81 | 2.7 |
| Expanded bed height, m | 2.97 | |
| Coal feed rate, kg/hr | 93 | 87 |
| Ca/S molar feed ratio - set | 1.49 | 1.00 |
| Ca/S molar feed ratio - calculated | 42.1 | 1.22 |
| Excess air, % | | |
| Sorbent | PD[a] | GL[b] |
| Coal | CH[c] | CH |
| Flue gas emissions | | |
| $SO_2$, ppm | 70 (5-160) | 30-90 |
| $NO_x$, ppm | 80 | 50-75 |
| CO, ppm | 105 | ~60 |
| $CO_2$, % | 13.7 | 15-16.3 |
| $O_2$, % | 3.8 | 3-4 |
| Results | | |
| Retention, % | 93.3 (99.5-84.8) | |
| Sulfation, % | | |
| lb $SO_2/10^6$ Btu | 0.16 (0.01-0.37) | |
| lb $NO_x/10^6$ Btu | 0.13 | |
| Regenerator operating conditions | | |
| Pressure, kPa | 705 | |
| Bed temperatures, °C | | |
| Reducing zone | 1010 | |
| Oxidizing zone | 1032 | |
| Superficial gas velocity, m/s | 0.84 | |
| Air-to-fuel equivalence ratio, $\phi$ | 1.4 | |
| Expanded bed height, m | 1.89 | |
| Solids recirculation rate, kg/hr | 15.4 | |

See footnotes at end of table, page A-5. (continued)

Table A-2. (Continued)

| Exxon PFBC run no.: | 104 | 105 |
|---|---|---|
| 1979 date: | 4/17-20 | 4/30-5/5 |
| Average regenerator flue gas emissions | | |
| $SO_2$, % | ~0.5 | - |
| CO, ppm | 1000-2000 | - |
| $CO_2$, % | 10-12 | - |

[a] PD = Pfizer dolomite.

[b] GL = Grove limestone.

[c] CH = Champion coal.

[d] ILL = Illinois coal no. 6.

## TABLE A-3. MINIPLANT PRESSURIZED FLUIDIZED-BED COAL COMBUSTION RUN SUMMARY

| Exxon PFBC run no.: | 106.1 | 106.2 | 106.3 | 107 | 108 |
|---|---|---|---|---|---|
| 1979 date: | 5/29-6/10 | 5/29-6/10 | 5/29-6/10 | 6/18-23 | 6/26-29 |
| Operating conditions | | | | | |
| Run length, hr | 43 | 5 | 217 | 108 | 71 |
| Pressure, kPa | 902 | 902 | 912 | 912 | 912 |
| Air flow rate, $m^3$/min | 20.6 | 19.7 | 20.2 | 16.5 | 16.4 |
| Temperature gradient, °C/m | -64.2 | -69.3 | -70.9 | -71.4 | -100 |
| Avg. bed temperature, °C | 914 | 904 | 908 | 872 | 877 |
| Superficial velocity, m/s | 1.71 | 1.62 | 1.64 | 1.31 | 1.31 |
| Settled bed height, m | | | | | |
| Initial | 2.04 | - | - | 2.12 | 2.03 |
| Final | - | - | 1.86 | 1.06 | 0.96 |
| Expanded bed height, m | 2.41 | 3.25 | 3.05 | 1.74 | 1.57 |
| Coal feed rate, kg/hr | 139 | 144.7 | 143.8 | 84.4 | 86.3 |
| Ca/S molar feed ratio - set | 1.35 | 1.19 | 1.25 | 1.25 | 1.25 |
| Ca/S molar feed ratio - calculated | - | - | - | 1.37 | 1.24 |
| Excess air, % | 15.6 | 5.8 | 9.0 | 31.4 | 23.0 |
| Sorbent | PD[a] | PD | PD | PD | PD |
| Coal | ILL[b] | ILL | ILL | CH[c] | CH |
| Flue gas emissions | | | | | |
| $SO_2$, ppm | 21.4 | 37.8 | 91.4 | 41.5 | 27.8 |
| $NO_x$, ppm | 47.5 | 42.4 | 64.1 | 26.4 | 44.6 |
| CO, ppm | 332 | 507 | 540 | 64.7 | 130.8 |
| $CO_2$, % | 14.8 | 16.4 | 13.4 | 12.8 | 14.2 |
| $O_2$, % | 3.1 | 1.1 | 2.1 | 5.1 | 4.0 |

See footnotes at end of table, page A-7.

(continued)

## TABLE A-3. (Continued)

| Exxon PFBC run no.: | 106.1 | 106.2 | 106.3 | 107 | 108 |
|---|---|---|---|---|---|
| 1979 date: | 5/29-6/10 | 5/29-6/10 | 5/29-6/10 | 6/18-23 | 6/26-29 |
| Results | | | | | |
| Retention, % | 98.8 | 96.9 | 99.2 | 99.6 | 98.7 |
| Sulfation, % | - | - | - | 72.57 | 79.78 |
| lb $SO_2/10^6$ Btu | 0.2 | 0.10 | 0.11 | 0.04 | 0.0 |
| lb $NO_x/10^6$ Btu | 0.06 | 0.06 | 0.08 | 0.13 | 0.08 |

[a] PD = Pfizer dolomite.

[b] ILL = Illinois coal no. 6.

[c] CH = Champion coal.

# APPENDIX B

## Mobile Baghouse Operational Problems

## CHRONOLOGICAL SUMMARY OF MOBILE BAGHOUSE PROGRAM OPERATIONAL PROBLEMS

| | |
|---|---|
| Tues. 5/29 | Initial preheat cycle started at 1705, discontinued at 2240. Insufficient heaters and insulation on slipstream to reach desired preheat level. |
| Wed. 5/30 | Additional band heaters and insulation put on slipstream. Preheat cycle started at 1315, switched over to miniplant process gas at 1430 with baghouse inlet temp. at 101°C. Initial gas flow extremely high, all flow measurement and static pressure gauges pegged. Turned off baghouse blower and closed manual gate valve downstream of blower. Leakage rate around valve gave flow of 180 acfm (7/1 A/C) |
| Thur. 5/31 | At 1216 miniplant shutdown due to plugged cyclone. Bags removed, inverted and lightly vacuumed to minimize possible blinding effect of extreme velocity during initial startup. Hopper assembly removed, cleaned, and replaced. Installed manual gate valve in baghouse inlet upstream of inlet sample ports for personnel protection due to positive pressure in line. Installed inlet and outlet orsat sample lines with toggle switch. |
| Fri. 6/1 | Bags rehung at 15 lb tension. Visible amount of dust still present in interstitial spaces. |

| | |
|---|---|
| | Miniplant restarted at 1800. Preheat cycle for baghouse started at 1913 after miniplant reached equilibrium. Pressure drop across bags appears normal for new bags; assume no blinding occurred or was corrected by vacuuming. Switched to miniplant flue gas at 2030. Flow rate still too high, 90 acfm or A/C of 3.4. Closed manual gate valve downstream of blower to reduce flow to 66 acfm or A/C of 2.5. Several leaks in baghouse compartment and ducting. Baghouse shutdown to repair leaks at 0235. Restarted at 0315. |
| Sat. 6/2 | Still experiencing leakage due to positive pressure. Repairs underway. Ran first sample set. |
| Sun. 6/3 | Flow from miniplant dropping off, may be due to blockage at Exxon valve, which is 90 percent closed. Exxon valve open and closed twice with baghouse in bypass mode. Flow problem corrected. Will repeat every 8 hours. |
| Mon. 6/4 | Day's sample set started at 0931. Miniplant switched to kerosene for 30 minutes at 1001, baghouse in bypass mode. Miniplant back on coal at 1025. |
| Tues. 6/5 | Experiencing erratic flow and pressure drop readings. Difficult to keep static taps cleaned out. Flow and temperature dropped at 1900--due to rain and ambient temperature effect on miniplant process lines. |
| Wed. 6/6 | Operating better; flow and bag pressure drop still somewhat erratic. |

| | |
|---|---|
| Thur. 6/7 | Miniplant off coal at 1630, firing kerosene for approximately 30 minutes. Caused significant changes in temperature and static pressure profiles. |
| Fri. 6/8 | Compressor failed, piped in miniplant air supply. |
| Sat. 6/9 | All outlet samples to date, mass and impactor, contaminated with extraneous debris; looks like rust flakes and condensable material.<br>Visible evidence of condensate noticed on bag compartment windows at temperature of 166°F. |
| Sun. 6/10 | Condensation again noticed on both bag compartment windows. Outlet samples still contaminated. |
| 6/11-17 | Miniplant down for routine maintenance. |
| Mon. 6/18 | Baghouse compartment and hopper sections completely dismantled and cleaned in attempt to solve outlet sample contamination problem. Lower rear panel and roof section showed severe condensation/corrosion. Reassembled baghouse with new gaskets. Windows and hopper removed, cleaned, and reasembled with all new gasket material. All flow and static taps on outlet duct cleaned, lines blown out, and reassembled. |
| Tues. 6/19 | Exxon 3" I.P.S. valve failed, stuck, in open position--could not be repaired without miniplant shutdown. Installed 1/2" orifice plate in 2 1/2" slipstream at a flanged joint. After startup flow measurement indicates orifice too small. Second orificie installed with 10 percent greater area. Flow level right for desired A/C ratio. Conference call with Ron Hoke, Exxon; Bob |

| | |
|---|---|
| | Hall, GCA; and Bruce Henschel, EPA, to decide whether or not to inject methane after third cyclone. Prupose being to raise pilot baghouse temperatures to avoid further acid condensation problems. Will not inject methane because of compromising GCA level 2 assessment. |
| Wed. 6/20 | Installed seven more 300 W band heaters on slipstream and two 250 W strip heaters on baghouse roof to minimize condensation problems. Outlet samples look better, but still seeing some contamination. Exxon fabricating new outlet duct section for span from bag compartment past outlet sample ports. |
| Thur. 6/21 | Installed new section of outlet duct at 1230. Miniplant fired kerosene from 0240 to 0340 last night. Baghouse back on line at 1530. Cannot preheat with no way to isolate slipstream from miniplant due to stuck valve. Samples (set #10) started at 1830. |
| Fri. 6/22 | Sample set #10 looked OK. Set #11 to be run today. |
| Sat. 6/23 | Miniplant and pilot baghouse shutdown at 0540 for weekend. |
| 6/26-29 | Operations normal, samples look good. |

# APPENDIX C

## ESP Inlet and Outlet Differential Size Distribution Curves

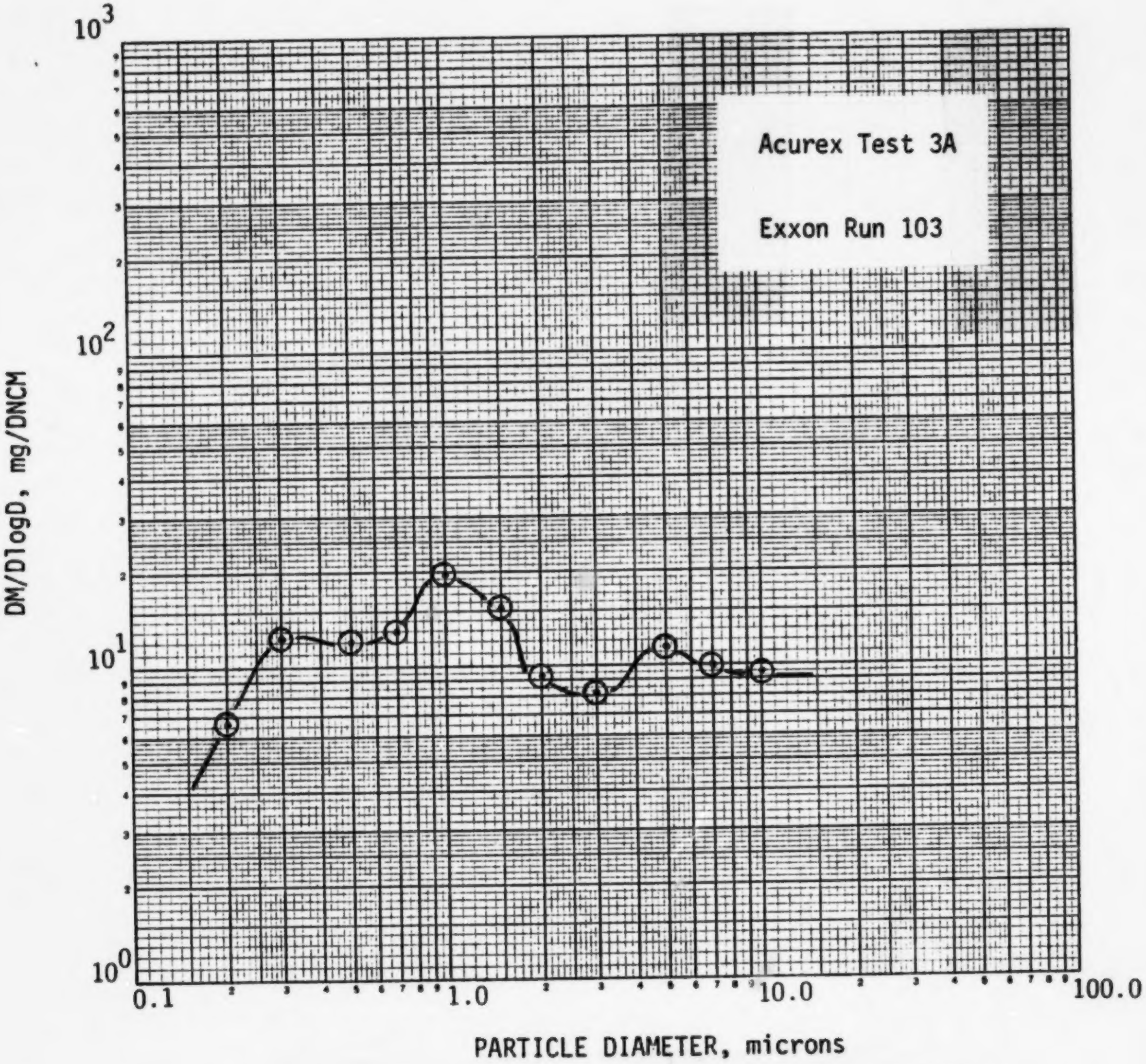

**Figure C-1. ESP inlet differential size distribution.**

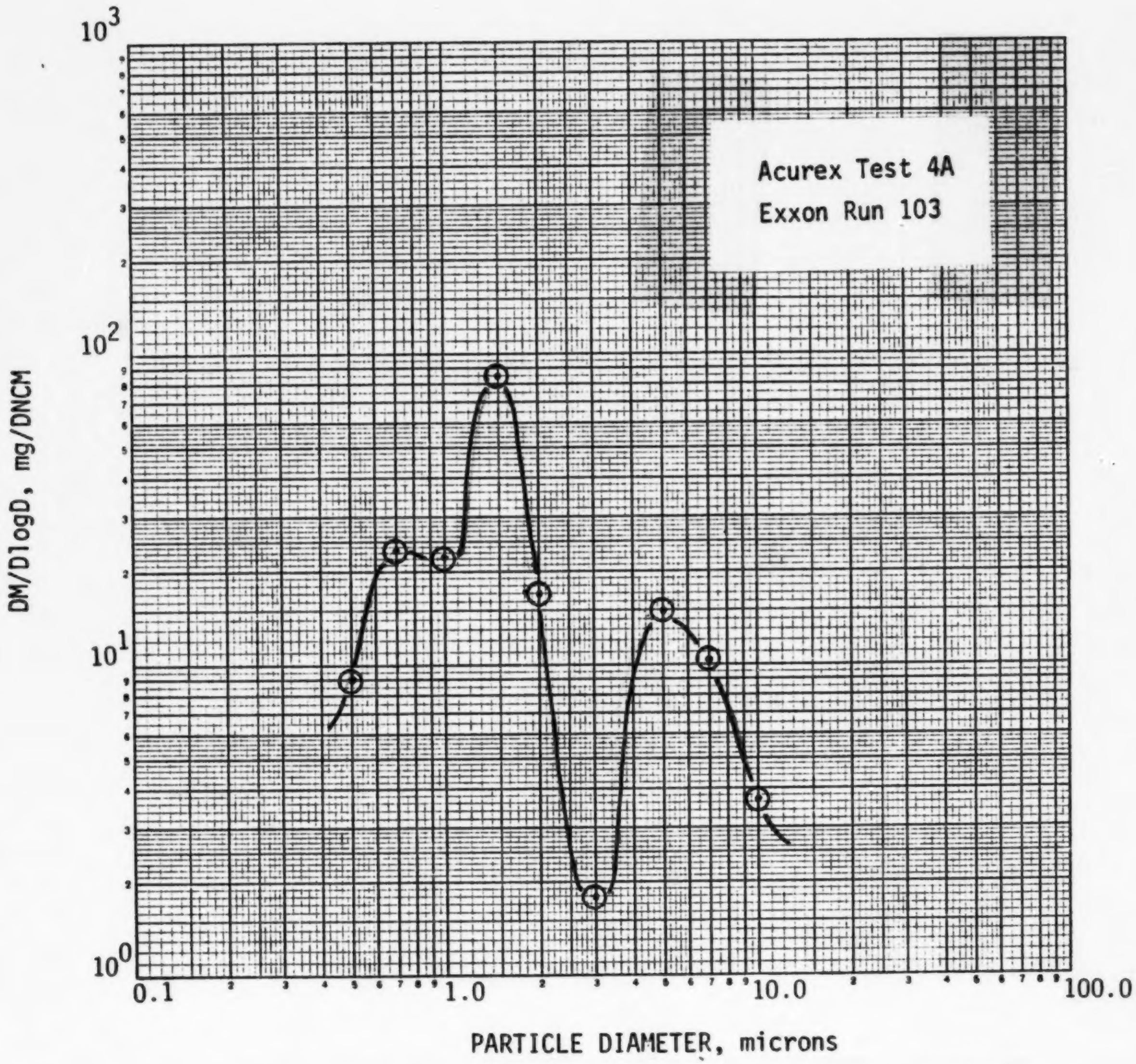

Figure C-2. ESP inlet differential size distribution.

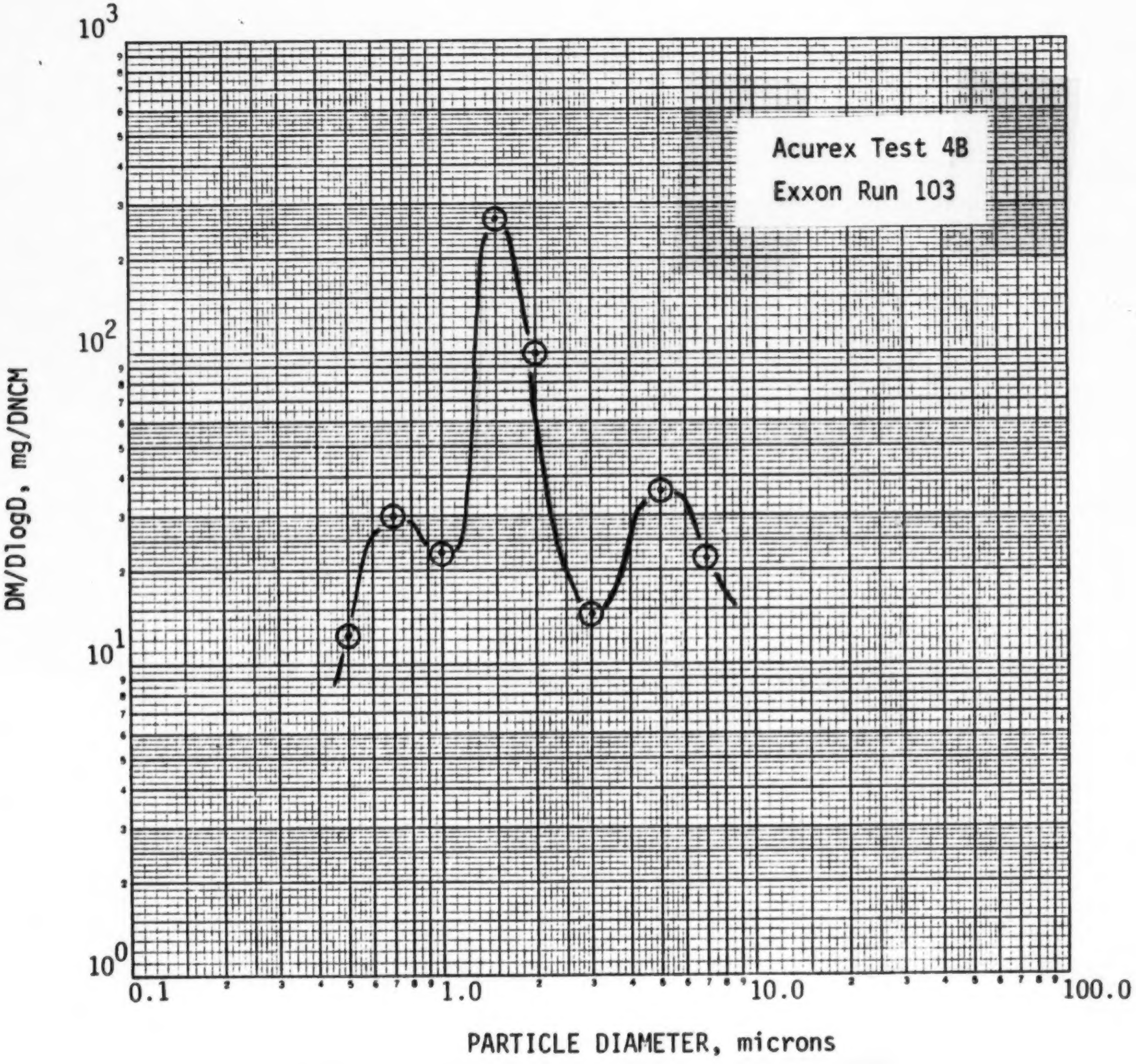

Figure C-3. ESP inlet differential size distribution.

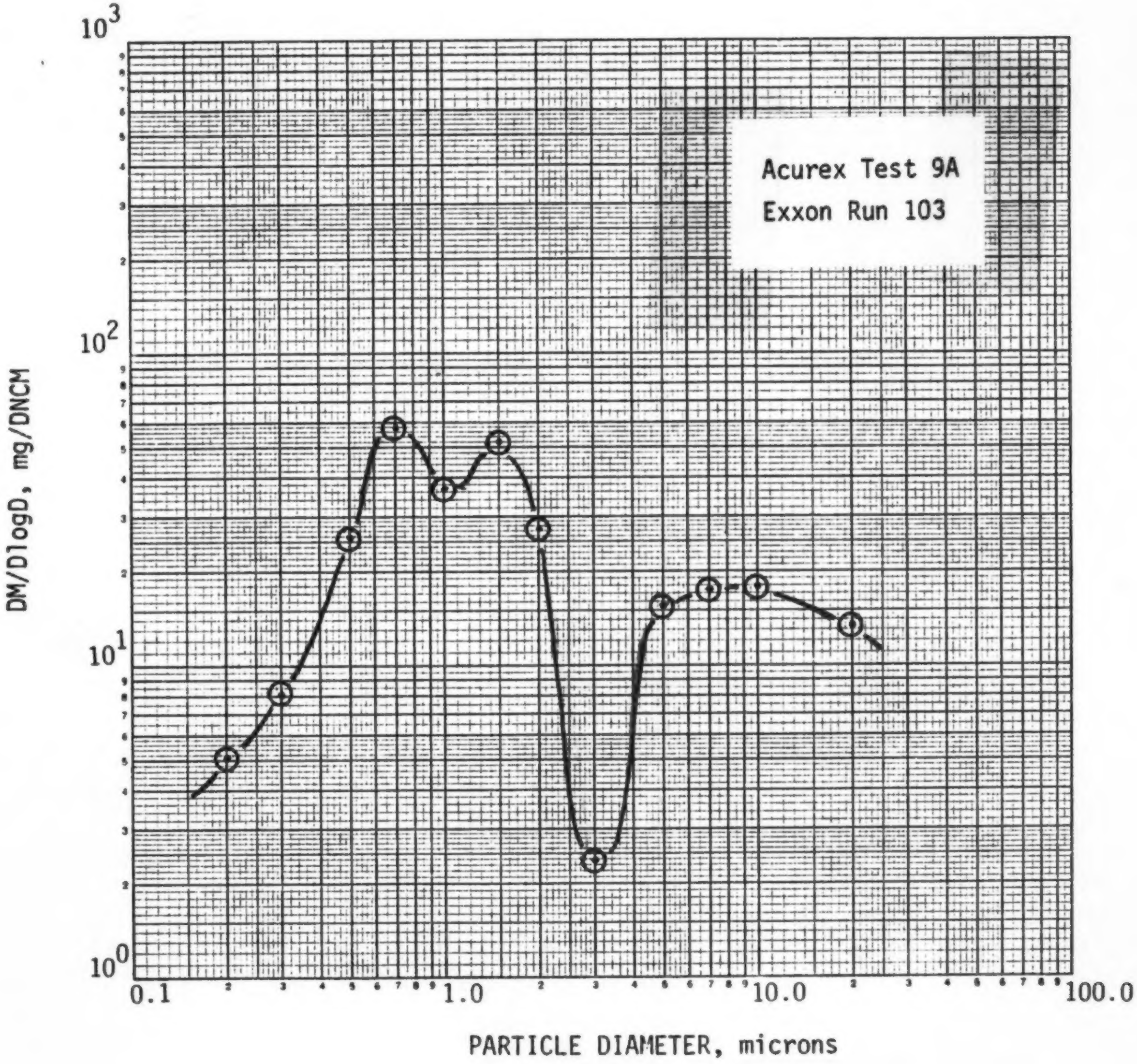

Figure C-4. ESP inlet differential size distribution.

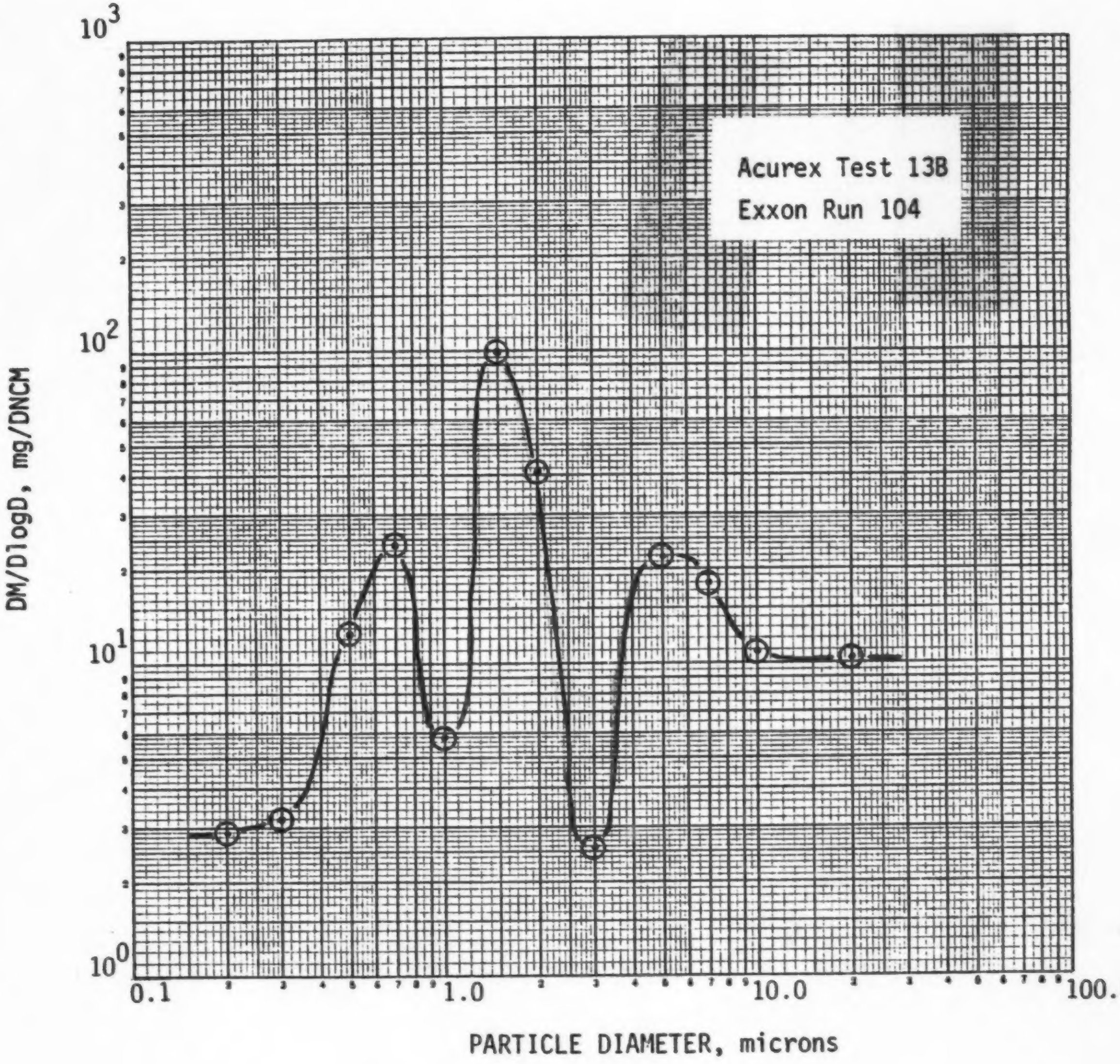

Figure C-5. ESP inlet differential size distribution.

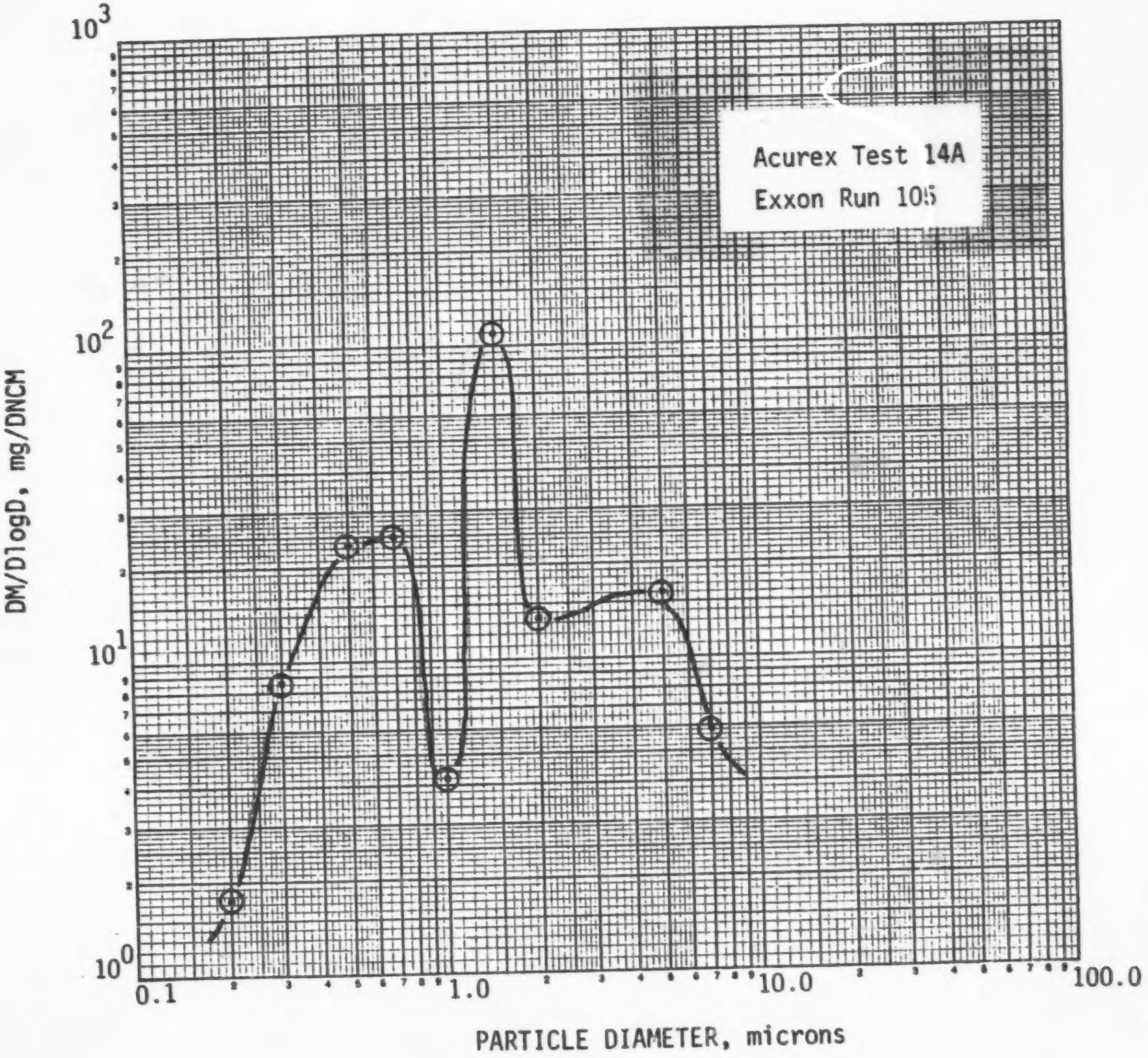

Figure C-6. ESP inlet differential size distribution.

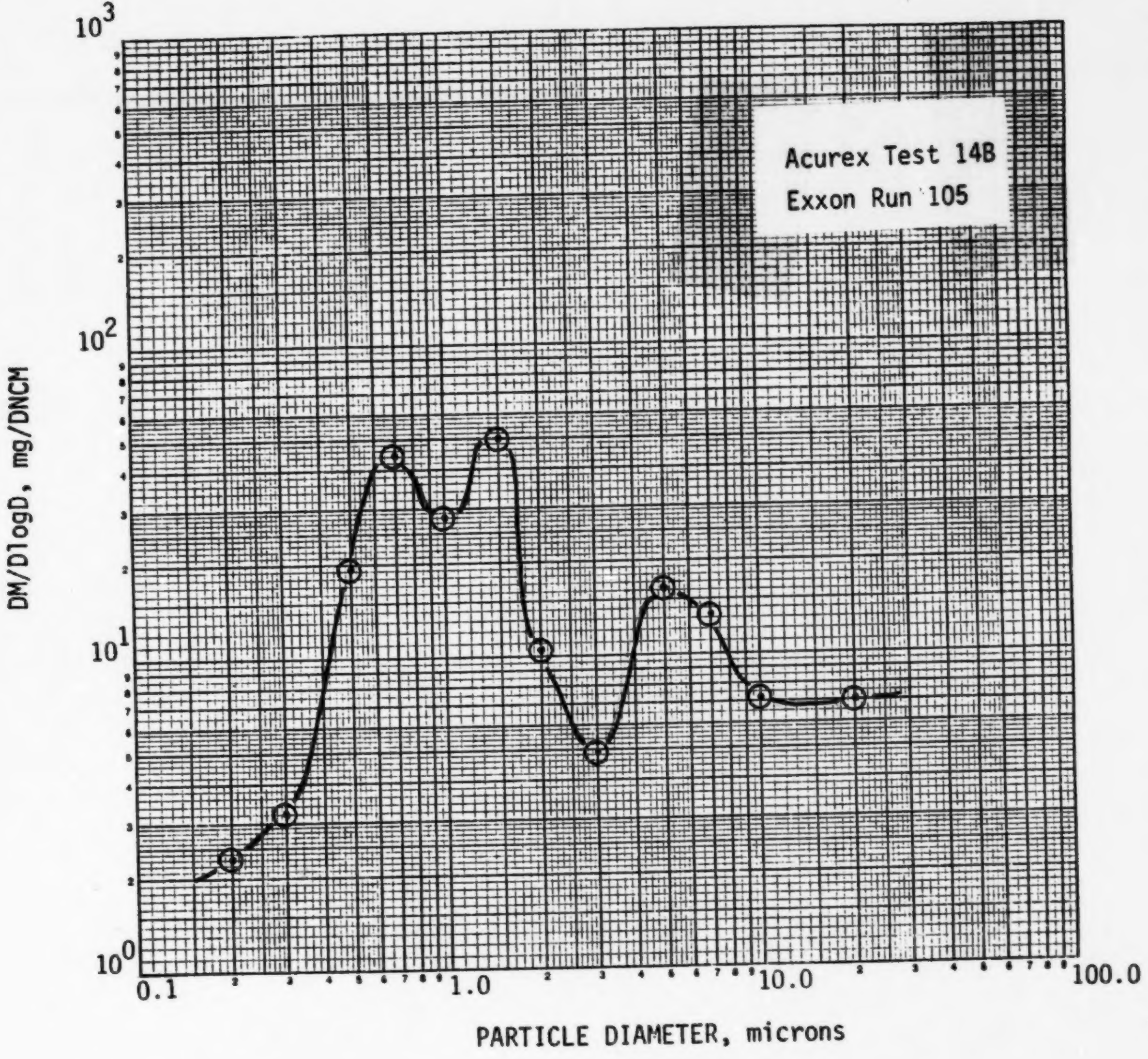

Figure C-7. ESP inlet differential size distribution.

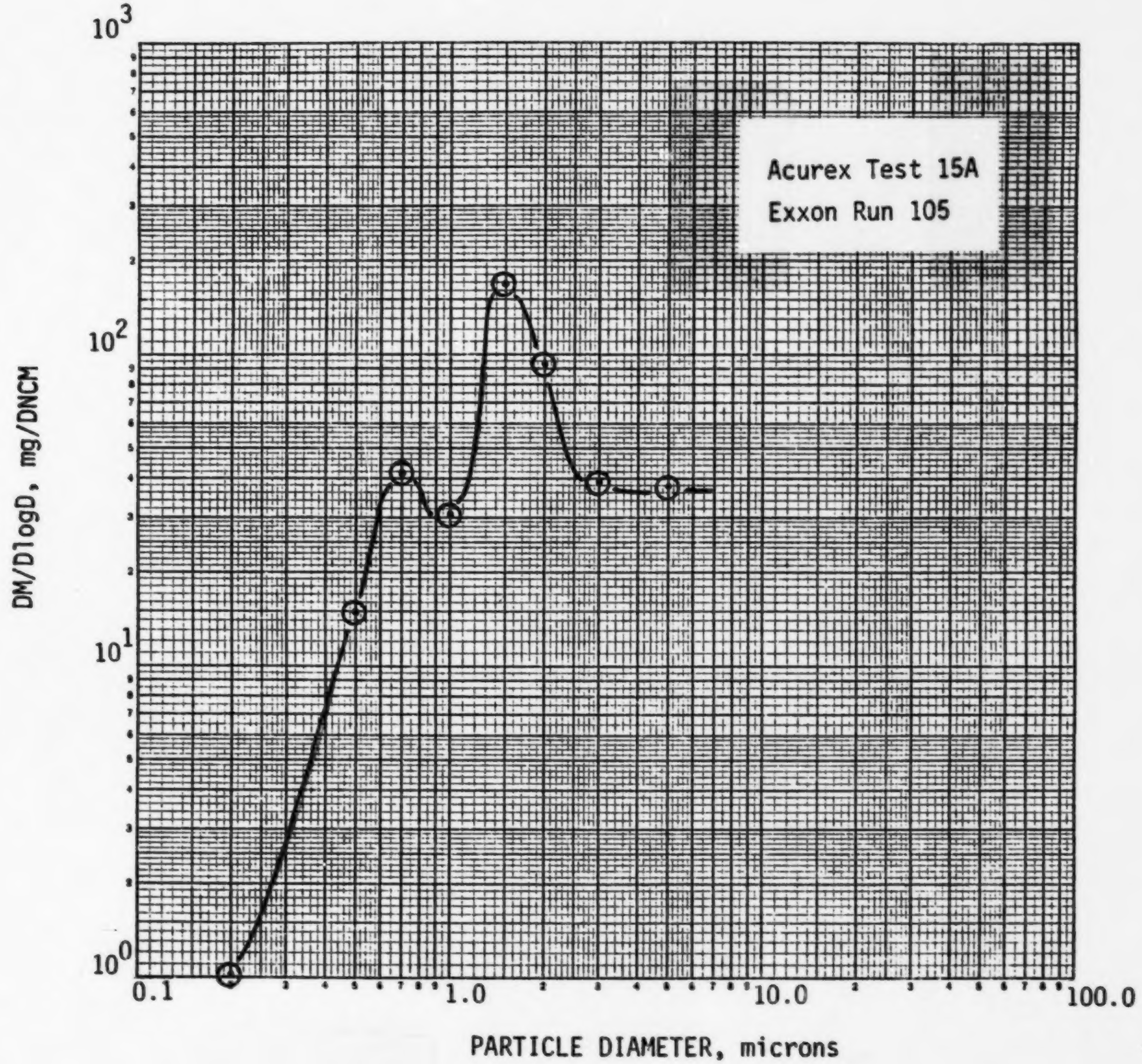

Figure C-8. ESP inlet differential size distribution.

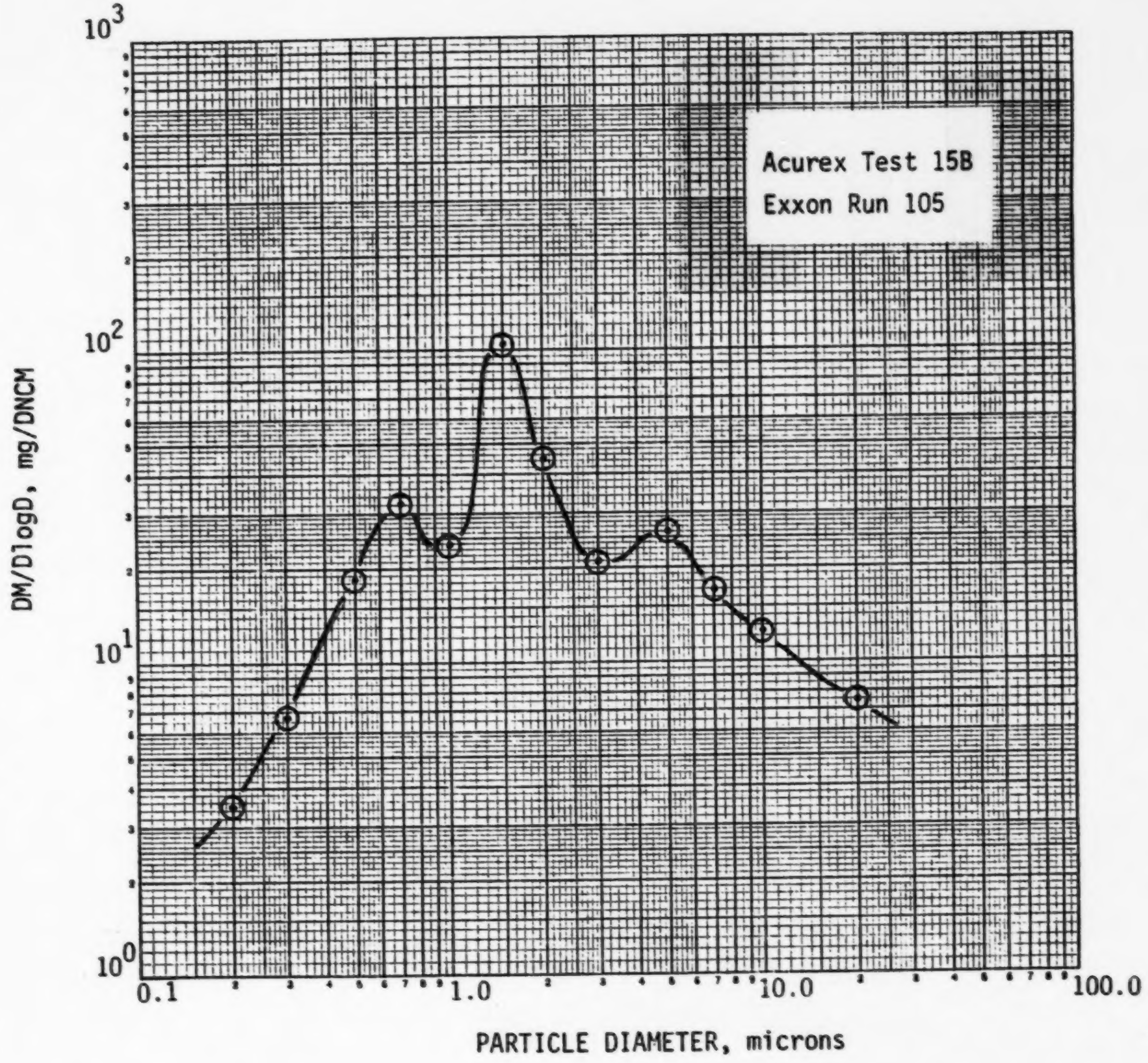

Figure C-9. ESP inlet differential size distribution.

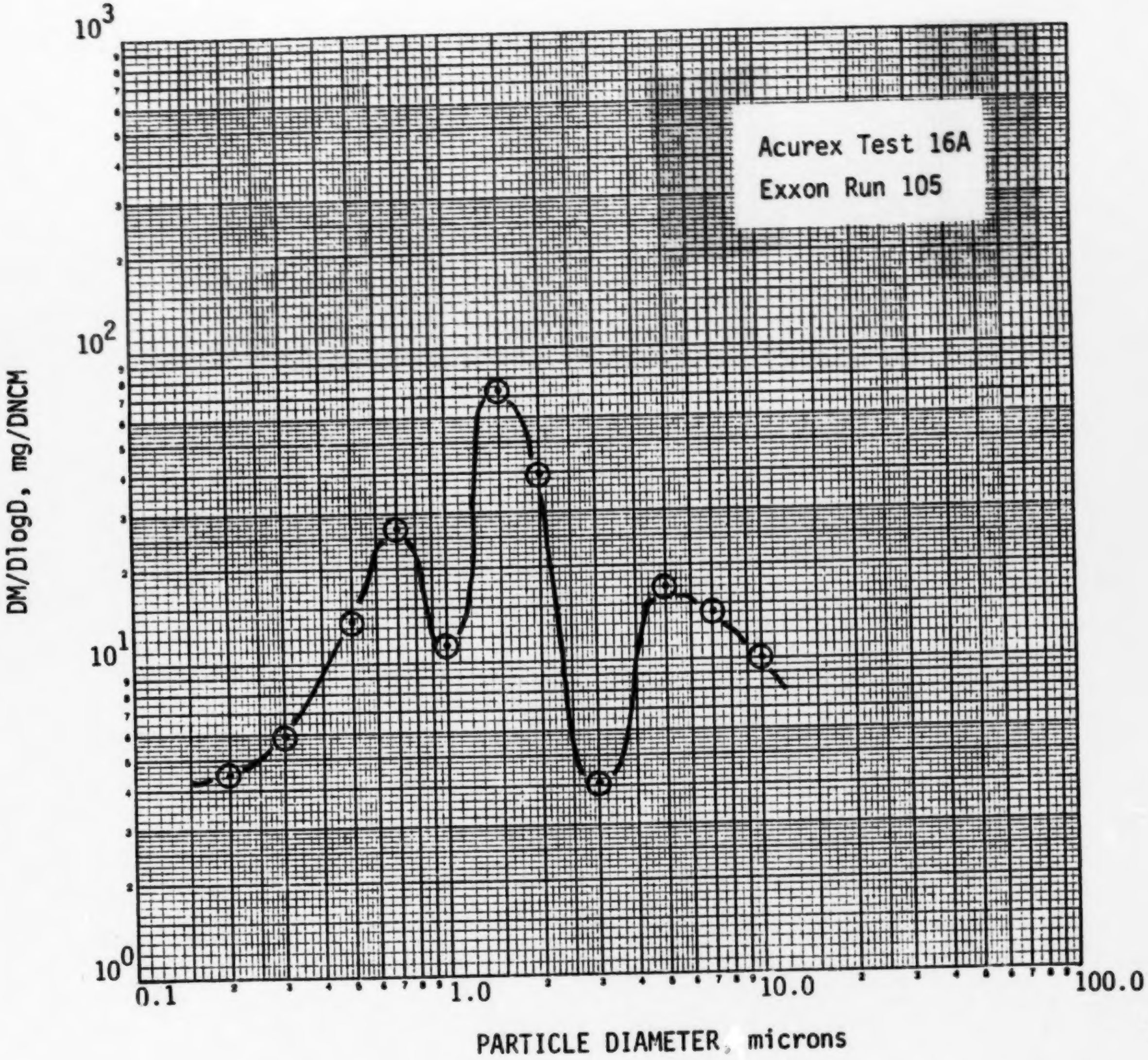

Figure C-10. ESP inlet differential size distribution.

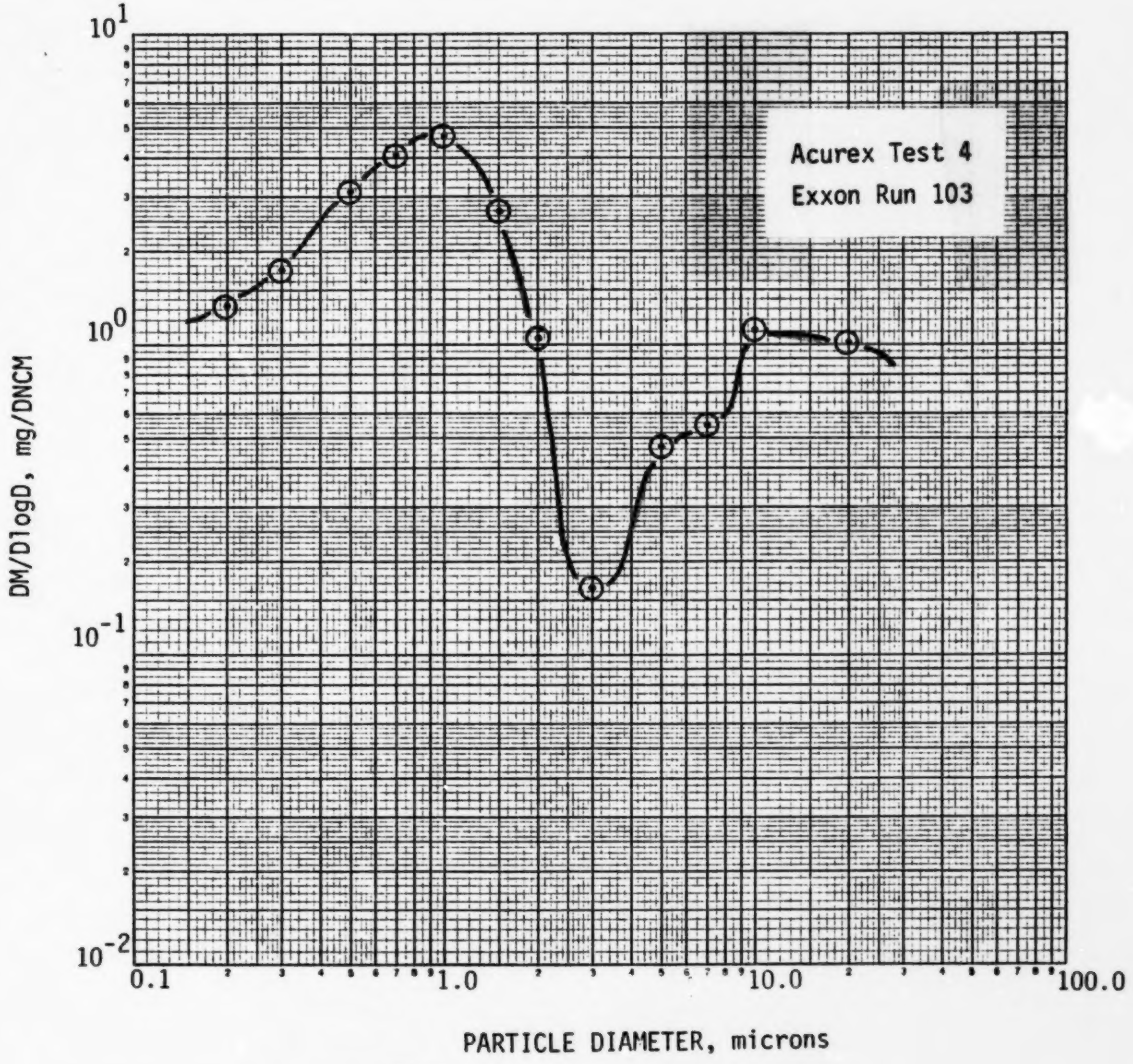

Figure C-11. ESP outlet differential size distribution.

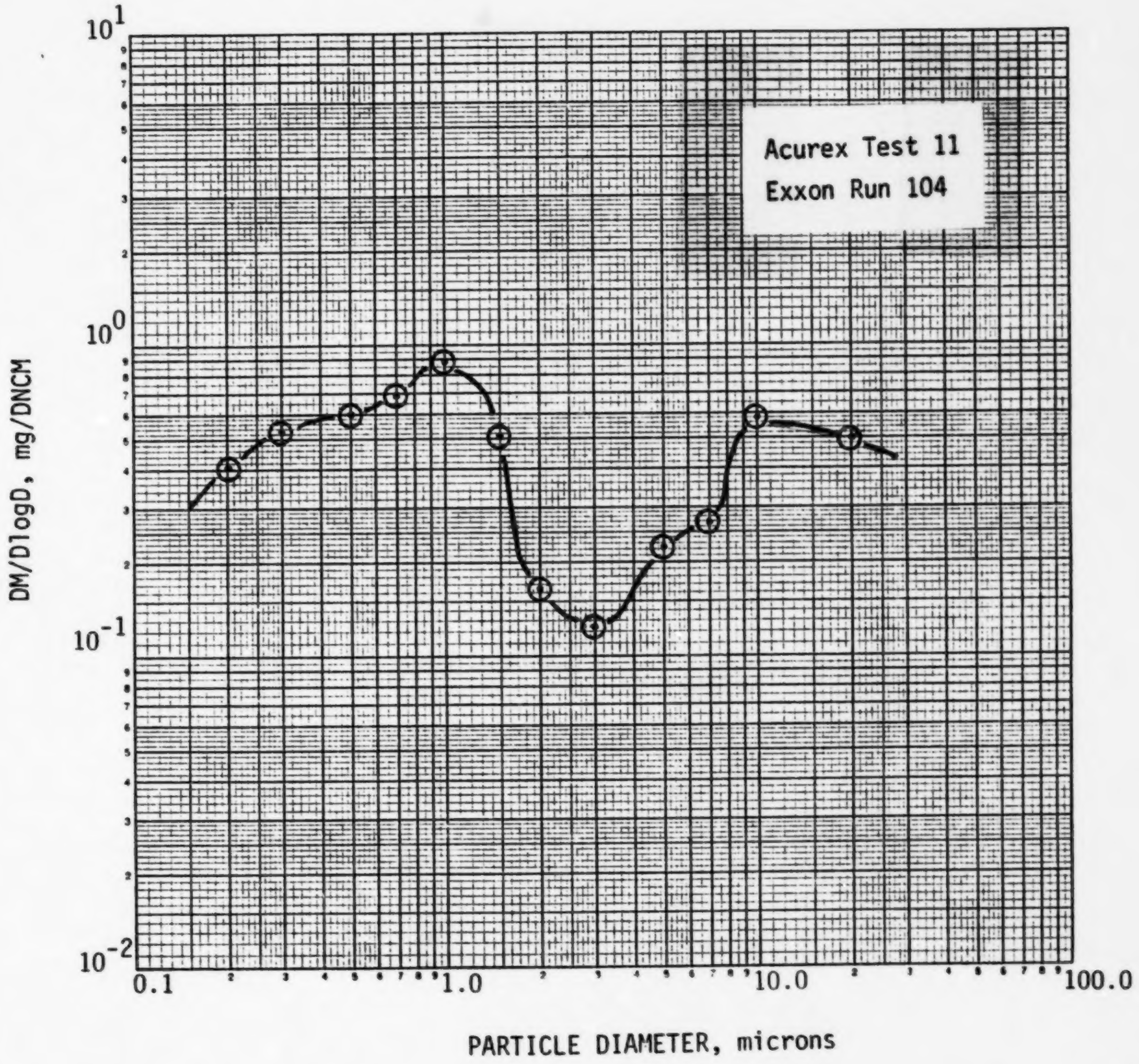

Figure C-12. ESP outlet differential size distribution.

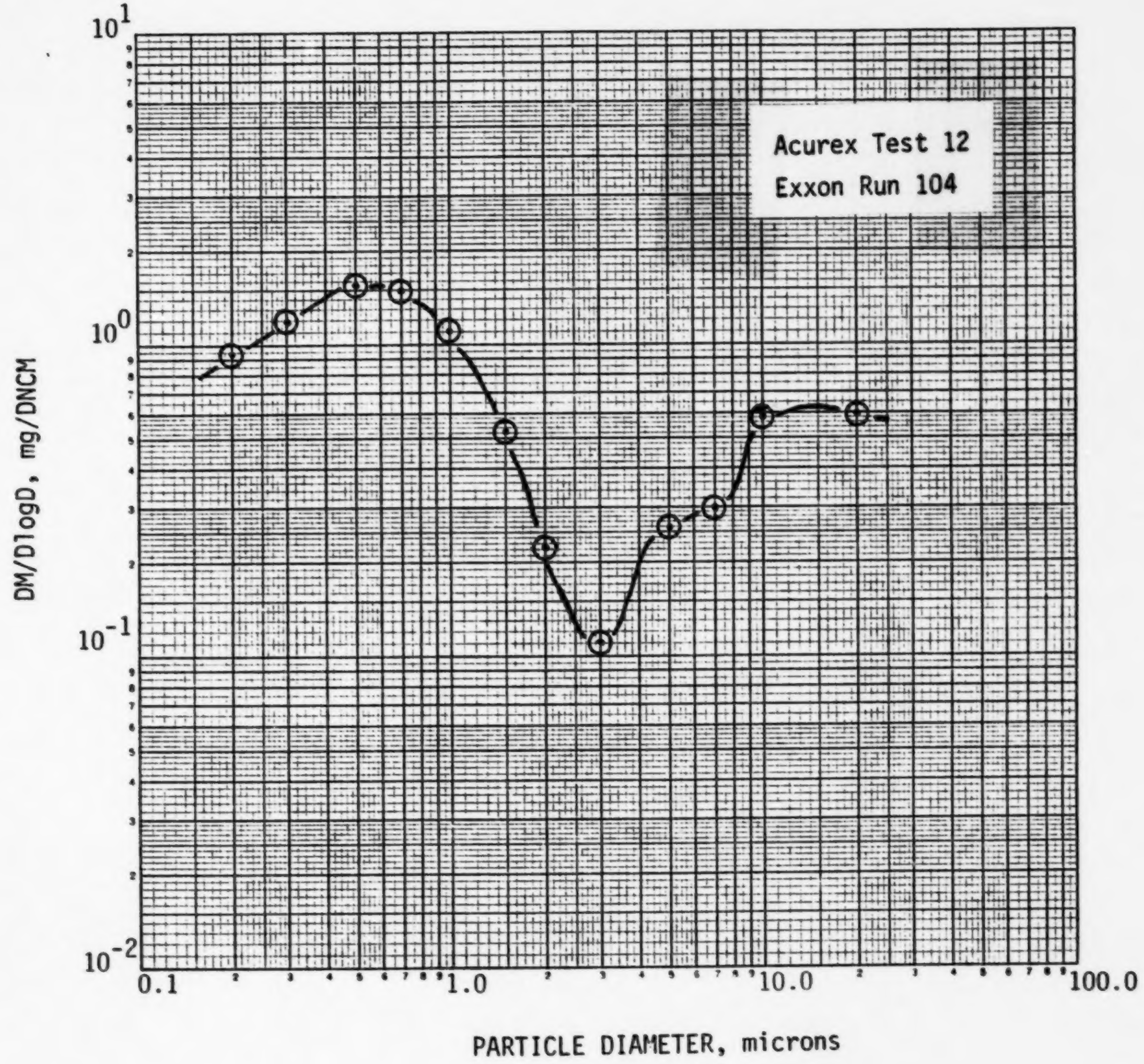

Figure C-13. ESP outlet differential size distribution.

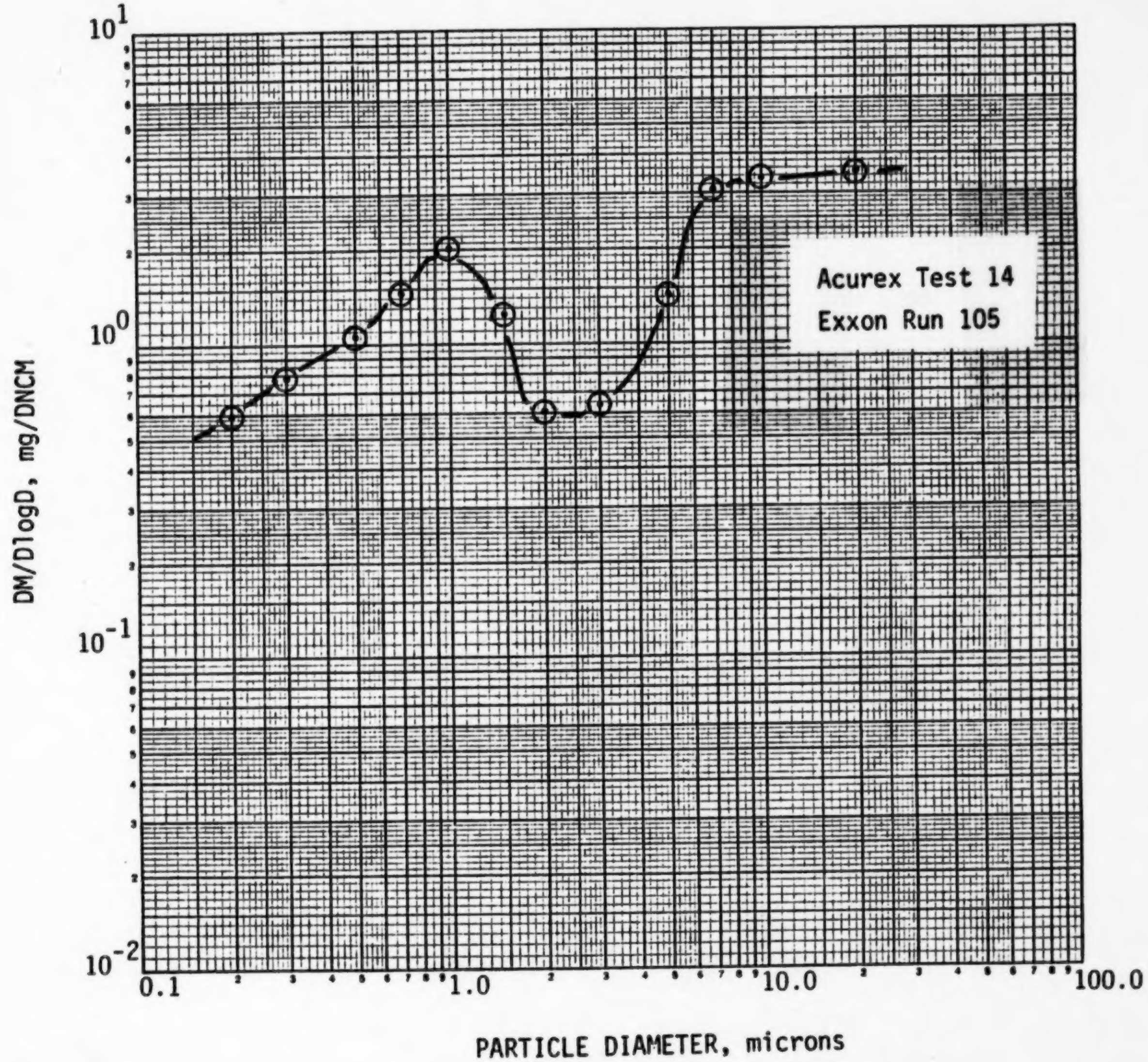

Figure C-14. ESP outlet differential size distribution.

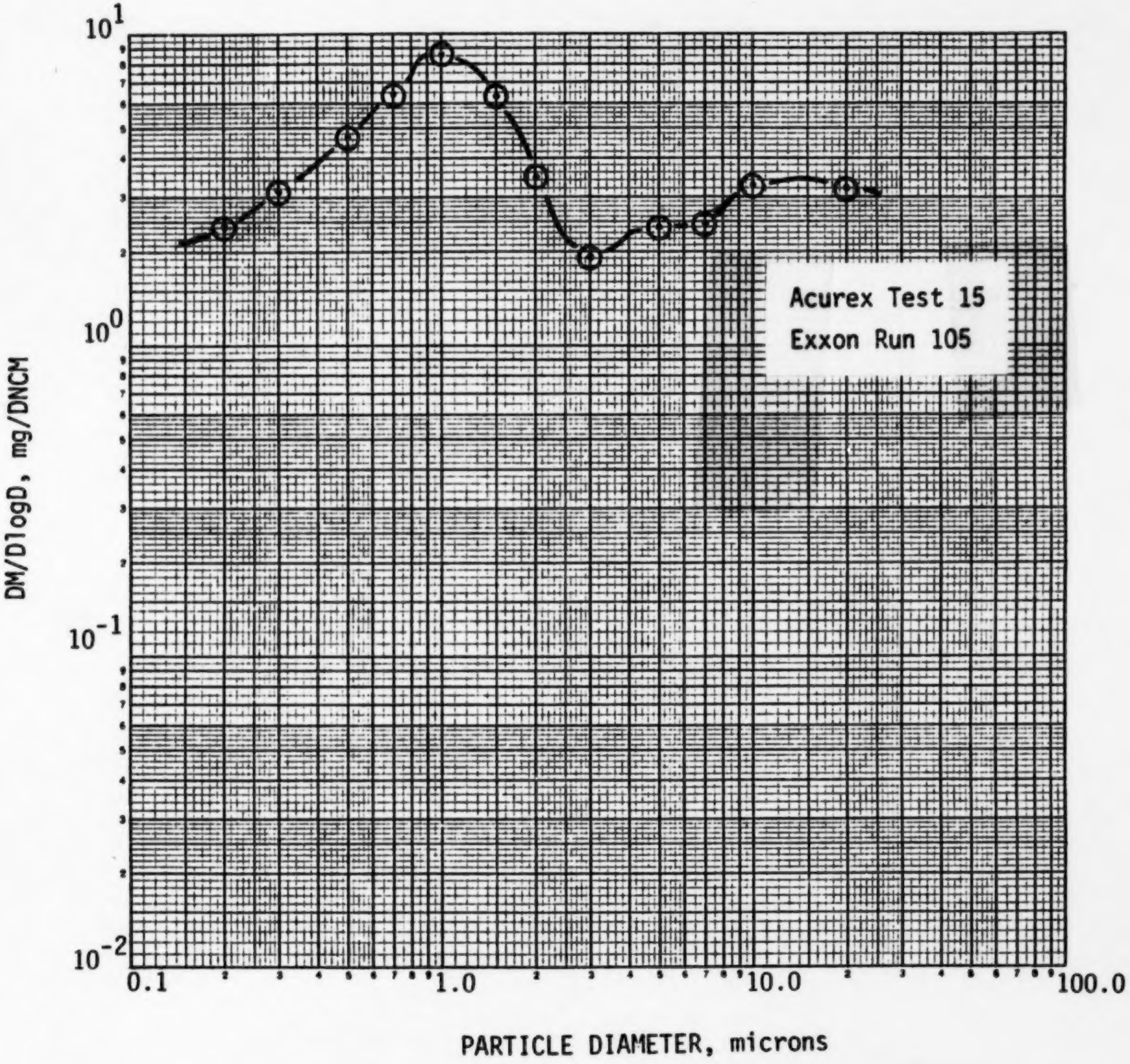

Figure C-15. ESP outlet differential size distribution.